

QC
807.5
U6
S3
00.75

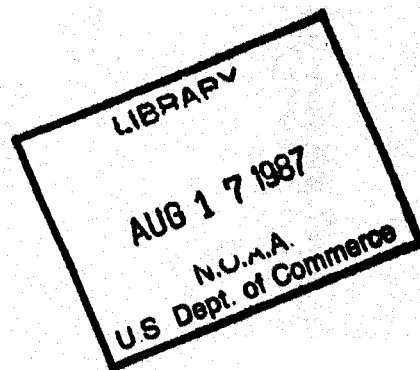
NOAA Technical Memorandum ERL SEL-75



THE TIROS - N / NOAA A-J
SPACE ENVIRONMENT MONITOR SUBSYSTEM

R. A. Seale
R. H. Bushnell

Space Environment Laboratory
Boulder, Colorado
April 1987



noaa

NATIONAL OCEANIC AND
ATMOSPHERIC ADMINISTRATION

Environmental Research
Laboratories

National Oceanic and Atmospheric Administration TIROS Satellites and Satellite Meteorology

ERRATA NOTICE

One or more conditions of the original document may affect the quality of the image, such as:

Discolored pages

Faded or light ink

Binding intrudes into the text

This has been a co-operative project between the NOAA Central Library and the Climate Database Modernization Program, National Climate Data Center (NCDC). To view the original document contact the NOAA Central Library in Silver Spring, MD at (301) 713-2607 x124 or Library.Reference@noaa.gov.

HOV Services
Imaging Contractor
12200 Kiln Court
Beltsville, MD 20704-1387
January 26, 2009

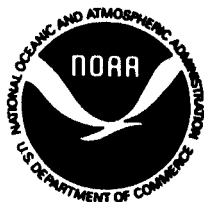
NOAA Technical Memorandum ERL SEL-75

QC
807.5
.4653
no. 75

// THE TIROS - N / NOAA A-J
SPACE ENVIRONMENT MONITOR SUBSYSTEM

R. A. Seale
R. H. Bushnell

Space Environment Laboratory
Boulder, Colorado
April 1987



**UNITED STATES
DEPARTMENT OF COMMERCE**

**Malcolm Baldrige,
Secretary**

**NATIONAL OCEANIC AND
ATMOSPHERIC ADMINISTRATION**

**Anthony J. Callo,
Administrator**

**Environmental Research
Laboratories**

**Vernon E. Derr,
Director**

NOTICE

Mention of a commercial company or product does not constitute an endorsement by NOAA Environmental Research Laboratories. Use for publicity or advertising purposes of information from this publication concerning proprietary products or the tests of such products is not authorized.

CONTENTS

	Page #
LIST OF FIGURES	iii
LIST OF TABLES	iv
ABSTRACT	1
1. INTRODUCTION	2
2. SPACECRAFT AND SEM	2
3. TOTAL ENERGY DETECTOR (TED)	8
3.1 General Description	8
3.2 Calibration for the TED	17
3.3 TED Data	18
3.4 TED Data Interpretation	19
3.5 TED Application	24
3.6 Data Displays for the TED	24
4. MEDIUM ENERGY PROTON AND ELECTRON DETECTOR (MEPED)	27
4.1 General Description	27
4.2 Proton Telescope	27
4.3 Electron Telescope	30
4.4 Omnidirectional Sensors	38
4.5 MEPED Application	40
5. HIGH ENERGY PROTON AND ALPHA DETECTOR (HEPAD)	42
5.1 Principle	42
5.2 HEPAD Operation	42
5.3 Response to radiation	47
5.4 HEPAD Application	49
5.5 Sample of HEPAD Data	49

6. DATA PROCESSING UNIT (DPU)	51
6.1 General Description	51
6.2 DPU Functions	51
6.3 Symbols & Data Conversion	57
7. INFLIGHT CALIBRATION IFC	62
8. TELEMETRY	71
8.1 Data Transmission and Processing	71
8.2 Data Formats	71
9. COMMAND	87
9.1 General Information	87
9.2 IFC and Format Commands	87
9.3 TED Commands	88
9.4 HEPAD Commands	89
10. ACKNOWLEDGMENTS	90
11. REFERENCES	91
12. REFERENCE DOCUMENTS	92
Appendix A: Table of the area F under the normal curve	93
Appendix B: SEM IFC	94
Appendix C: TED IFC Details	94
Appendix D: MEPED IFC Details	95
Appendix E: HEPAD IFC Details	97
Appendix F: Detector and Level Sensor Cross Reference	99
Appendix G: Integration Time	101
Appendix H Digital A Telemeter Assignments	102
Appendix I Acronyms and Letter Groups	108

LIST OF FIGURES

Figure	Title	Page #
1	TIROS-N Spacecraft Diagram	4
2	SEM on TIROS-N	5
3	Energy Coverage of the TIROS-N Space Environment Monitor	6
4	Performance Requirements	7
5	Total Energy Detector	9
6	TED Analyzer	10
7	TED Block Diagram	11
8	Particle Pitch Angle	13
9	TED Ramp Characteristics	16
10	Relationship Between Field Lines and Spacecraft	20
11	Variation of Particle Pitch Angle along Field Line	22
12	Northern Hemisphere Auroral Particle Energy Influx	25
13	Hemispherical Power Input	26
14	Medium Energy Proton and Electron Detector	28
15	MEPED Block Diagram	29
16	MEPED Proton Telescope	31
17	Energy Loss in Aluminum Contact vs Incident Ion Energy	32
18	MEPED Proton Telescope Response	33
19	MEPED Electron Telescope	34
20	MEPED Electron Detector Response	36
21	MEPED Electron Detector Efficiency	37
22	Omnidirectional Spectrometer	39
23	MEPED Data	41
24	High Energy Proton and Alpha Detector	43
25	HEPAD Block Diagram	44
26	HEPAD Telescope Assembly	45
27	HEPAD Telescope Response	48
28	Comparison of Flux Spectra by Kolasinski	50
29	Data Processing Unit	53
30	DPU Block Diagram	54
31	Output Circuits	81
32	Spacecraft-Powered Temperature TLM Output Circuits	82
33	SEM-Powered Temperature TLM Output Circuit	83
34	HEPAD and TED HV Power Supply Monitor Analog TLM Output Circuit	84
35	HEPAD/MEPED Detector Bias Voltage TLM Output Circuit	85
36	TED LV Ramp TLM Output Circuit	86
37	DPU IFC Ramp TLM Output Circuit	86

LIST OF TABLES

Table	Title	Page #
1	Energy Bands of the TED	17
2	TED Conversion From Telemetered Values	18
3	MEPED Detector Data and Passbands	35
4	Omnidirectional Proton Sensor Data	38
5	HEPAD Outputs	46
6	Algebraic Conversion of Log Function to Count	59
7	Look-up Conversion of Log Function to Count	60
8	TED Prescaler True Count	62
9	IFC Data	64
10	Complete Counts	65
11	FWHM Data	66
12	Coincidence Efficiency	68
13	Coincidence Efficiency	68
14	Digital A Subcom Words	76
15	Housekeeping Subcom in Digital A	77
16	Digital B Telemetry	78
17	Analog Subcom Telemetry	79
18	Equations for Analog Telemetry	80

The TIROS-N / NOAA A - J
SPACE ENVIRONMENT MONITOR SUBSYSTEM

R. A. Seale

Robert H. Bushnell

ABSTRACT. The Space Environment Monitor (SEM), which is incorporated as a subsystem in the TIROS-N and NOAA A-J satellites, is described. The SEM consists of a Total Energy Detector (TED), a Medium Energy Proton and Electron Detector (MEPED), a High Energy Proton and Alpha Detector (HEPAD) and a Data Processing Unit (DPU). The detectors are intended to provide near real time particle data for use in the Space Environment Service Center of NOAA and to provide a long term scientific data base. Telemeter codes, data reduction, and test instructions are given.

Key Words: Polar Orbiting Satellite, particles, monitoring, space.

1. INTRODUCTION

The objective of this report is to bring together in convenient form all the information on the SEM pertinent to use of the data and understanding its operation. The TIROS-N Space Environment Monitor (SEM) makes measurements of the Earth's charged particle environment. The data from the SEM detectors are used operationally by the Space Environment Services Center (SESC) of the US National Oceanic and Atmospheric Administration (NOAA) in Boulder, Colorado. The SESC, which is operated jointly by NOAA and the USAF Air Weather Service, has the US national responsibility for the preparation and dissemination of monitoring and forecasting information on solar activity and the state of the Earth's space environment, and the effects of these on man's activities. In addition, it is designated as the World Warning Agency by the International Union of World Data Centers (IUWDC). Affected activities are as diverse as the scheduling of geophysical surveying using the Earth's magnetic field, the planning of scientific experiments and the reduction of data from such experiments; to the radiation hazards to people in space or, during occasional giant solar particle events, to passengers and crew of high flying aircraft on polar routes.

The TIROS-N polar orbit affords the opportunity to make direct measurements of phenomena at high latitudes where the Earth's magnetic field geometry permits the free access of charged particles to the polar cap areas surrounding each magnetic pole, and to the region where particles trapped in the outer magnetosphere can be precipitated into the Earth's atmosphere during magnetic disturbances.

The TIROS-N SEM was provided by Ford Aerospace and Communications Corp. (FACC) as a subcontractor to the Space Environment Laboratory. A list of the major individuals involved is given in the acknowledgments. Much of the graphic material is from contractors' publications.

2. SPACECRAFT AND SEM

The TIROS-N/NOAA-A-G spacecraft, shown in Figures 1 and 2, is a five-sided box-like structure which is 3.71 meters long and 1.88 meters in diameter. Four of the side faces are equal in size and accommodate thermal control louvers in each face. The fifth side is wider than the other four to accommodate the earth-facing communications antennas and some of the earth viewing sensors. The spacecraft has a mass of 1421 kg at launch including expendables.

At one end of the central body known as the Equipment Support Module is the Reaction Support Structure which includes the last stage launch injection motor, an attitude control propulsion system and a boom-mounted solar cell array. The 11.6 sq. meter solar array is motor driven to rotate once per revolution in orbit so that it will continuously face the sun during the daylight portion of the orbit.

The Manipulated Information Rate Processor (MIRP) processes the high rate data from the Advanced Very High Resolution Radiometer (AVHRR) in order to

provide separate, real time outputs for Automatic Picture Transmission (APT) and High Resolution Picture Transmission (HRPT), recorded Global Area Coverage (GAC) of reduced resolution data and recorded Local Area Coverage (LAC) of high resolution data. By command these are read out at the CDA's and processed in the NOAA central computer facility at Suitland, Maryland. The four data formats are put out simultaneously. LAC is similar to the recorded HRPT data of the ITOS system known as VREC.

In addition to formatting, the MIRP adds synchronization, identification, time code, telemetry and the TIROS Information Processor (TIP) output to the AVHRR data. The high resolution AVHRR is reduced in resolution by averaging techniques for use in the APT and GAC formats. The HRPT and LAC are put out from the MIRP at 0.66 megabits per second while the APT is in analog form.

The instrument data which are processed by the TIP include the TIROS Operational Vertical Sounder (TOVS), the Space Environment Monitor (SEM), and the Data Collection System (DCS). NOAA-F and -G have been designated Advanced TIROS N (ATN) and have a somewhat different complement of instruments which varies with the particular spacecraft. A Search and Rescue (SAR) receiver is included.

The individual instrument data rates going into the TIP are as follows:

HIRS/2	2880 bits per second
SSU	480 " " "
MSU	320 " " "
SEM	160 " " "
DCS	720 " " "

The TIP data are put out as one channel of serial digital words at 8320 bits per second included in the real time beacon transmission and recorded data.

The NOAA-A SEM consists of three detector and analog electronics sections which feed a common Data Processing Unit (DPU). The three SEM detectors, a Total Energy Detector (TED), a Medium Energy Proton and Electron Detector (MEPED) and a High Energy Proton and Alpha Detector (HEPAD), measure the flux and spectrum of charged ambient particles at the spacecraft. In addition, the TED and, in the low energy portion of its range, the MEPED measure two points on the spatial distribution function by having two detectors make directional measurements at different angles to the geomagnetic field.

The division of the detectors into the three groups reflects the three different detector technologies used to cover the wide energy range between 300 eV and 850 MeV. Figure 3 and Figure 4 show the outputs of the SEM.

The three SEM sensors are shown in Figure 2. The DPU is located inside the Equipment Support Module and is therefore not visible.

The mass of each, less cables, is:

TED 3200 g, MEPED 3200 g, HEPED 3300 g, DPU 3100 g; total 12800 g.

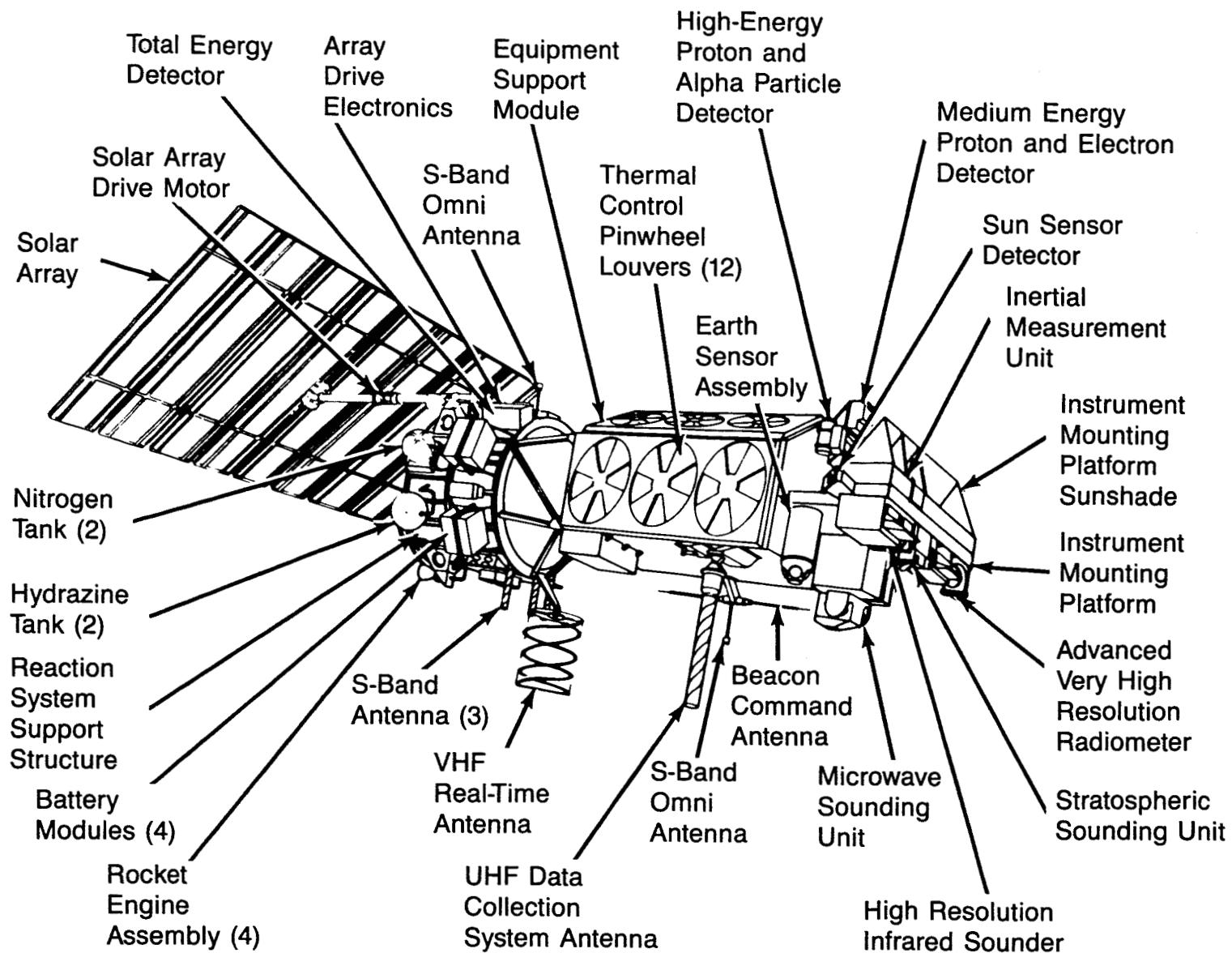


Figure 1.—TIROS-N Spacecraft Diagram

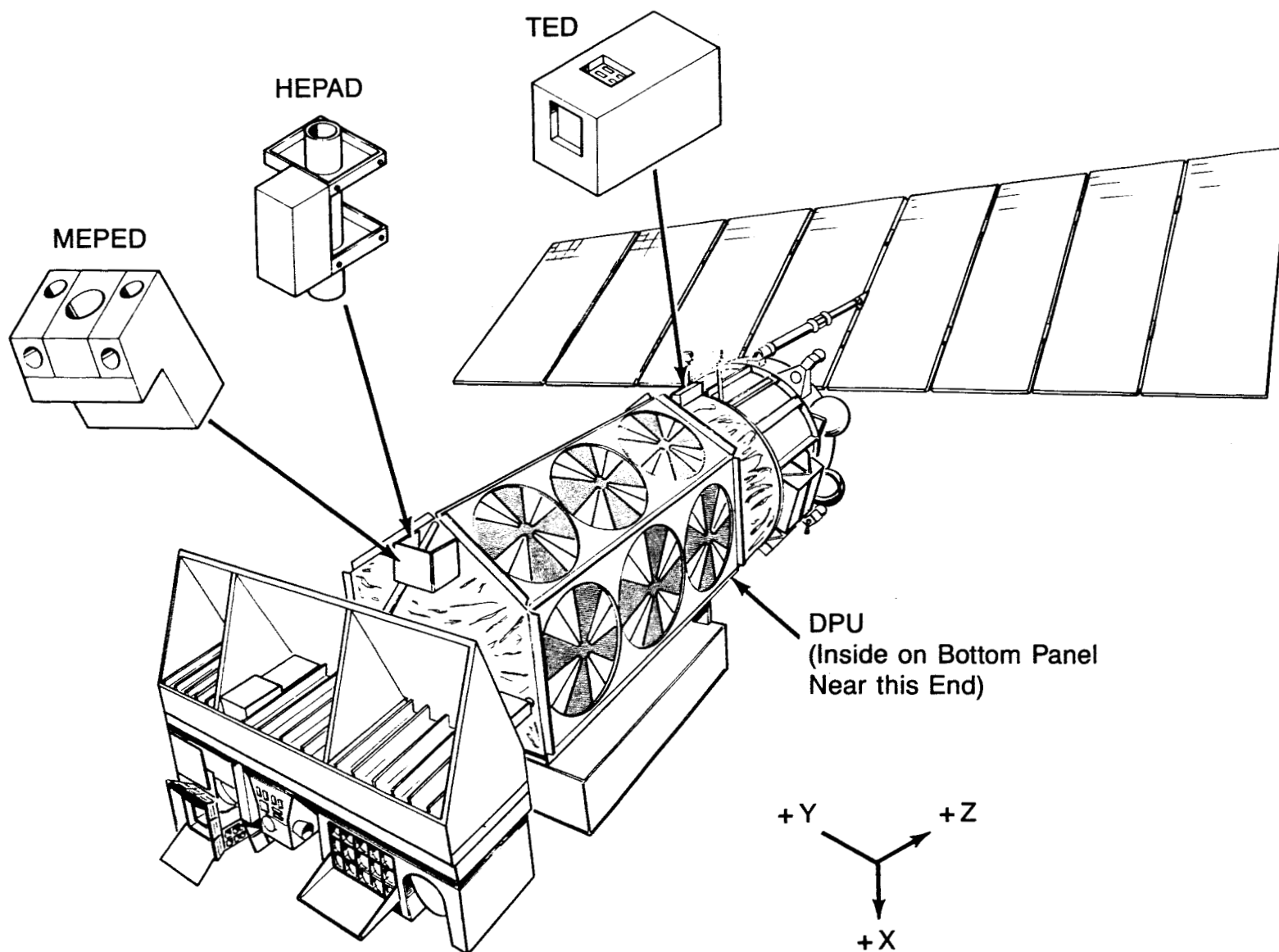
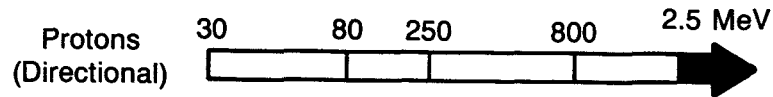


Figure 2.—SEM on TIROS-N

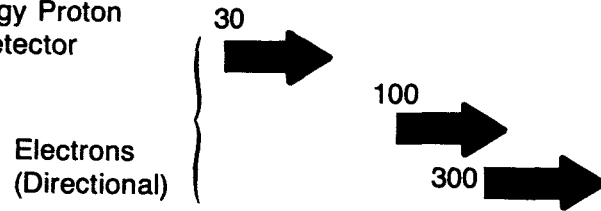
Electrons & Positive Ions



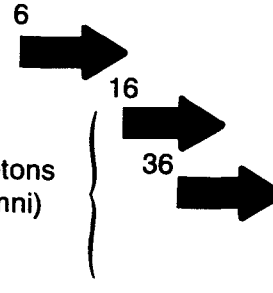
Total Energy Detector (TED)



Medium Energy Proton
& Electron Detector
(MEPED)



Alphas
(Directional)



High Energy Proton
& Alpha Detector
(HEPAD)

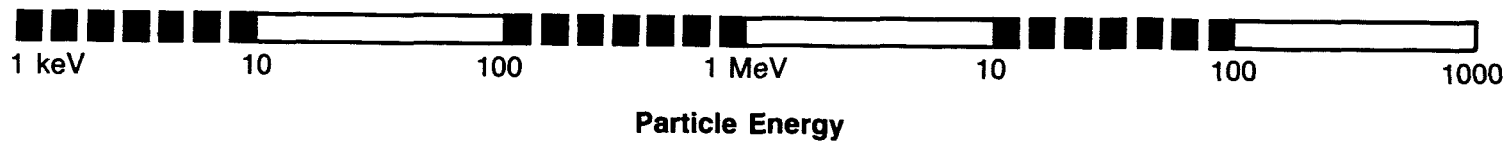
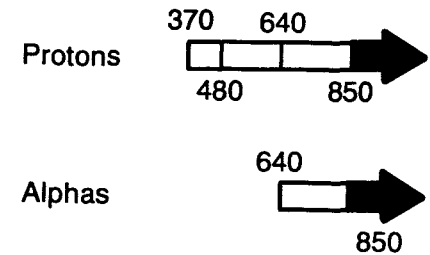


Figure 3.—Energy Coverage of the TIROS-N Space Environment Monitor

	Data Channel	Particle Type	Energy Range	Field of View		Max. Counting Rate pps	Data Sampling Interval	Other	
				Aperture Axis	Cone Half Angle				
TED	$F_D(\alpha), (DE)_m, E_m$	Electrons	0.3-20 Kev	0° (Zenith)	~3°	4×10^5	2 sec	$F_D(\alpha)$ accuracy: $\pm 50\%$ (DE) _m accuracy: $\pm 50\%$ E _m accuracy: $\pm 30\%$ Resolution: Statistical in weak fluxes < $\pm 6\%$ in strong fluxes Insensitive to sunlight, moonlight. IFC: Preserves 7 1/2% accuracy.	
	"	Protons	"	"	"				
	"	Electrons	"	30°	"				
	"	Protons	"	"	"				
	(DE) _{1,3,5,7}	E.P	Four Differential	0°, 30°	"		4 or 8 sec		
MEPED Telescopes	P ₁ P ₂ P ₃ P ₄ P ₅	Protons	30-80 Kev 80-250 Kev 250-800 Kev 800-2.5 Mev >2.5 Mev	0° (Zenith)	14°	5×10^7	2 sec	Noise Resolution: 7 Kev FWHM tele. 60 Kev FWHM OMNI Telescopes insensitive to incorrect particle type Energy Interval Stability: < $\pm 20\%$ at 5×10^6 counting rate IFC: Provides energy intervals; " noise resolution in telescopes Lifetime: Operation within specification for 5 years for all channels except P1 and E1.	
	Same as above box	Protons	Same as above box	90°	"				
	E ₁ E ₂ E ₃	Electrons	> 30 Kev > 100 Kev > 300 Kev	0°	"				
	Same as above box	Electrons	Same as above box	90°	"				
	$0^1 90^1$	Positive Ions (Z ≥ 2)	> 6 Mev	0°, 90°	"	Not Specified	16 sec		
	MEPED OMNI	P ₆ P ₇ P ₈	Protons	> 16 Mev > 36 Mev > 80 Mev	0° (Zenith)	60°	2×10^5		2 sec
HEPAD		P ₁ P ₂ P ₃ P ₄	Protons	370-480 Mev 480-640 Mev 640-850 Mev > 850 Mev	0° (Zenith)	24°	7×10^4	4 sec	Accuracy: < $\pm 20\%$ in count rate and energy intervals. IFC: Verifies accuracy specifications
		α_1 α_2	Alpha Particles	640-850 Mev Nucleon > 850 "	"	"	10^4		
	S ₁ , S ₂ , S ₃ S ₅ S ₄	All p, α Am ²⁴¹ α	All > 65 Mev/Nucleon ~5.4 Mev	- 0° (Zenith) -	180° 24° -	2×10^5			

Figure 4.—Performance Requirements

3. TOTAL ENERGY DETECTOR (TED)

3.1 General Description

The TED measures electrons and positive ions (often assumed to be protons) in the energy range 300 eV to 20 keV. Four separate detector assemblies measure the negatively charged and positively charged particles, respectively, at two angles; one approximately parallel to the magnetic field at high latitudes and the other at 30° to the first. Figure 5 shows a general view of the TED.

The detector assembly (Figure 6) uses a cylindrical-plate electrostatic analyzer with approximately a 13% energy resolution. A voltage difference is impressed on the analyzer plates. The polarity of this voltage determines whether positively charged ions (assumed always to be protons) or negatively charged particles (assumed to be electrons) are detected. The magnitude of this voltage selects a band of particle energies centered at some energy E for which the particles are passed through the analyzer.

The analyzer is followed by a "spiraltron" type channel electron multiplier (called a channeltron in Figure 7) which produces a relatively large pulse of electrons for input particles of either positive or negative charge, independent of the original particle energy. It does this in an electron avalanche (regardless of the charge or species of the input particle) of secondary emission. Preacceleration fields of appropriate polarity are applied between the electrostatic analyzer exit and the spiraltron cathode to ensure that even the lowest energy particles produce enough electrons at the cathode surface to be counted. The channel electron multiplier counts those charged particles which have passed through the analyzer.

A block diagram of the TED detector and analog electronics is shown in Figure 7. The basic signal chain between the detector spiraltrons and the logic pulse output to the DPU consists of linear amplification and pulse shaping followed by a "level comparator". There are four "levels" in the level comparator, set by the two attenuator levels and by the two reference levels shown at the right side of Figure 7. Two signal chains are used which are multiplexed sequentially between the detectors at 0° and those at 30° . See p. 91 for commands for these levels.

To allow for the loss of electron multiplication gain which occurs over the lifetime in orbit (basically a function of the number of events detected) the channeltron gain can be adjusted by varying its high voltage power supply (HVPS); 8 voltage steps are provided for this purpose. To determine the correct setting, a crude distribution of pulse heights from each detector is obtained by calibrating with the four comparator levels. Provision is made for this automatic "In-Flight Calibration" (IFC) under control of a sequence generated by the DPU which is started by ground command.

Four separate but identical analyzers, mounted in pairs, are included in the TED. Each pair views charged particles coming from different directions so that observations can be made of the directional energy flux at two different angles to the local geomagnetic field direction. One pair of

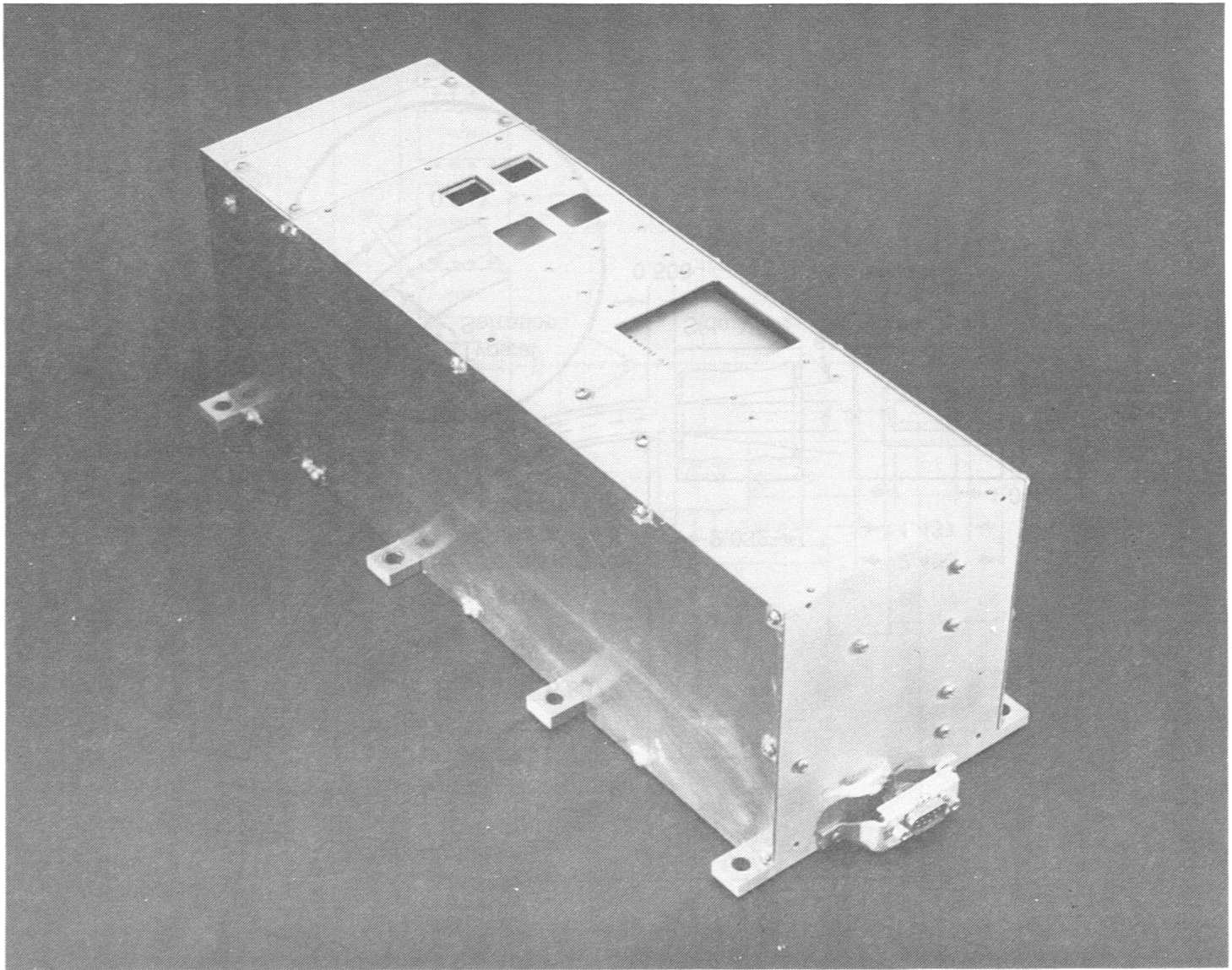


Figure 5.—Total Energy Detector

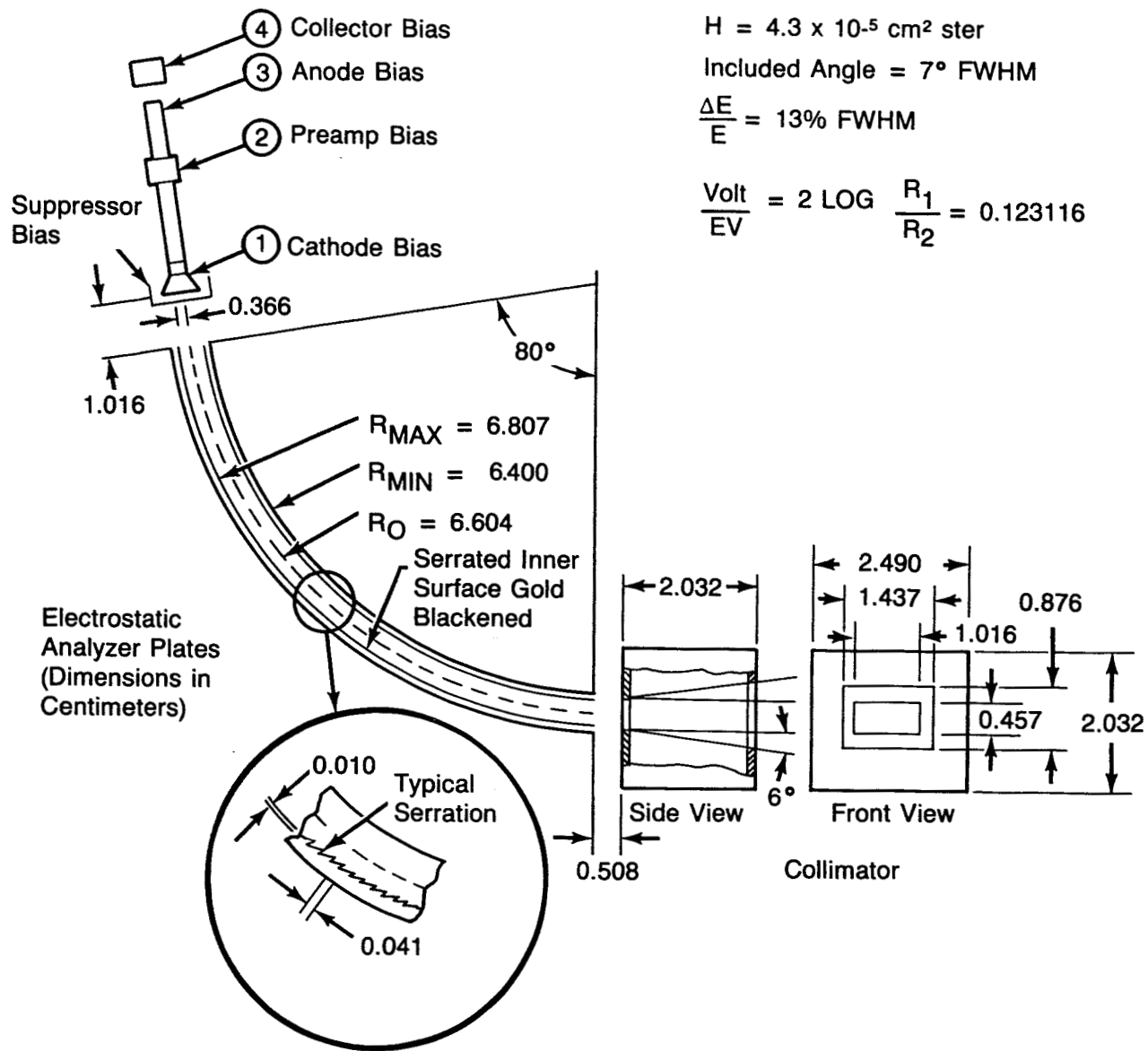


Figure 6.—TED Analyzer

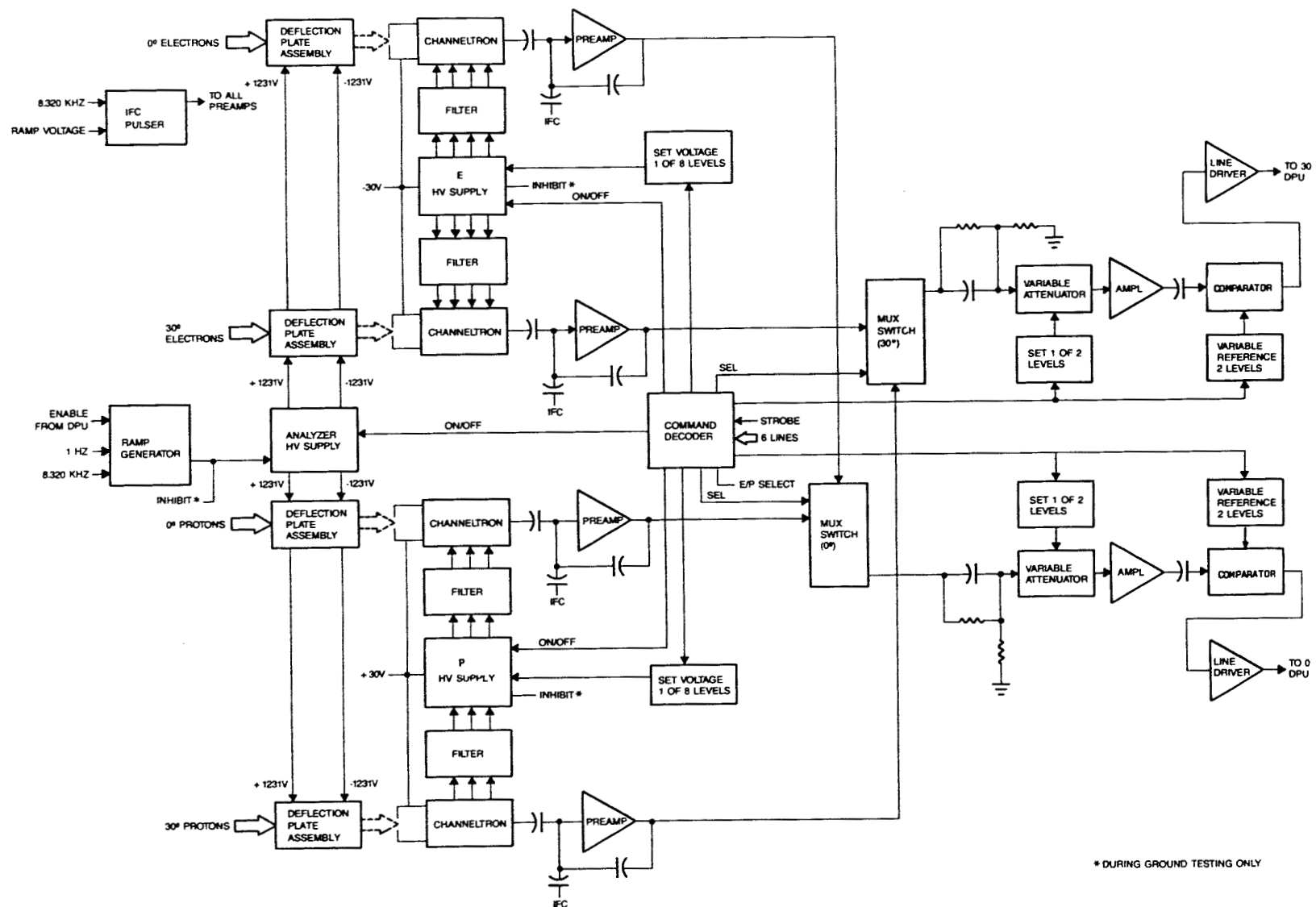


Figure 7.—TED Block Diagram

detectors views outwards parallel to the earth-center radial vector so that it measures charged particles whose velocities are toward the earth along this radial vector. The other pair views at an angle of 30° from the first. It is stressed that these two angles are defined with respect to the earth-center satellite vector and have nothing to do with the pitch angle α associated with the charged particles being measured.

One detector within a detector pair measures electrons and alternates in the data segment with the other detector which measures positive ions. The time taken for a full cycle is two seconds. The first half cycle (one second) is devoted to measuring electrons. The total count during this sweep is telemetered to the ground as a measure of the integrated (from 300 eV to 20,000 eV) directional energy flux carried by the electrons observed by that analyzer. During the second half cycle (one more second) the process is repeated for positive ions using the other detector in the pair.

For a cylindrical electrostatic analyzer being operated at a "center energy" E , the count rate is related to the physical quantity $j(E)$, the differential directional particle number flux, by the expression

$$j(E) = \frac{A \text{ CR}(E)}{E}$$

where $\text{CR}(E)$ is the count rate and A is a nearly energy-independent number characterizing the analyzer. $j(E)$ is the number of particles of energies E , coming from a point within a solid angle about some direction, passing through a unit area oriented normal to that direction vector, per unit time per unit energy; units: particles / (cm²·s·sr·keV). In practice, the direction from where these particles come is specified in terms of the "pitch angle" between that direction and the direction of the local geomagnetic field (see Figure 8).

Given $j(E)$ one can define a differential directional energy flux by

$$j(E)E = A \text{ CR}(E).$$

It is seen that $j(E)E$ is determined by the detector count rate independent of what particle energy happens to be studied. A given count rate for low energy particles converts to the same differential directional energy flux as the same count rate would for high energy particles. The units of the differential directional energy flux, $j(E)E$, are energy per (unit area · unit time · steradian · unit energy).

The directional energy flux carried by charged particles (either electrons or protons as chosen by the plate voltage polarity) having energies between E_1 and E_2 is defined by

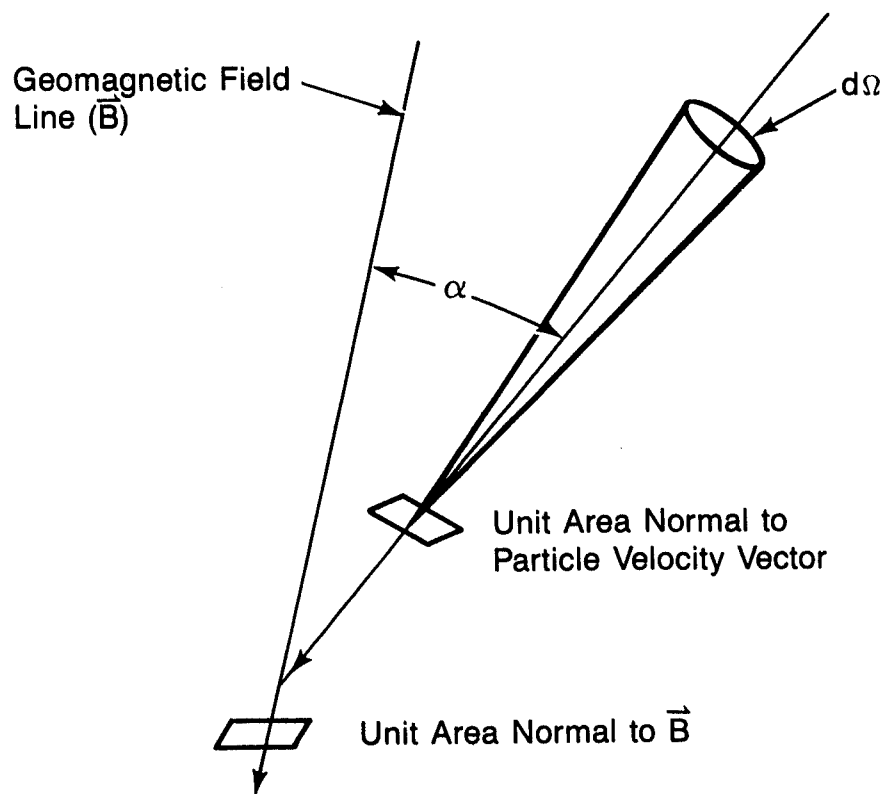


Figure 8.—Particle Pitch Angle α

$$\begin{aligned}
F_D &= \int_{E_1}^{E_2} j(E) E dE \\
&= \int_{E_1}^{E_2} A CR(E) dE
\end{aligned}$$

Here the detector count rate $CR(E)$ is shown as an explicit function of the particle energy E which, in turn, is directly proportional to the voltage between the analyzer plates. If this plate voltage is varied linearly with time from measuring charged particles of energy E_1 to particles of energy E_2 , then a shift of variable from the explicit E to the implicit variable t (time) may be made and the integral may be rewritten as

$$\begin{aligned}
F_D &= k \int_{T_1}^{T_2} CR(t) dt \\
&= k CR_T
\end{aligned}$$

where CR_T is the total count accumulated by the detector during the time period when the analyzer was being swept between energy E_1 and E_2 . The constant k is determined by a combination of the detector system sensitivity (the constant A) and the rate at which the energy setting of the analyzer is being varied.

The units of F_D are energy per (unit area · unit time · steradian).

Ordinarily the directional energy flux F_D will be dependent upon the pitch angle of the particles being detected (the TIROS detector has a small field of view and will detect particles within a small range of pitch angle). In order to obtain a measure of the total energy flux carried by these particles through a unit area oriented normal to the geomagnetic field B , F_D must be integrated over the pitch angle α .

If F_D is known as a function of α at the top of the atmosphere, normally taken to be 120 km altitude, then the energy flux through a unit area normal to B will be

$$F_T = 2\pi \int_0^{\pi/2} F_D(\alpha) \sin \alpha \cos \alpha d\alpha$$

The units of F_T are energy per (unit area · unit time).

For all latitudes relevant to the TIROS observations (i.e. poleward of 40 degrees latitude) the inclination of B to the horizontal is greater than 60°.

Thus, identifying the energy flux through a unit area normal to B with the actual energy flux into the atmosphere will introduce an error of no more than $(1 - \cos 30)$ which is 15%.

The prime function of the TIROS-N instrument is to measure the directional energy flux F_D for each of the two particle species, electrons and protons, at each of two pitch angles. This is sufficient to estimate the total energy fluxes F_T for each of the particle species and the sum of these two energy fluxes.

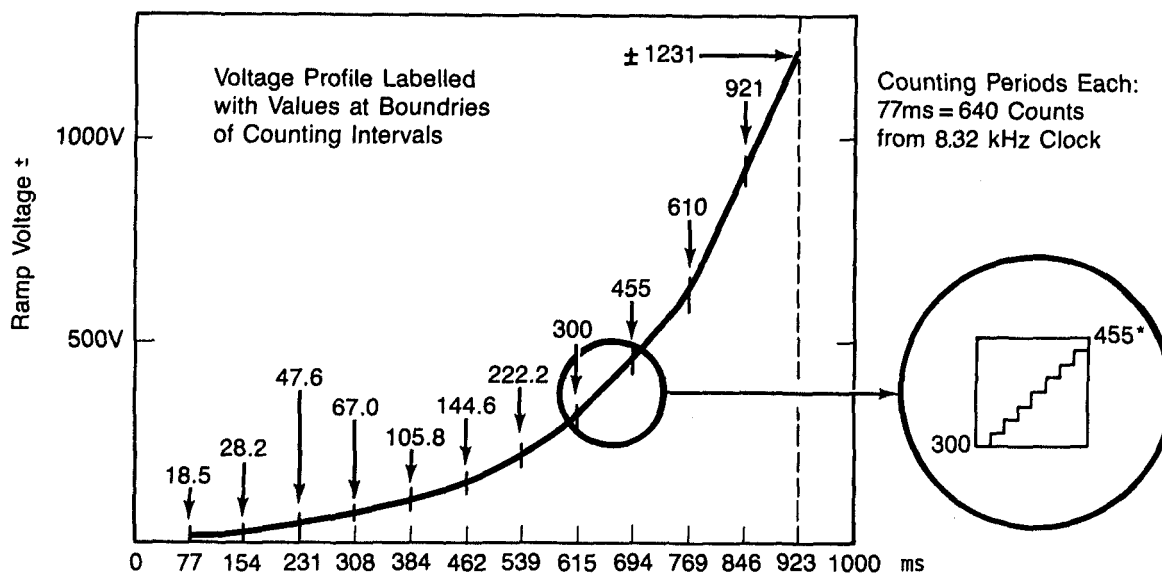
While the main output of the TED, as its name implies, is the total incident energy flux, the electrostatic analyzer sorts particles by their charge and energy. The energy flux measurement is accomplished by sweeping the analyzer voltage in synchronism with the data processing and telemetry in the DPU. The total flux is formed by adding up the sorted counts.

For simplicity of ground processing and to minimize telemetry requirements, this sum is done in the SEM by sweeping the electrostatic analyzers with a piecewise linear ramp voltage. Figure 9 shows some details of the sweep. Measurements of a single particle species are made over a 1-second period. The 1-second period is split into 13 equal intervals. Background (particle count) is measured over the first interval (78 ms), when the ramp voltage applied to the electrostatic analyzer is set to zero. The energy sweep from 300 eV to 20,000 eV takes 11/13 second. Counts are accumulated during each successive 1/13 s interval for 11 intervals. There is one interval at the end to allow the ramp voltage to reset.

During the sweep of the 11 intervals a 5-bit binary prescaler is reduced by factors of two in synchronism with increases in the slope, which is also changed by factors of two, of the piecewise linear ramp voltage, so as to weight each contribution to the final accumulated count in proportion to its energy content, thus arriving at the total energy.

Of the 11 values generated by a single detector during an energy sweep, four are telemetered every fourth sweep. The four represent the counts accumulated during intervals 2, 4, 6, and 8 corresponding to energy bands 1, 3, 5, and 7.

An additional piece of information derived for each sweep is the energy band number containing the highest count thus giving an indication of the predominant energy in the incident spectrum. This is done so that an estimate can be made as to what energy particles are carrying the bulk of the energy flow and, thus, what altitude in the atmosphere this energy is ultimately deposited. Part of this information is telemetered at a slower rate in submultiplexed words.



Channel Energy (Kev)	Ramp Range (V)	Energy Interval (Kev)			Data Channel Label	Number of Pre-Scaling Bits in F_D (a) comp
		Width	Center	Width Center		
0	0	---	---	---	BKGND	---
0.300- 0.458	18.5- 28.2	0.158	0.379	0.42	DE 1	5
0.458- 0.773	28.2- 47.6	0.315	0.616	0.51	DE 2	4
0.773- 1.088	47.6- 67.0	0.315	0.931	0.34	DE 3	4
1.088- 1.718	67.0- 105.8	0.630	1.403	0.45	DE 4	3
1.718- 2.349	105.8- 144.6	0.630	2.033	0.31	DE 5	3
2.349- 3.610	144.6- 222.2	1.261	2.979	0.42	DE 6	2
3.610- 4.870	222.2- 299.8	1.261	4.250	0.30	DE 7	2
4.870- 7.392	299.8- 455.0	2.522	6.131	0.41	DE 8	1
7.392- 9.914	455.0- 610.2	2.522	8.653	0.29	DE 9	1
9.914-14.957	610.2- 920.6	5.043	12.436	0.41	DE10	0
14.957-20.000	920.6-1231.0	5.043	17.479	0.29	DE11	0
0.300-20.0	18.5-1231.0				F_D (a)	

Ramp Characteristics

Figure 9.—TED Ramp Characteristics

The count accumulated during a single subinterval of the energy sweep relates to the directional energy flux within the limited energy range swept by the detector in the 1/13-second subinterval. By dividing this directional energy flux by the width of the energy band sampled, the directional differential energy flux at the center energy of the band may be obtained.

Table 1 lists the details of each of these 11 energy bands.

TABLE 1. ENERGY BANDS OF THE TED					
Energy Band #	Edges of Band (eV)	Center Energy (eV)	Conversion from Count to Directional Energy Flux (ergs/(cm ² ·s·sr))		Altitude at Which Energy is Deposited km
			electrons	protons	
1	300- 458	379	5.97 x 10 ⁻⁵	4.69 x 10 ⁻⁵	>300
2	458- 773	616	1.19 x 10 ⁻⁴	9.38 x 10 ⁻⁵	215
3	773- 1088	931	1.19 x 10 ⁻⁴	9.38 x 10 ⁻⁵	190
4	1088- 1718	1403	2.38 x 10 ⁻⁴	1.88 x 10 ⁻⁴	165
5	1718- 2349	2033	2.38 x 10 ⁻⁴	1.88 x 10 ⁻⁴	145
6	2349- 3610	2979	4.76 x 10 ⁻⁴	3.75 x 10 ⁻⁴	130
7	3610- 4870	4250	4.76 x 10 ⁻⁴	3.75 x 10 ⁻⁴	120
8	4870- 7392	6131	9.52 x 10 ⁻⁴	7.50 x 10 ⁻⁴	115
9	7392- 9914	8653	9.52 x 10 ⁻⁴	7.50 x 10 ⁻⁴	108
10	9914-14957	12436	1.90 x 10 ⁻³	1.50 x 10 ⁻³	105
11	14957-20000	17479	1.90 x 10 ⁻³	1.50 x 10 ⁻³	104

The telemetered number is multiplied by the conversion factor to obtain the desired quantity in physical units.

3.2 Calibration for the TED

Calibration data are contained in the End Item Data package prepared for each SEM by the manufacturer, Ford Aerospace and Communication Corporation (FACC) which gives the results of instrument calibration performed at the low-energy particle calibration facility at Rice University.

The conversions between these telemetered values and the corresponding directional energy flux in physical units are given in Table 2. The difference in conversion between electrons and protons reflects a difference in detection efficiency for the two particle species.

TABLE 2. TED CONVERSION FROM TELEMETERED VALUES		
Directional Energy Flux		
ergs/(cm ² ·s·sr) per count		
Electrons:	1.905 x 10 ⁻³ x	0EFD or 30EFD
Protons:	1.50 x 10 ⁻³ x	0PFD or 30PFD
Directional Energy Flux in Each Band		
erg/(cm ² ·s·sr·eV) per count at the center energy		
Electrons	3.78 x 10 ⁻⁷	
Protons	2.97 x 10 ⁻⁷	

3.3 TED Data

The following are the data obtained by the TED, their meaning, and the frequency/timing with which they are obtained.

0EFD, 30EFD	The TED directional count from each of two pitch angles for each of the two particles species at the location of the satellite. These numbers are proportional to the directional energy flux between 300 eV and 20 keV. The full set of four values is transmitted continuously every two seconds (about 15 km of spacecraft travel).
0PFD, 30PFD	
Total Energy	The total energy flux into the atmosphere at 120 km as computed from the four individual directional measurements every two seconds.
0DEM, 0EM	The energy channel number EM or PM within which the maximum count rate was observed together with the value DEM or DPM of that count rate. This data set is transmitted continuously every two seconds.
30DEM, 30EM	
0DPM, 0PM	
30DPM, 30PM	

ODE1, ODE3	These four sets of differential directional energy flux values for energy bands 1, 3, 5 and 7 (sweep intervals 2, 4, 6 and 8) are transmitted in a sequence requiring 8 seconds. These data appear only in record types 1, 2 and 3. Record type means one of the four 8-second parts of the 32-second telemeter period listed in Appendix H.
ODE5, ODE7	
3ODE1, 3ODE3	
3ODE5, 3ODE7	
ODP1, ODP3	
ODP5, ODP7	
3ODP1, 3ODP3	
3ODP5, 3ODP7	
OEBC, 3OEBC	The count accumulated during the first 1/13 second (background interval) of each of 16 energy sweeps associated with labeled detector and particle species. These data are transmitted every 32 seconds and appear in output record type 4 only.
OPBC, 3OPBC	

The four observations (OEFD, 3OEFD, OPFD, and 3OPFD), which constitute a measure of the total energy, are the prime data from the TED instrument and are transmitted continuously every two seconds (about 15 km of spacecraft travel).

Because there are four detectors there are a total of four directional data sets (or 16 points) available every two seconds. Only one in four such sets are actually transmitted, the sequence being:

first two seconds	ODE1, ODE3, ODE5, ODE7
next two seconds	3ODE1, 3ODE3, 3ODE5, 3ODE7
next two seconds	ODP1, ODP3, ODP5, ODP7
last two seconds	3ODP1, 3ODP3, 3ODP5, 3ODP7

The data channel identification here includes the detector direction (0 or 30), the particle species (E or P) and the energy band (1, 3, 5, 7).

3.4 TED Data Interpretation

All these physical variables listed so far are those measured at the satellite at 850 km altitude. These measured values are manipulated, together with a geomagnetic field model (IGRF) to obtain the truly relevant variable: the magnitude of the energy flow into the atmosphere and the location at which this energy input is occurring.

Figure 10 illustrates this situation. Charged particles measured at the satellite are guided along the magnetic field lines. Because these magnetic lines of force are not radial, the point at which the field line passing through the satellite intersects the atmosphere may be displaced considerably from the subsatellite point. The magnetic field model is used to trace the field line passing through the satellite to the point where the field line intersects the atmosphere at 120 km. (This point is called the "foot of the

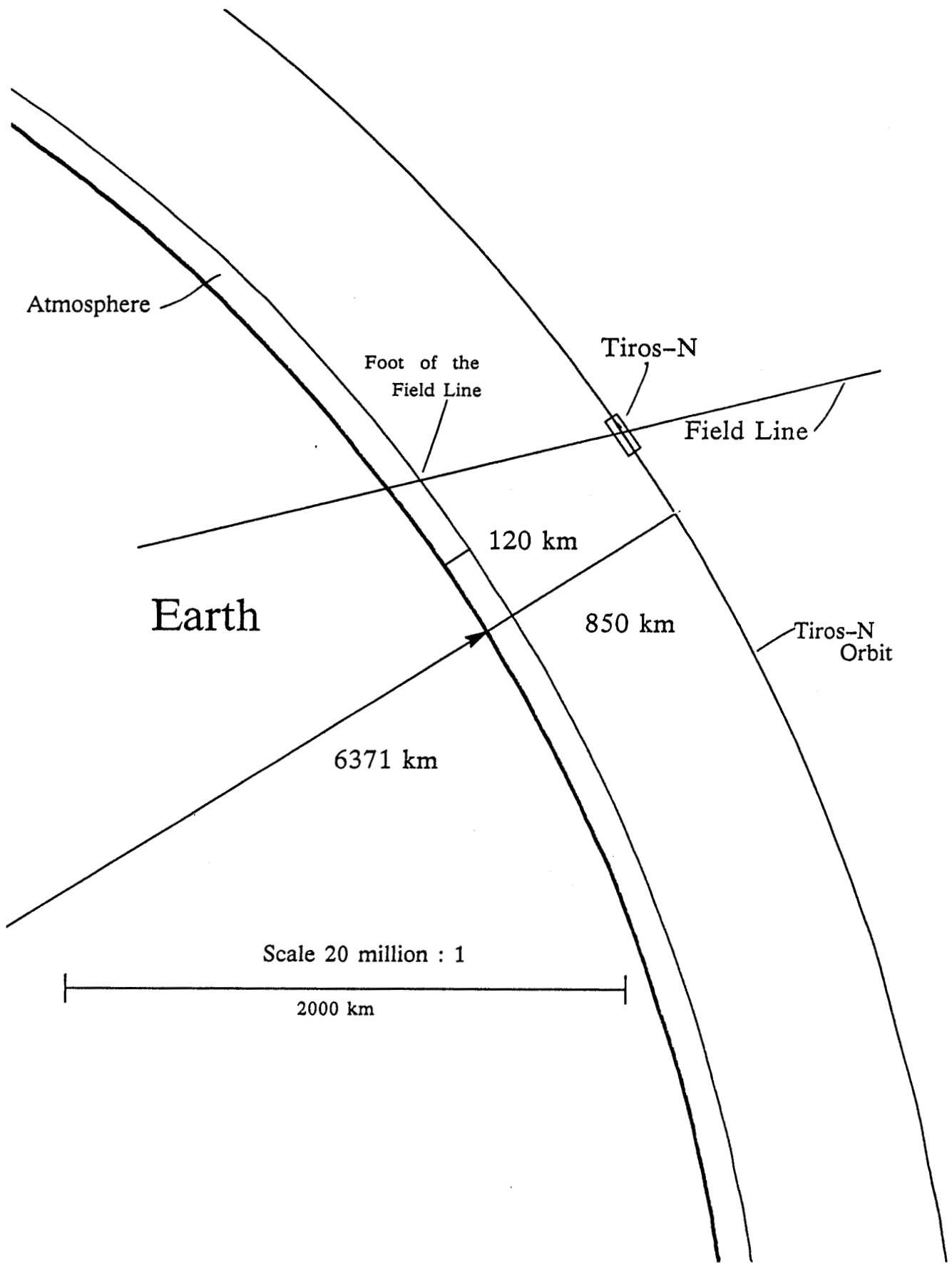


Figure 10.—Relationship Between Field Lines and Spacecraft

field line", FOFL). The co-ordinates of this point, both geographic and geomagnetic, together with the solar time and magnetic time are calculated and given in the header records of an archive tape made for all data. Zero of magnetic time occurs when the sun crosses the lower branch of the meridian through the geographic pole and the northern magnetic pole. By convention, if TIROS-N is north of the geomagnetic equator, the FOFL is taken to be in the northern hemisphere. Otherwise the FOFL is in the southern hemisphere.

The angles between the geomagnetic field direction and the look direction of the two detectors are also computed using the geomagnetic field model. These two angles are the local pitch angles of the charged particles being studied by the two detectors. However, because of the "magnetic mirror effect" on the motion of charged particles, the pitch angles these particles have at the location of the satellite are not the same pitch angles they have at the top of the atmosphere. The relation between the pitch angles a particle has at these two points in space is

$$\sin \alpha_{120} = \sqrt{\frac{B_{120}}{B_{850}}} \sin \alpha_{850}$$

where

α_{850} = pitch angle at the TIROS-N spacecraft 850 km

α_{120} = pitch angle at 120 km (the foot of the field line)

B_{850} = geomagnetic field strength at the TIROS-N spacecraft

B_{120} = geomagnetic field strength at the FOFL

Figure 11 illustrates how the pitch angle of a charged particle varies as it moves along the geomagnetic field line between TIROS-N and the atmosphere. Note that convention defines a particle's pitch angle as the angle between the particle's velocity vector and the direction of the magnetic field. This means that in the northern hemisphere charged particles moving downwards toward the atmosphere have pitch angles between 0° and 90° . In the southern hemisphere charged particles moving towards the atmosphere have pitch angles between 180° and 90° .

Note also that it is possible for $\sin \alpha_{120}$ to exceed 1.0 such that $\sin \alpha_{120}$ is not defined. Physically, this occurs when the charged particles going downwards toward the atmosphere at TIROS-N in fact magnetically mirror before reaching 120 km and return back up the magnetic field line. Such particles cannot be counted as contributing to the energy influx into the earth's atmosphere.

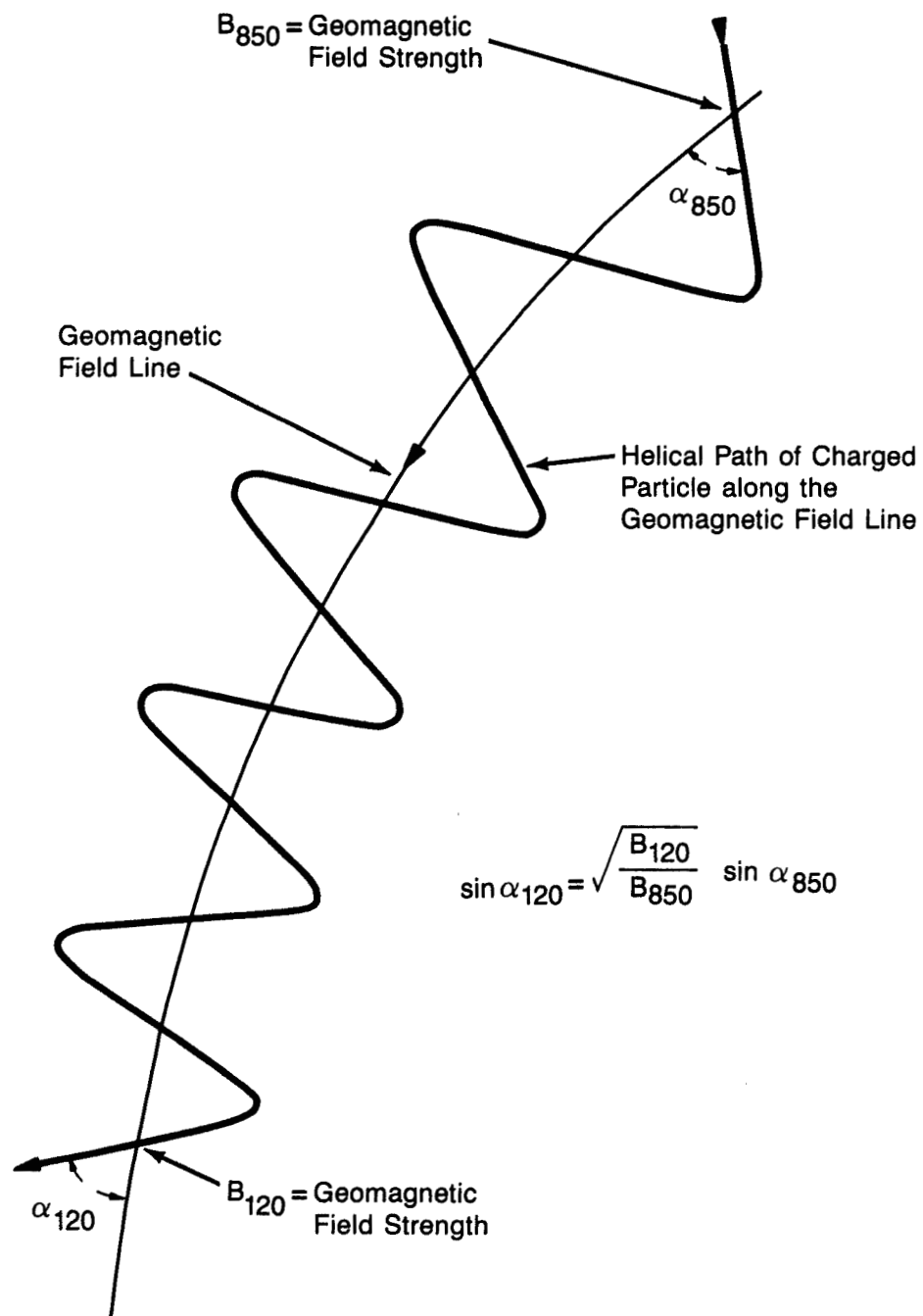


Figure 11.—Variation of Particle Pitch Angle Along Field Line

Using the measurements of OEFD, 3OEFD, OPFD, and 3OPFD, together with the pitch angles at which the measurements were made (as transformed to 120 km) F_T , the integral shown on p. 14, may be evaluated independently for both electrons and ions. The sum of these two, converted to physical units $\text{erg}/(\text{cm}^2 \cdot \text{s})$, becomes the Total Energy Flux.

During the creation of the archive tapes at SEL, all variables concerning the geomagnetic field are computed once each eight seconds and given in the header format. Amongst these variables are:

- A. The three vector components of the geomagnetic field at TIROS-N together with the scalar magnitude of the field.
- B. The geographic coordinates of the FOFL.
- C. The geomagnetic coordinates of the FOFL.
- D. Local solar time and geomagnetic time of the FOFL.
- E. The three vector components of the geomagnetic field at the FOFL together with the scalar magnitude of the field.
- F. The pitch angles of the charged particles being observed by the two TED detectors as transformed to the FOFL.

If neither of the two detectors is viewing charged particles which reach the earth's atmosphere, then the value of the total energy is set to 0 on the archive tape. However, the values of OEFD, 3OEFD, OPFD, and 3OPFD remain available in the record. The situation where neither detector views charged particles which can reach the atmosphere is confined to low geographic latitudes where energy flow into the atmosphere is small.

The TED was originally designed to operate in any one of three different modes in order to compensate for possible detector failures. However, the TED has thus far proven reliable. This fact, coupled with the additional data processing complexity in handling varying instrument modes of operation, led to the policy that the TED is operated only in its normal mode.

As a quality check on the operation of the TED, the counts during the first 1/13 second (background phase) of each sweep are accumulated for 16 sweeps - a total of 1.23 seconds. The accumulated count is transmitted once each 32 seconds in place of the normal transmission of ODE1, ODE3, ODE5, and ODE7. There are 4 such numbers abBK where $a = 0, 30$ and $b = E, P$ while BK means background. These numbers are generally less than 50. Should they exceed 200, detector malfunction may have occurred.

When analyzing TED data, take care in treating total energy flux values which exceed $100 \text{ ergs}/(\text{cm}^2 \cdot \text{s})$. Experience has shown that a high percentage of such data (~50%) are in fact associated with telemetry noise and do not represent valid observations.

3.5 TED Application

The TED instrument was included in the TIROS-N SEM to monitor the total energy fluxes carried to the atmosphere by energetic charged particles (energies between 0.3 keV and 20 keV). The purposes for doing so are twofold.

1. To provide a measure in near real time of the general level of particle precipitation activity. In this respect, it should be mentioned that the particles being measured are those that produce auroras. Thus the data provides a direct measure of the intensity and extent of the aurora beneath the track of the satellite and allows estimating the potential effects on radio communications and navigation equipment operating in the auroral zone. Several aspects of the data can be used to generate usable indices of activity. Among these are:

- a. The most equatorward latitude for which the energy flux exceeds a given value. This provides an index of the general level of activity.
- b. The maximum energy influx recorded during a given satellite pass. This is equivalent to a measure of the brightest aurora beneath the satellite.
- c. The latitude and longitude integrated total energy input. This value weights both the intensity and the extent of the energy input, and provides an estimate of global auroral activity.

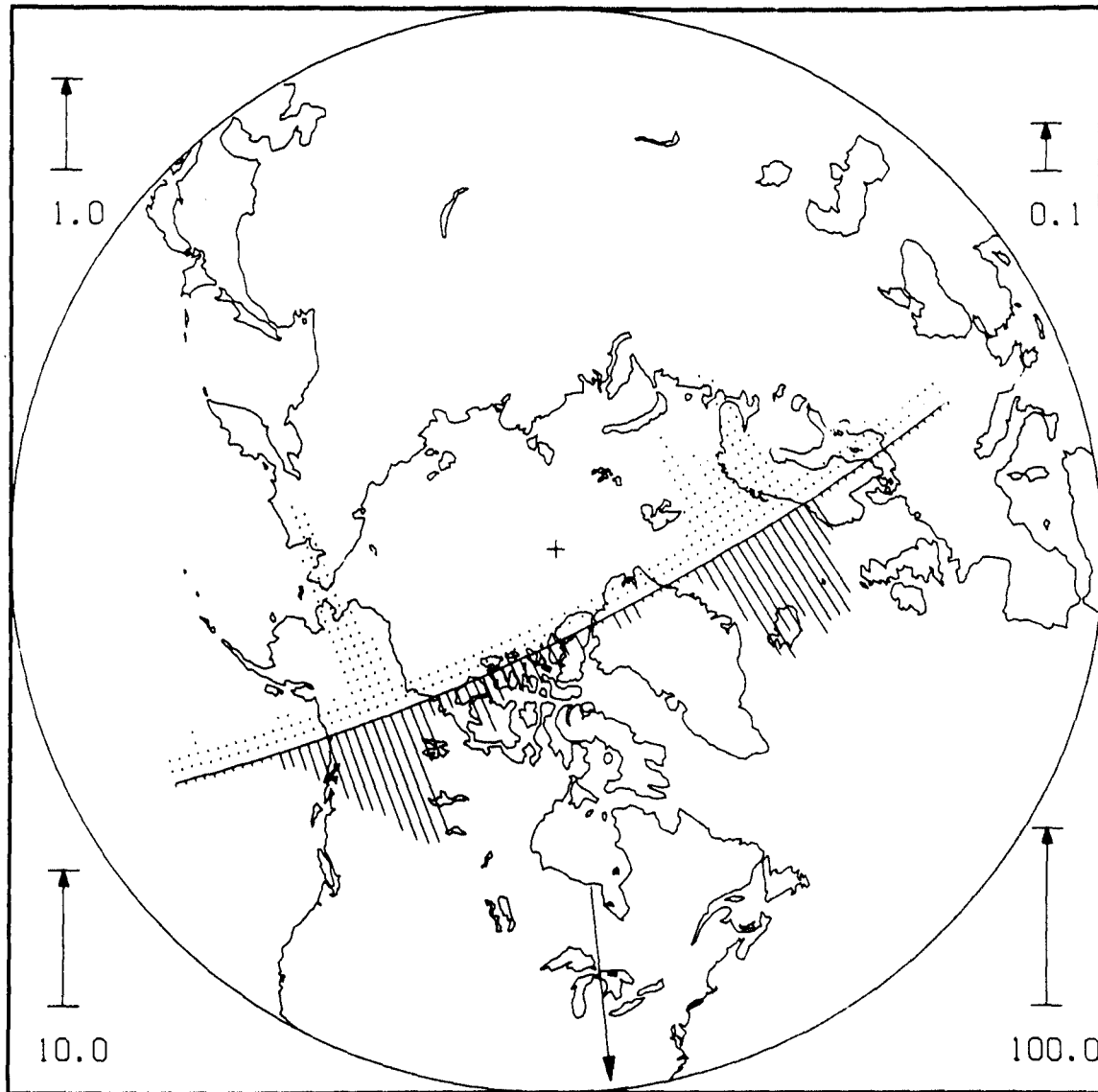
2. The second purpose of the instrument is to generate a data base useful to the study of the response of the upper atmosphere to the energy input from the magnetosphere. A measure of the energy input to the atmosphere above 100 km is useful (and relevant) for correlation with atmospheric data.

3.6 Data Displays for the TED

TED data may be displayed as a graph of the particle energy influx for a particular orbit, as shown in Figure 12. Such data may be used to estimate the total amount of particle energy being deposited into the entire auroral atmosphere. Figure 13 shows these power input estimates averaged over an entire day (about 29 satellite passes) for an entire month.

It should be pointed out that the power input due to particles is only 30% of the total power input to the atmosphere from magnetospheric processes. The rest comes from Joule heating caused by ionospheric currents driven from the magnetosphere. The total of both power inputs to the upper atmosphere often exceeds the energy input to the same altitude range from solar radiance.

NOAA-6
NORTHERN HEMISPHERE AURORAL PARTICLE ENERGY INFLUX
PASS STARTED AT 1736 UT ON 16 JAN, 1983 ENDED AT 1802



REFERENCE SCALES ARE IN UNITS OF ERGS/CM2/SEC

Figure 12

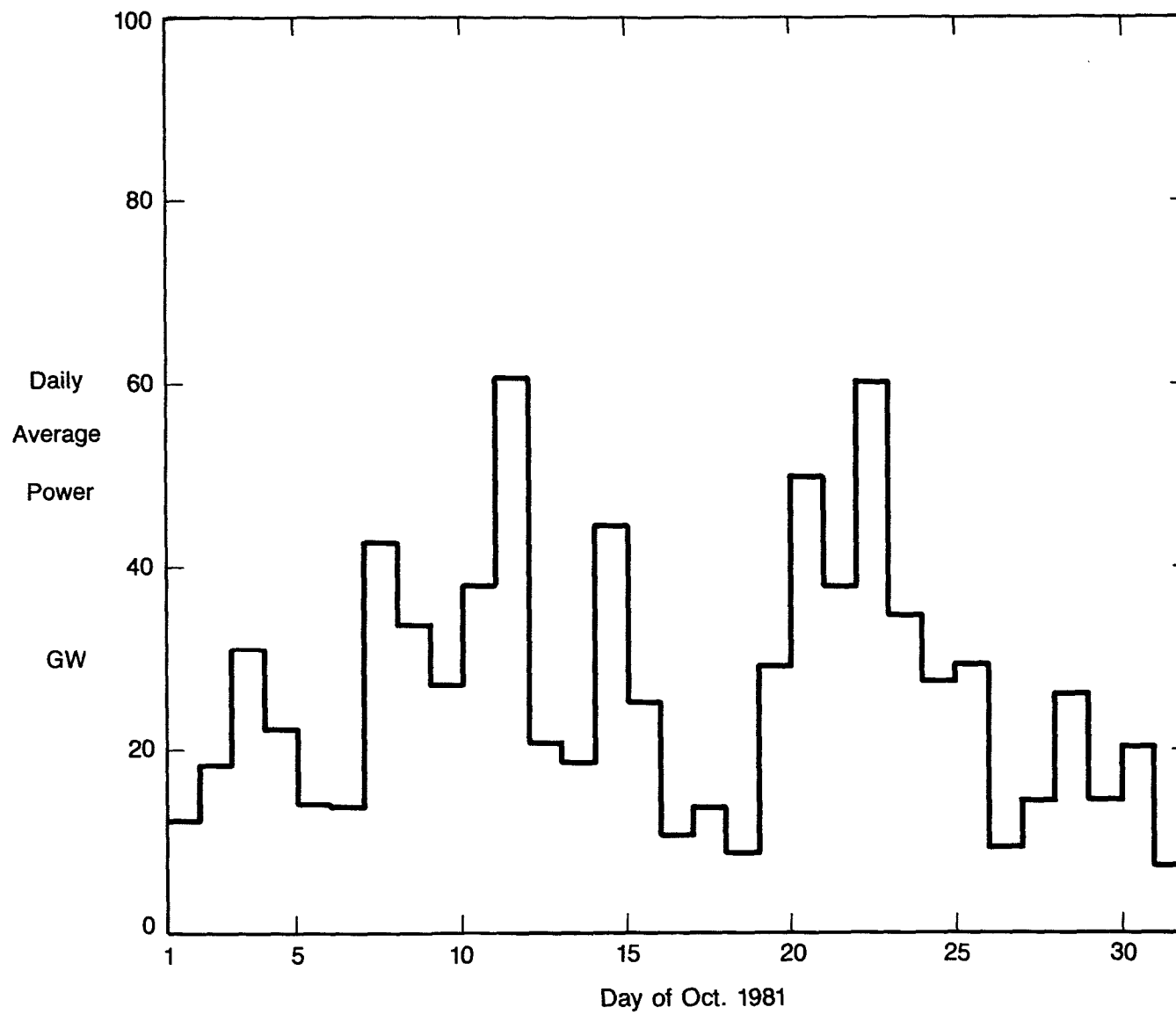


Figure 13.—Hemispherical Power Input

4. MEDIUM ENERGY PROTON AND ELECTRON DETECTOR (MEPED)

4.1 General Description

The MEPED uses solid-state silicon detectors to detect electrons, protons, and alpha particles over an energy range of >30 keV to >80 MeV. The silicon detectors are linear detectors which produce a quantity of charge directly proportional to the quantity of energy deposited in the active volume of the detector by an incident particle. This makes possible the energy analysis of the particle flux by analyzing the distribution of the charge pulses produced by the incident particles. A general view of the instrument is shown in Figure 14. Separate pairs of proton and electron "telescopes" are used, one pointing at approximately 0° to the magnetic field at high latitudes, the second of the pairs nominally perpendicular to the first.

In addition three simple sensors measure omnidirectional fluxes of higher energy protons. These use detectors in a dome moderator arrangement in which the energy threshold is basically defined by the energy loss in the shielding moderators.

A functional block diagram of the MEPED is shown in Figure 15.

Each detector has its own charge sensitive preamplifier. The output of each of the six preamps associated with the 0° and 90° telescopes are multiplexed into three signal chains consisting of linear amplifiers and pulse shaping networks which drive a set of pulse amplitude discriminators. The three high energy integral channels have individual, separate signal chains with only a single discriminator. These discriminators, either directly or in logical combination or in the case of the proton telescopes, after time coincidence gating and logical combination, produce logic level pulses for transmission to the DPU which correspond to the intensity of a given incident particle species in particular energy bands.

It is of interest to note that at the lowest threshold of this sensor, 30 keV, the linear signal electronics is detecting an event producing only 10^4 electrons at the input to the charge sensitive preamplifier.

The MEPED telescopes consist of four sensors, a pair of which view the local zenith and a pair of which "look" $\sim 90^\circ$ to this direction. Each pair of sensors consists of a proton telescope and an electron telescope. The zenith is the spacecraft -X axis as shown in Figure 3 and +Y is the direction of spacecraft velocity. The 90° sensors "look" nominally along the -Z axis. In order that the viewing cone of these sensors be unobstructed by a sunshade the collimator axes were rotated (around the Y axis) away from -Z toward -X by 7° and 9° for the electron and proton detectors respectively.

4.2 Proton Telescope

Each proton telescope responds to protons (actually to all positive ions) with energy >30 keV in five discrete energy intervals. Low energy electrons are removed by a broom magnet. Higher energy electrons and ions are discriminated against by anticoincidence logic between the two solid state detectors in the telescope. The proton telescope also identifies the intensity of ions with $Z \geq 2$ in one energy interval.

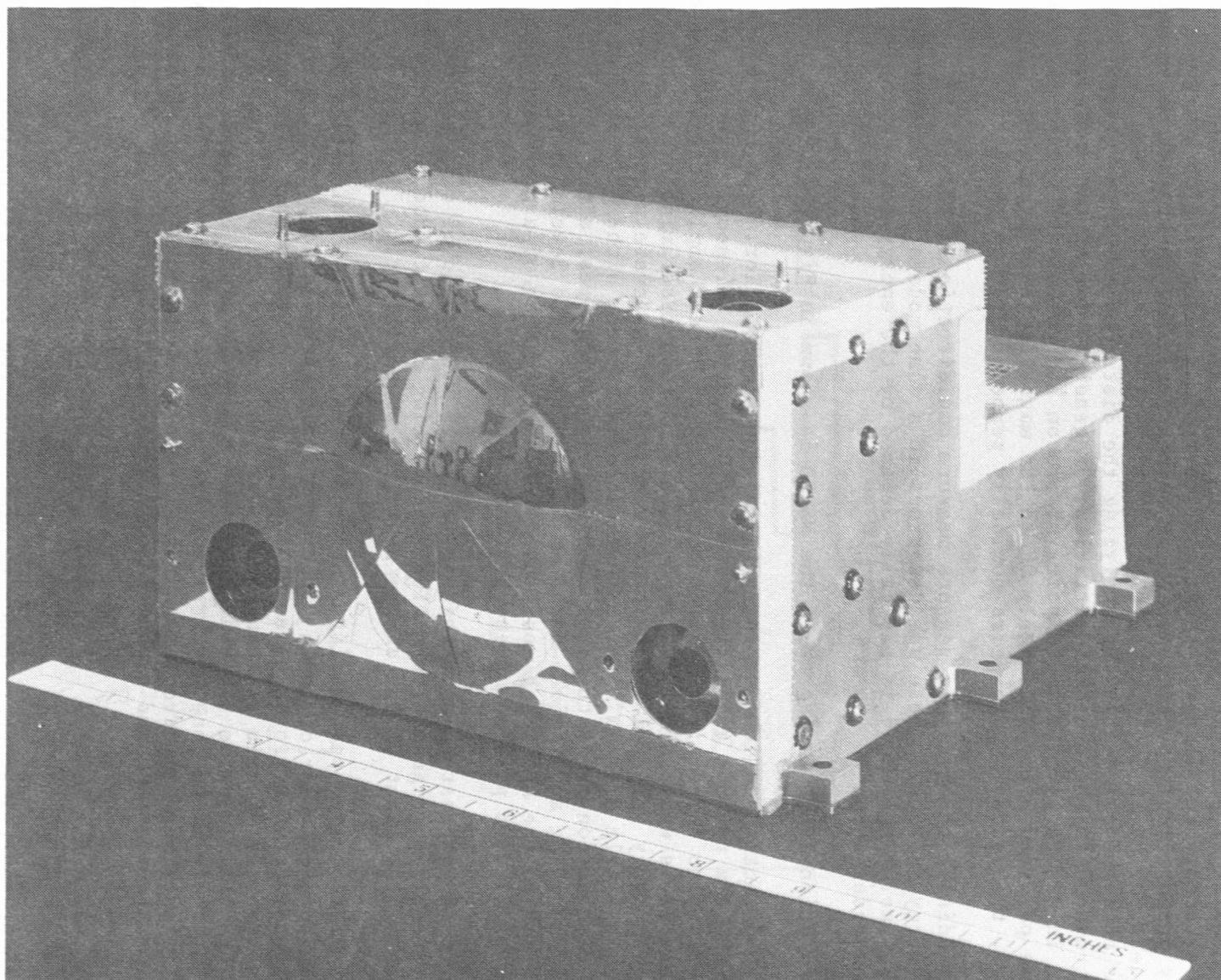


Figure 14.—Medium Energy Proton and Electron Detector

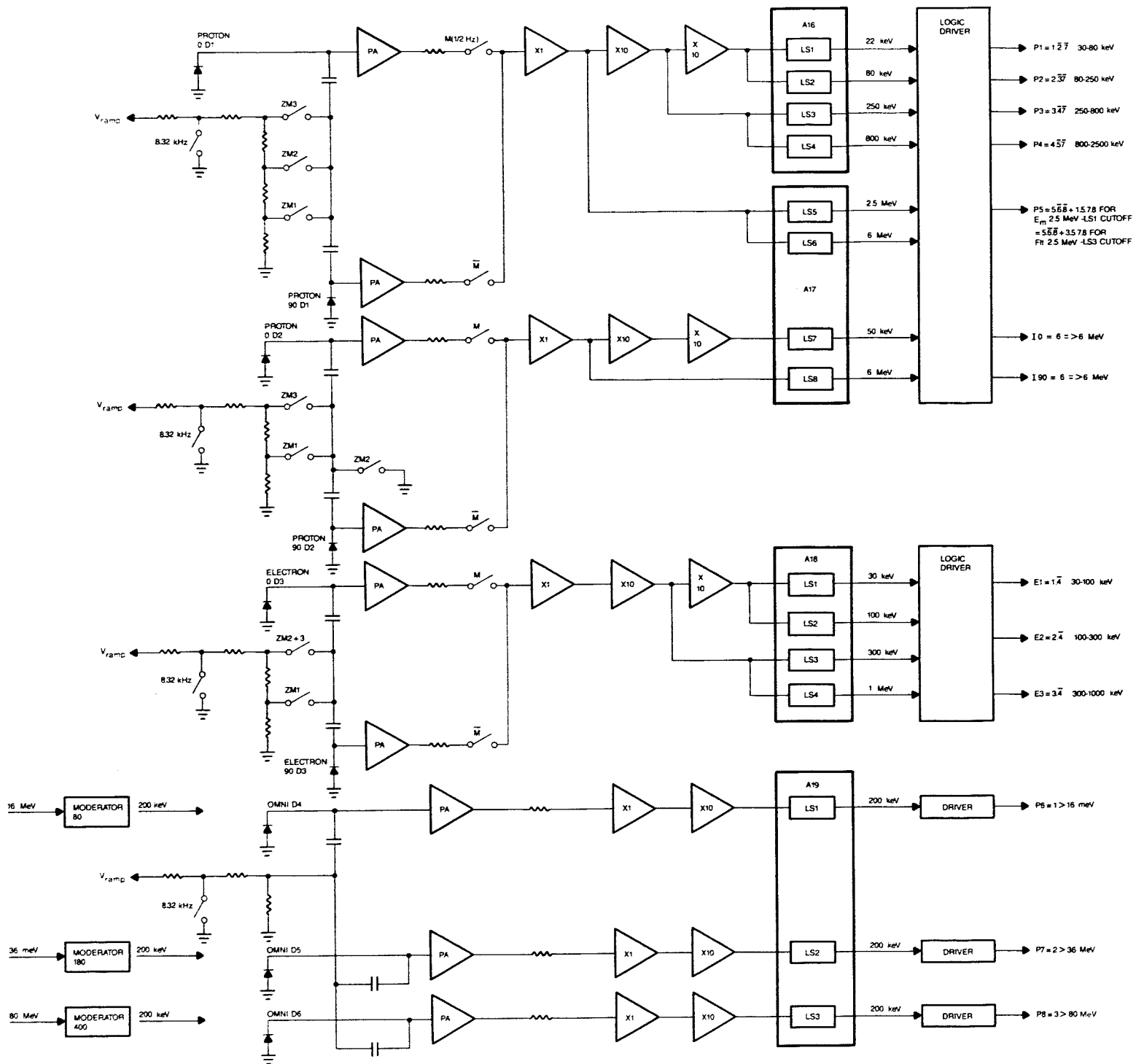


Figure 15.—MEPED Block Diagram

The broom magnet, made of Alnico VIII, has a strength of at least 2.48 kilogauss. No particle with a magnetic rigidity of less than 6200 gauss-cm (6.2 mT·m) can strike the detector (unless it scatters). This rigidity corresponds to an energy of 1.5 MeV for electrons and about 2 keV for protons. Electrons with energy below about 1.5 MeV are therefore prevented from contaminating the proton telescope response.

A proton with an energy of 30 keV has a radius of curvature of about 100 mm in the field of the broom magnet. Therefore the broom magnet significantly skews the view of the proton telescope for the lowest energy channel (30 - 80 keV) by about 10° .

The proton telescope, shown schematically in Figure 16, has a geometric factor of $9.5 \times 10^{-3} \text{ cm}^2 \cdot \text{sr}$. It consists of two 200 micrometer thick silicon surface barrier detectors. The front detector (D1) has an effective area of 25 mm^2 and is mounted with its ohmic (Aluminum) contact exposed to the incoming radiation. The second detector (D2) has an effective area of 50 mm^2 and is mounted with its gold (Au) contact forward. The detectors were procured from Ortec, Inc. with nominal $40 \mu\text{g}/\text{cm}^2$ Au contacts. The critical aluminum contact of the D1 detector was specified to be $18 \mu\text{g}/\text{cm}^2$ thick. As part of the SEM development, the uniformity and actual thickness of this contact was measured for all flight D1 detectors. The energy loss in the Al contact of each D1 detector as a function of incident ion energy was determined using a particle accelerator at NASA/GSFC. Figure 17 illustrates a representative result of these determinations. With knowledge of the electronic threshold it is possible to determine the proton telescope thresholds to an accuracy of 0.5 keV.

Each proton telescope measures ions in six energy passbands labelled P1 through P5 over the range 30 keV to $>2.5 \text{ MeV}$ and a channel I which is sensitive to $Z \geq 2$ ions with energy between 6 MeV and 55 MeV. The logic of the passbands is given in Figure 18. The identification of the detectors and the actual passbands are given in Table 4 for each satellite.

4.3 Electron Telescope

The electron telescope, which consists of a single detector mounted behind a thin nickel foil, responds to electrons with energy $>30 \text{ keV}$ and positive ions $>200 \text{ keV}$ in three integral energy channels. The true electron response can be calculated by subtracting the proton response determined by the proton telescope.

The electron telescope is shown schematically in Figure 19. It has the same geometric factor as the proton telescope, $9.5 \times 10^{-3} \text{ cm}^2 \cdot \text{sr}$. The detector is a 1700 micrometer thick, 25 mm^2 silicon surface barrier type. The system incorporates a thin nickel foil in front of the detector to reduce the proton contribution to the counting rate. These foils for TIROS-N were $0.696 \mu\text{m}$ (27.4 microinches) thick but the foils for subsequent satellites were reduced to an average value of $0.511 \mu\text{m}$ (20.1 microinches). There are three energy thresholds at nominal energies of 30 keV, 100 keV, and 300 keV. A fourth threshold was included at approximately 1 MeV, used as a veto signal to

Tiros Meped Proton Telescope

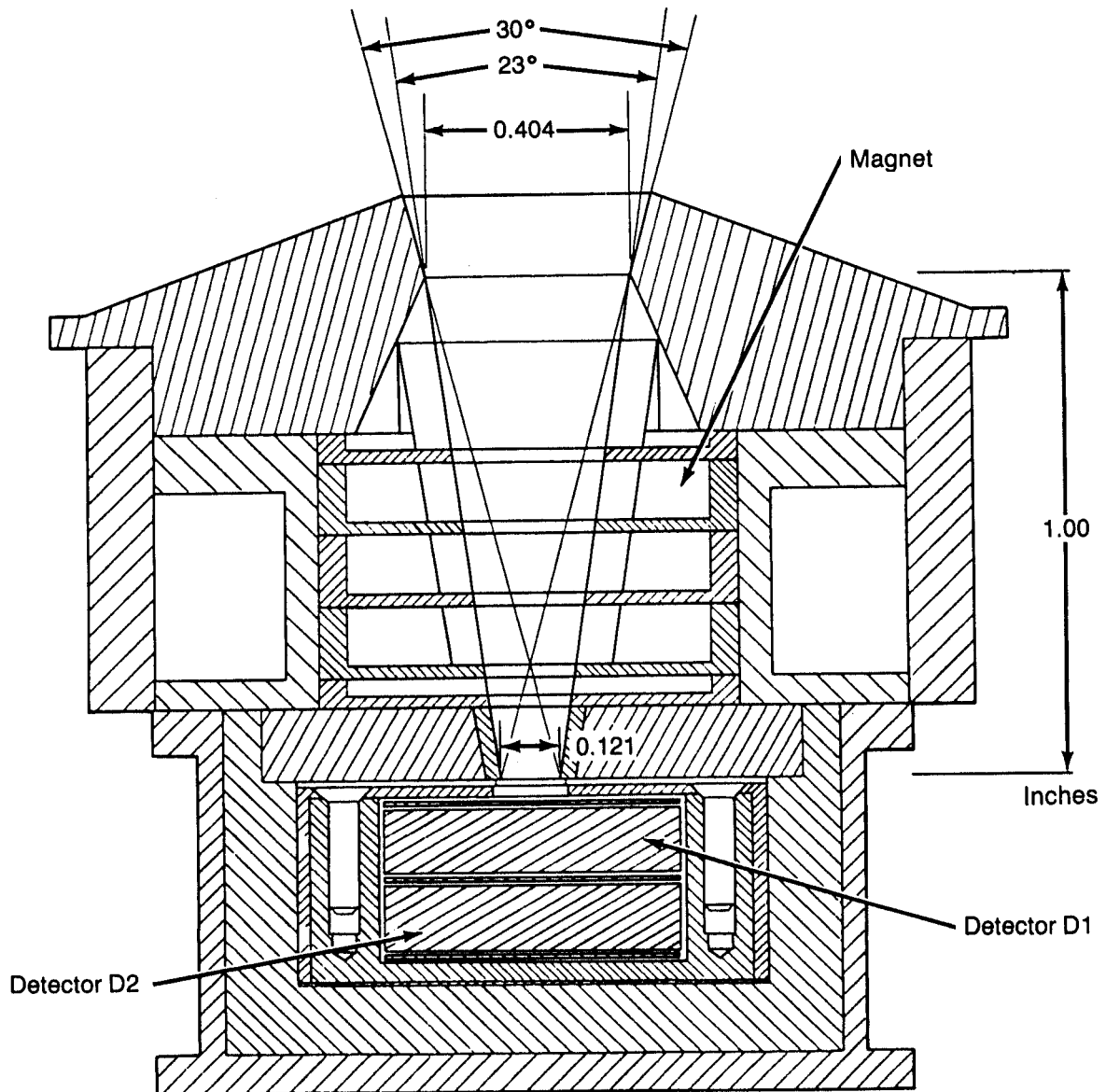


Figure 16.—MEPED Proton

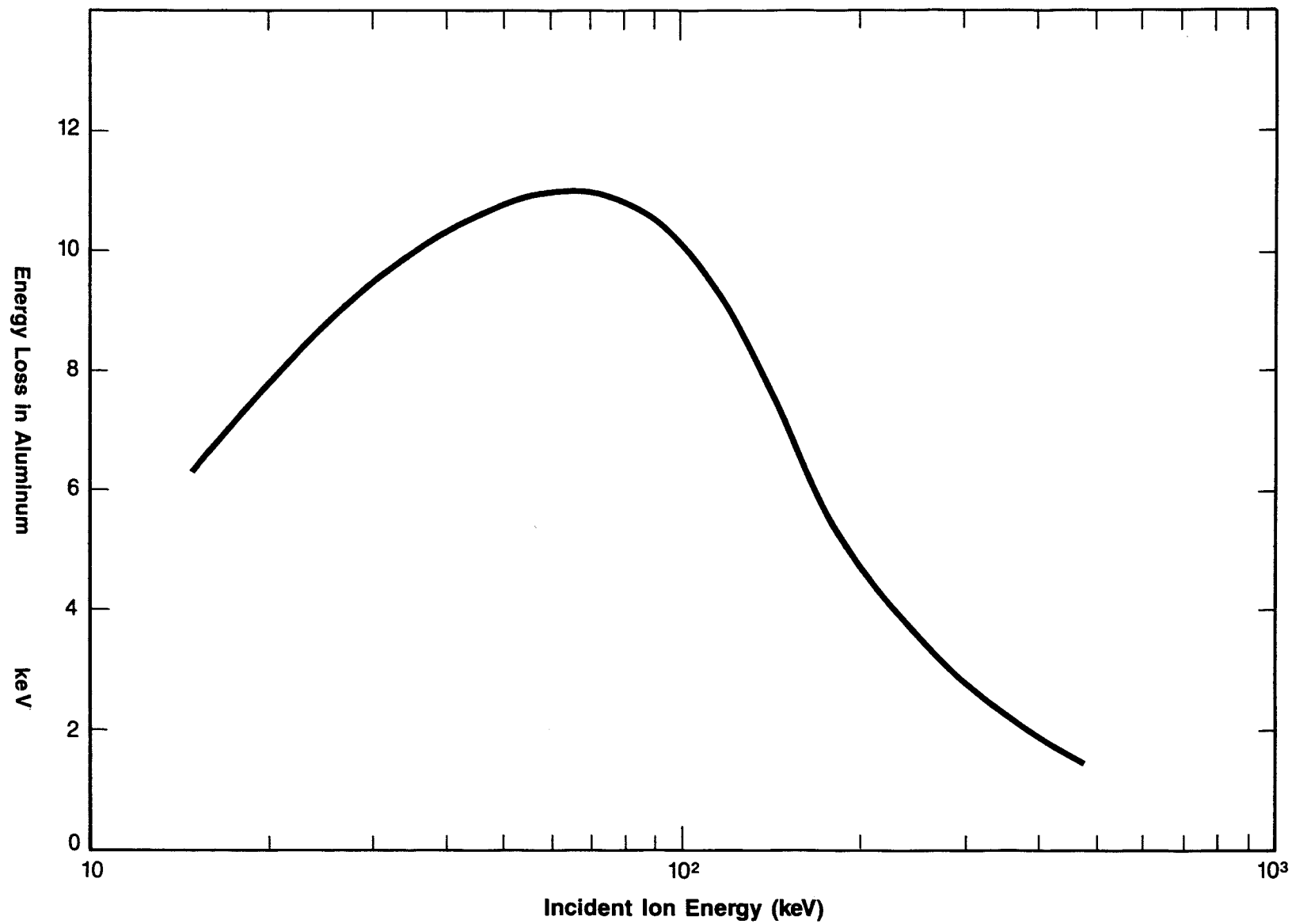
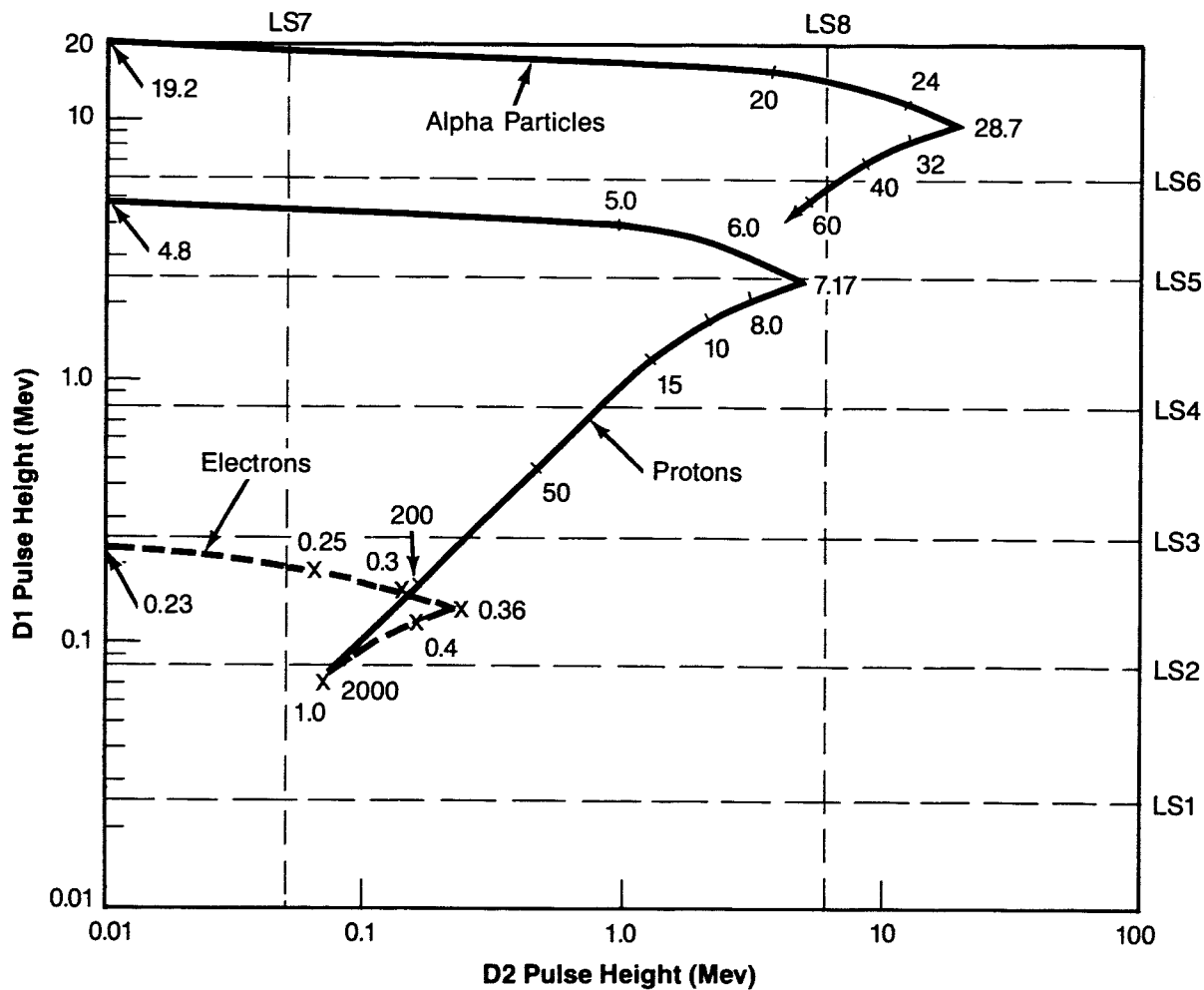


Figure 17.—Energy Loss in A1 Contact vs Incident Ion Energy



		25mm ²	50mm ²
		200μ	200μ
		→	
		Channel	LS Logic
PROTONS	30-80 Kev	1	$\bar{2}$ $\bar{7}$
	80-250	2	$\bar{3}$ $\bar{7}$
	250-800	3	$\bar{4}$ $\bar{7}$
	800-2500	4	$\bar{5}$ $\bar{7}$
	>2500	5	$\bar{6}$ $\bar{8}$ OR
IONS	> 6000	6	$\bar{5}$ $\bar{7}$ $\bar{8}$

Curves Labelled With
Particle Energy (Mev)

Figure 18.—MEPED Proton Telescope Response

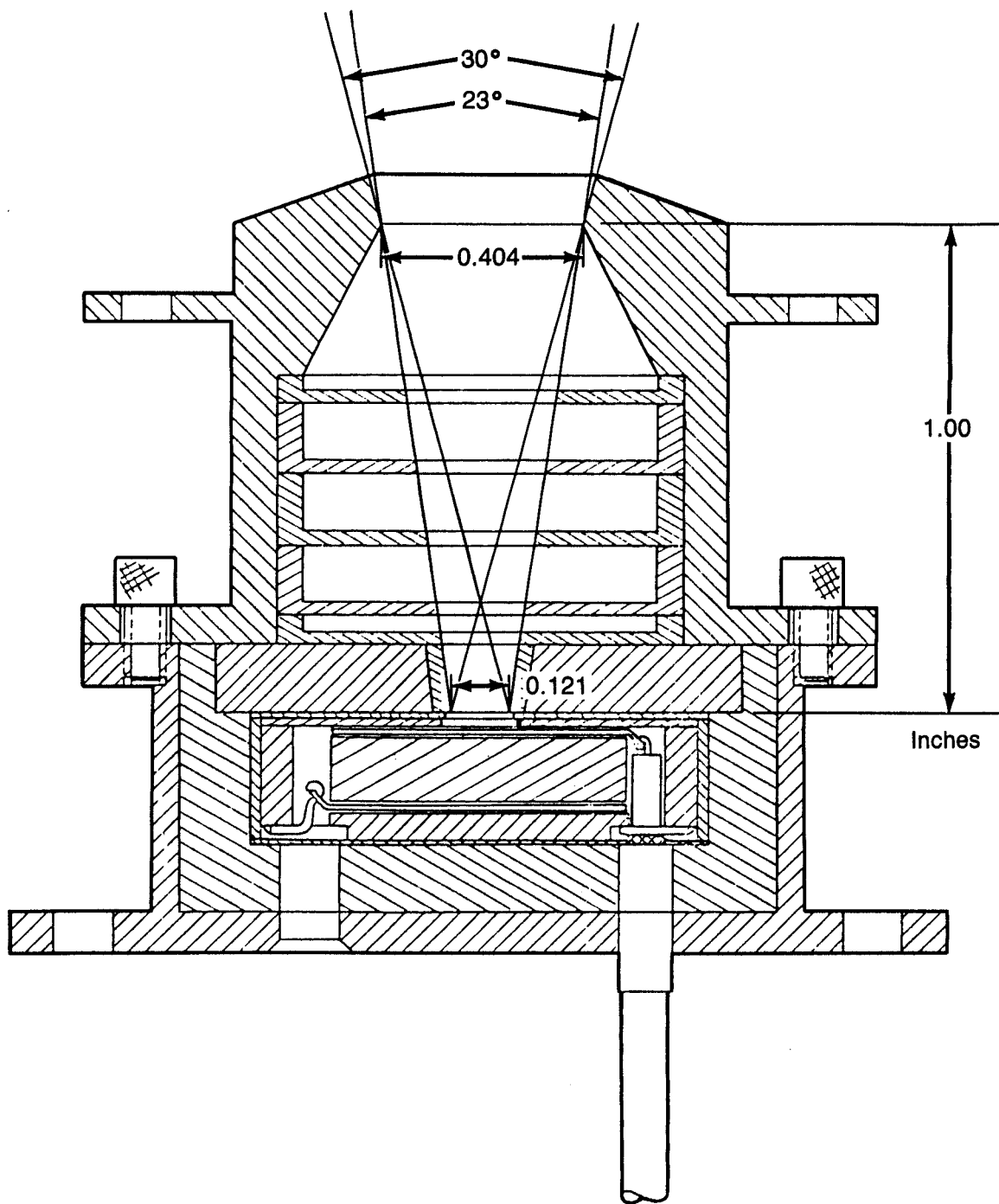


Figure 19.—MEPED Electron Telescope

effectively remove any sensitivity to protons above 1.1 MeV. Figure 20 presents the nominal pulse height response of the electron detector.

The actual thresholds for TIROS-N (0.696 μ m (27.4 microinch) Ni foil) were determined from electron beam calibrations, presented in Figure 21, using the accelerator facilities at NASA/GSFC. No detailed calibrations were performed on the subsequent satellite assemblies. The electron incident energy thresholds have been estimated by simply adding 5 keV to the electronic thresholds for the subsequent units. The actual thickness of the Ni-foils for NOAA-A and -B are not known but a nominal or average value for all foils was used to make the estimate. These thresholds are given in Table 3 along with the range of proton energies to which that channel is sensitive (enclosed in brackets).

TABLE 3. MEPED Detector Data and Passbands					
TIROS-N Protoflight Model					
D1	17-294E	17-294I	D3	17-097B	17-098D
D2	17-107E	17-108I	foil	27.4 microinch Ni	
P1	41.7-82.9keV	39.6-79.6 keV	E1(e)	>40 keV	>40 keV
P2	82.9-265	79.6-254	E1(p)	(177-1128)	(176-1119)
P3	265-860	254-820	E2	>107(262-1128)	>105(260-1119)
P4	860-2784	820-2655	E3	>322(453-1128)	>318(450-1119)
P5	>2.78 MeV	>2.66 MeV	I	6.32-(55) MeV	6.01-(55)MeV
NOAA-A Flight Model 2					
D1	17-102I	17-103E	D3	17-099C	17-098G
D2	17-108D	17-107F	foil ave	20.07 microinch Ni	
P1	30.6-82.6 keV	30.3-80.4 keV	E1(e)	>29	>29.2
P2	82.6-247	80.4-242	E1(p)	(135-1320)	(135-1320)
P3	247-853	242-834	E2	>117(230-1320)	>117(230-1320)
P4	853-2636	834-2579	E3	>350(445-1320)	>350(445-1320)
P5	>2.64 MeV	>2.58 MeV	I	6.94-(55) MeV	6.79-(55) MeV
NOAA-B Flight Model 1					
D1	17-103E	17-101G	D3	17-099F	17-717B
D2	12-122C	17-108A	foil ave	20.07 microinch Ni	
P1	32.9-83.7keV	32.5-81.6 keV	E1(e)	>28 keV	>28
P2	83.7-252	81.6-247	E1(p)	(135-1050)	(135-1040)
P3	252-813	247-801	E2	>105(220-1050)	>104(220-1040)
P4	813-2681	801-2649	E3	>317(415-1050)	>313(410-1040)
P5	>2.68 MeV	>2.65 MeV	I	6.08-(55) MeV	6.0-(55) MeV

D1,D2,D3 refer to the detectors. Serial numbers are listed.
P1, etc. refer to the output data channels from these detectors.

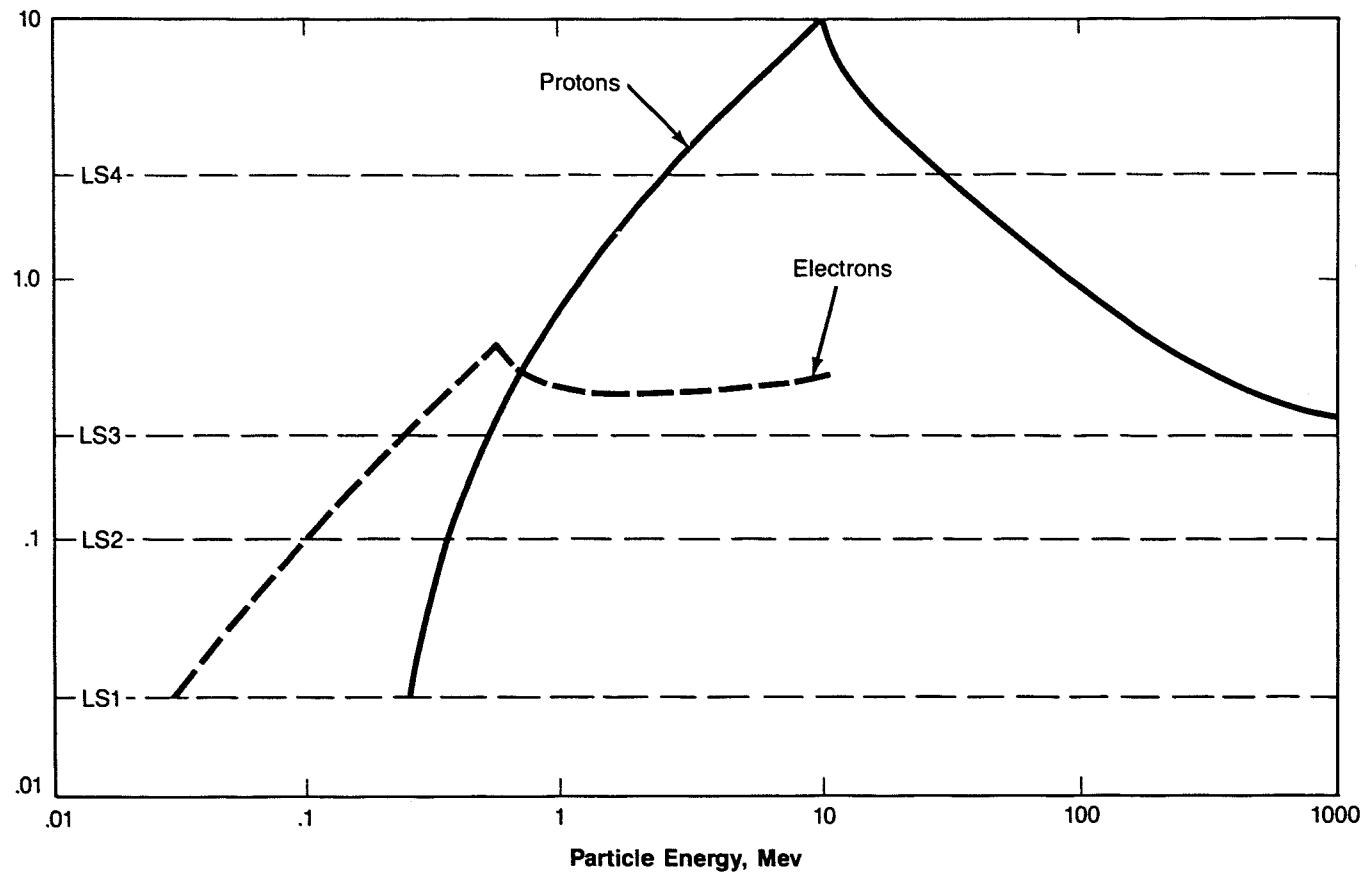


Figure 20.—MEPED Electron Detector Nominal Pulse Height Response

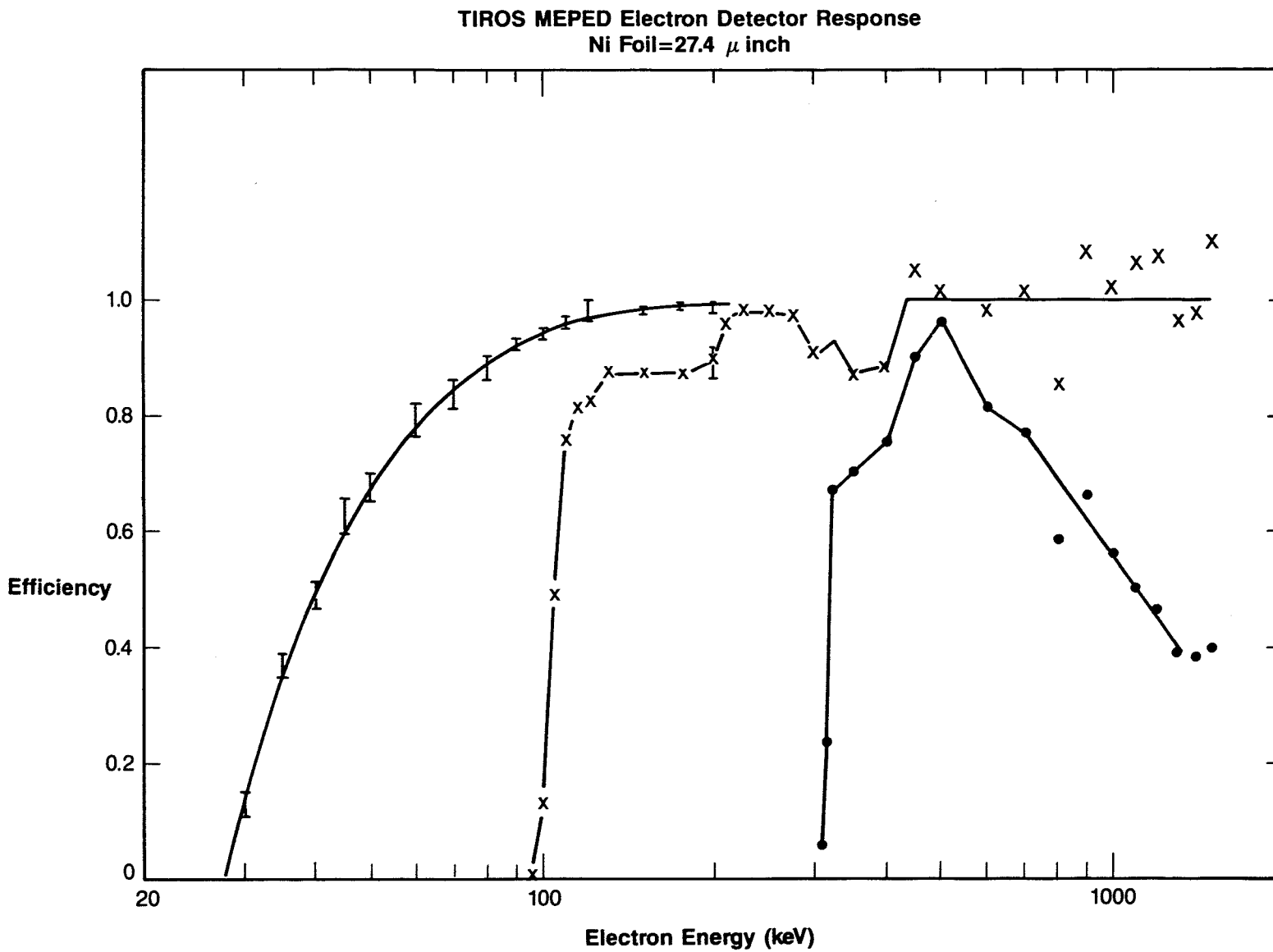


Figure 21.—MEPED Electron Detector Efficiency

4.4 Omnidirectional Sensors

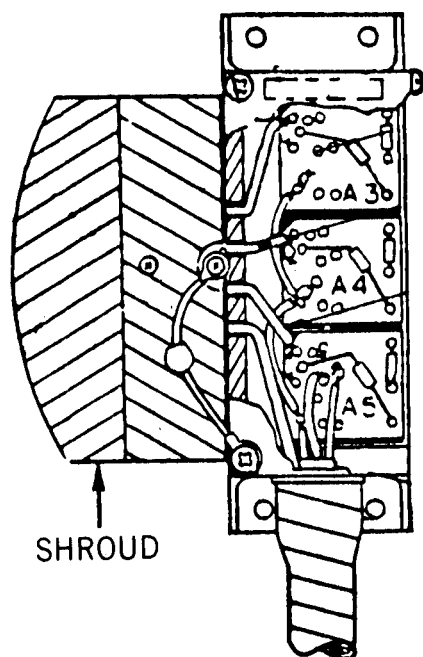
The MEPED omnidirectional sensors, essentially identical to units flown on the GOES-2 & -3 spacecraft, comprise three (3) nominally identical Kevex Si(Li) solid state detectors of 0.50 cm² area by 3 mm thickness, independently mounted under spherical shell moderators, domes, to provide measurements in three channels. The viewing angle of each of the detectors has a full opening angle of 120° in the zenithal direction as mounted. The pertinent data for the detectors are as follows:

TABLE 4. OMNIDIRECTIONAL PROTON SENSOR DATA						
Channel	Energy Band MeV	Area cm ²	Solid Ang. sr	Omnidirectional GEOM Factor * cm ²	Moderator Material	Thickness
P6	16- 80	0.50	1 pi	0.09375	Aluminum	.050 in.
	80-215	0.43	4 pi	0.215		1.27 mm
P7	36- 80	0.50	1 pi	0.09375	Copper	.230 in.
	80-215	0.43	4 pi	0.215		5.84 mm
P8	80-215	0.43	4 pi	0.215	Mallory	.086 in. 2.18 mm

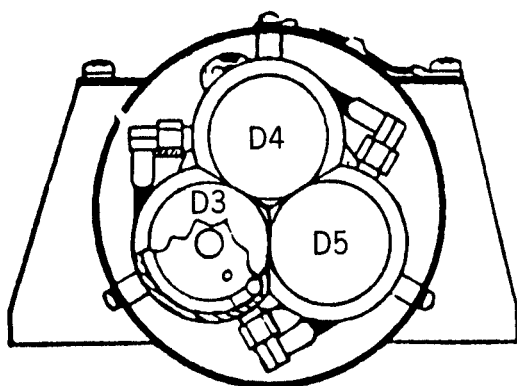
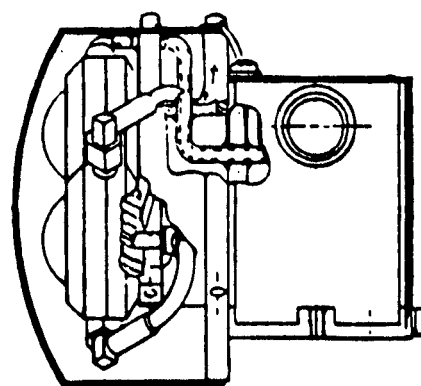
* The omnidirectional flux is defined as the flux through a unit cross section sphere; Flux = Counts/omni GEOM factor.

The overall shielding of the instrument stops protons of less than 80 MeV. Therefore the detectors respond to protons of energy >80 MeV over the entire 4 pi solid angle as indicated above. The effective solid angle of the flight units will of course be somewhat less, determined by the shielding provided by the satellite body itself. Because of the usual relatively steep spectrum for both galactic and solar cosmic rays, the counting rates of the 16-80 MeV and 36-80 MeV channels are not severely compromised by the >80 MeV background. However, the response of the 80-215 MeV detector will be uncertain to a factor of the order of two.

Calibration of the omnidirectional detectors was performed using a uniform axial proton beam, at the Harvard University Cyclotron Facility, which confirmed the detector thresholds. Figure 22 is a diagram of the detector.



SIDE VIEWS



"KEVEX"
Si (Li)
DETECTOR 3 PLACES

D3 = ALUMINUM DOME
D4 = COPPER DOME
D5 = TUNGSTEN DOME

DOME DETECTORS

Figure 22.—Omnidirectional Spectrometer

4.5 MEPED Application

The principal operational use of the particle detectors comprising the MEPED is the reliable and accurate determination of the flux and spectrum of energetic particle fluxes produced by the sun during solar disturbance events. These energetic particles, mostly protons in the energy range of some tens of kilovolts to, in major events, greater than a billion electron volts, produce additional ionization of the Earth's upper atmosphere and ionosphere which has substantial consequences on radio propagation. The particles themselves and their atmospheric secondaries may in extreme cases pose a significant radiation hazard to high flying aircraft and to those engaged in extra-terrestrial activities. These data therefore provide an important input to the data base of the Space Environment Services Center for real time analysis and distribution to their interested customers.

MEPED data are an important information source for validation of photochemical models of the stratosphere and ionosphere. Crutzen et al, 1975, have determined that the additional production of nitric oxide (NO) in the stratosphere by large solar proton events produces substantial reductions in the earth's stratospheric ozone concentration. Nitric oxide, through several coupled catalytic reactions, is efficient in removing ozone from the atmosphere. Atmospheric ozone is important in screening us from a large portion of the sun's damaging ultraviolet radiation.

Additionally, however, the lower energy protons and electrons detected by the MEPED can provide information on the state of, and dynamical processes occurring within, the magnetosphere. Many questions still exist concerning the entry of solar particles into the magnetosphere and the subsequent processes which act upon them. Low energy protons are more sensitive to the properties of the geomagnetic field and the electromagnetic processes they are subject to. The lowest energy threshold of the MEPED has been reduced to 42 keV (in NOAA-A) in channel P1 from the 270 keV threshold of the monitors aboard the previous TIROS series. Subsequent S/C will have 30 keV. This reduction of minimum threshold enhances the tracer use of solar protons.

In the early part of at least some solar cosmic ray events, an asymmetry has been observed between the fluxes seen over the northern and southern polar caps. In comparison with corresponding measurement of the particle fluxes outside the magnetosphere, this asymmetry supports the hypothesis that the interplanetary magnetic field is interconnected with the polar field of the earth. The sense of the connection depends on the direction of the interplanetary field, whether toward or away from the sun. In this manner, observation of solar protons over the polar caps says something about the topology of the geomagnetic fields at high latitudes as well as about the mean orientation of the interplanetary field. Further, solar protons of a given energy have essentially free access to the polar caps of the Earth to some minimum geomagnetic latitude which is dependent upon energy, the so-called cutoff latitude. The cutoff latitude for a given energy is dependent on the local time, an expression of the longitudinal asymmetry of the magnetospheric fields, and is dependent as well on the geomagnetic disturbance level of the magnetospheric fields. A better understanding of the behavior of solar

protons will help define the dynamical changes in the topology of the magnetic field of the earth.

Figure 23 shows data from a portion of one revolution of NOAA-8 in which the satellite went through the auroral zone. The base lines (where log count = 0) are each offset by 10. Longer-term observations are shown in Sauer 1984.

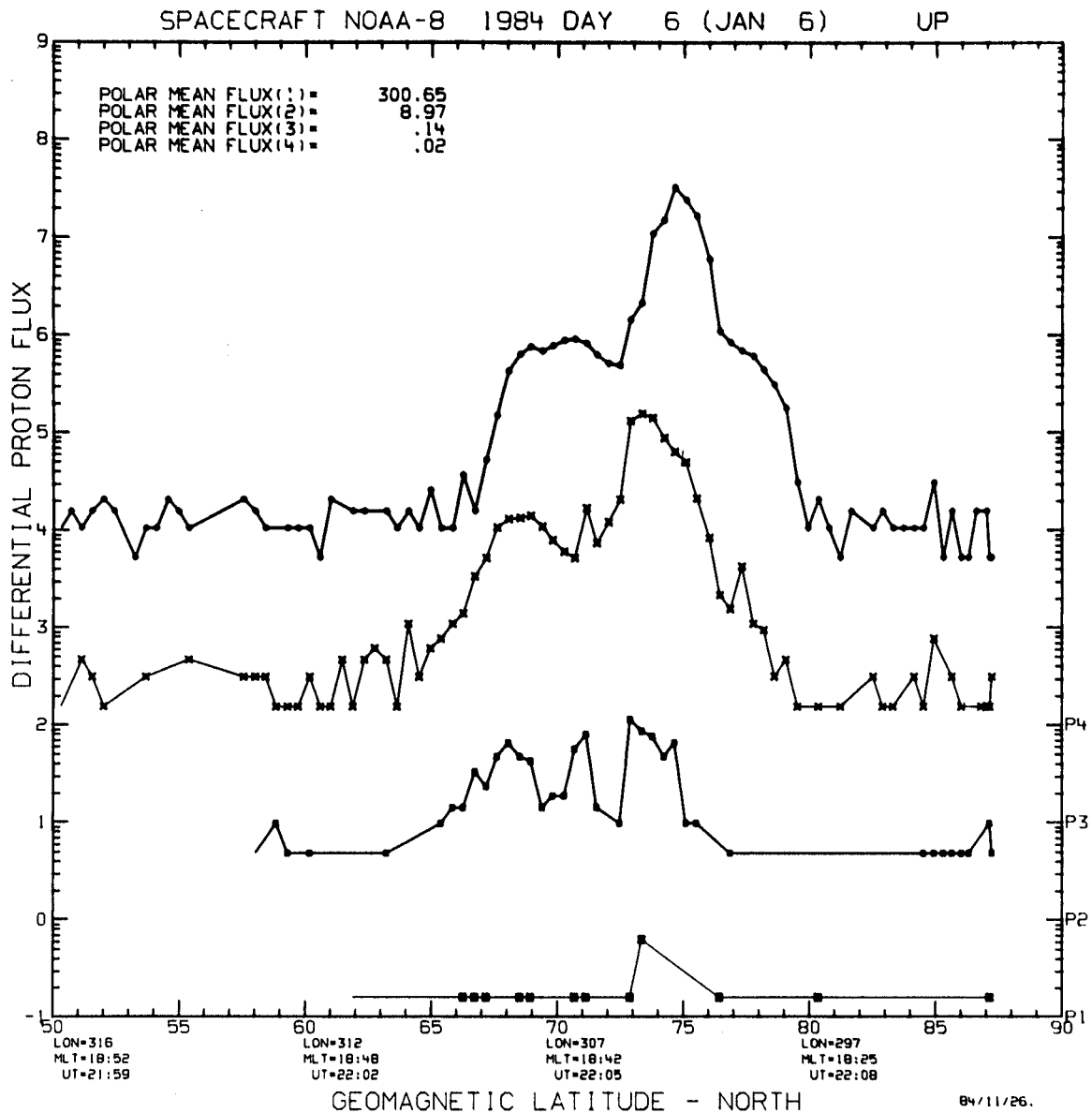


Figure 23.—MEPED Data

5. HIGH ENERGY PROTON AND ALPHA DETECTOR (HEPAD)

5.1 General Description

The HEPAD uses Cerenkov light to detect protons with energy above 370 MeV and alpha particles with energy above 640 MeV. Cerenkov radiation of light occurs when an incident particle travels at greater than the local speed of light in a high-refractive-index material. The material chosen in this case is fused silica. The light is collected by total internal reflection at the boundaries of the material and detected by a Photo Multiplier Tube (PMT) whose faceplate is integral with one end of the material.

Figure 24 shows a view of the HEPAD. A block diagram of the HEPAD is shown in Figure 25. Figure 26 shows the overall arrangement of the sensor which is a 3-element telescope.

Each particle event must provide a fast triple time coincidence between the two front solid-state detectors and the PMT. The three detectors define the solid angle of the response. Directionality forward or backward is determined by the shape of the material and the character of the Cerenkov light emitted preferentially in the same direction as the particle travel. The geometric factor of the telescope acceptance aperture is $\sim 0.9 \text{ cm}^2 \cdot \text{sr}$ with a half-angle field of view of $\sim 24^\circ$. Spectral intensity data is telemetered at a rate of one sample every four seconds. Events are sorted for energy and discriminated as protons or alpha particles on the basis of the detector outputs.

As high event rates may occur in any of the individual detectors due to energetic electrons which can penetrate the instrument shielding, the "single" and "double coincidence" counting rates from the solid-state detectors are also telemetered.

Energy measurement is obtained from the number of photoelectrons produced at the PMT photocathode by each event. This PMT output is a nonlinear function of the energy deposited by the incident particle. Because it is a function of secondary emission efficiency and a very rapid function of accelerating voltage the PMT gain must be controlled to maintain calibration. This is done by incorporating a small radioactive isotope scintillator light "pulser" which provides a reference number of photoelectrons which can be monitored on the ground. The PMT overall voltage, and therefore gain, can be adjusted as needed.

5.2 HEPAD Operation

The HEPAD outputs are listed in Table 5.

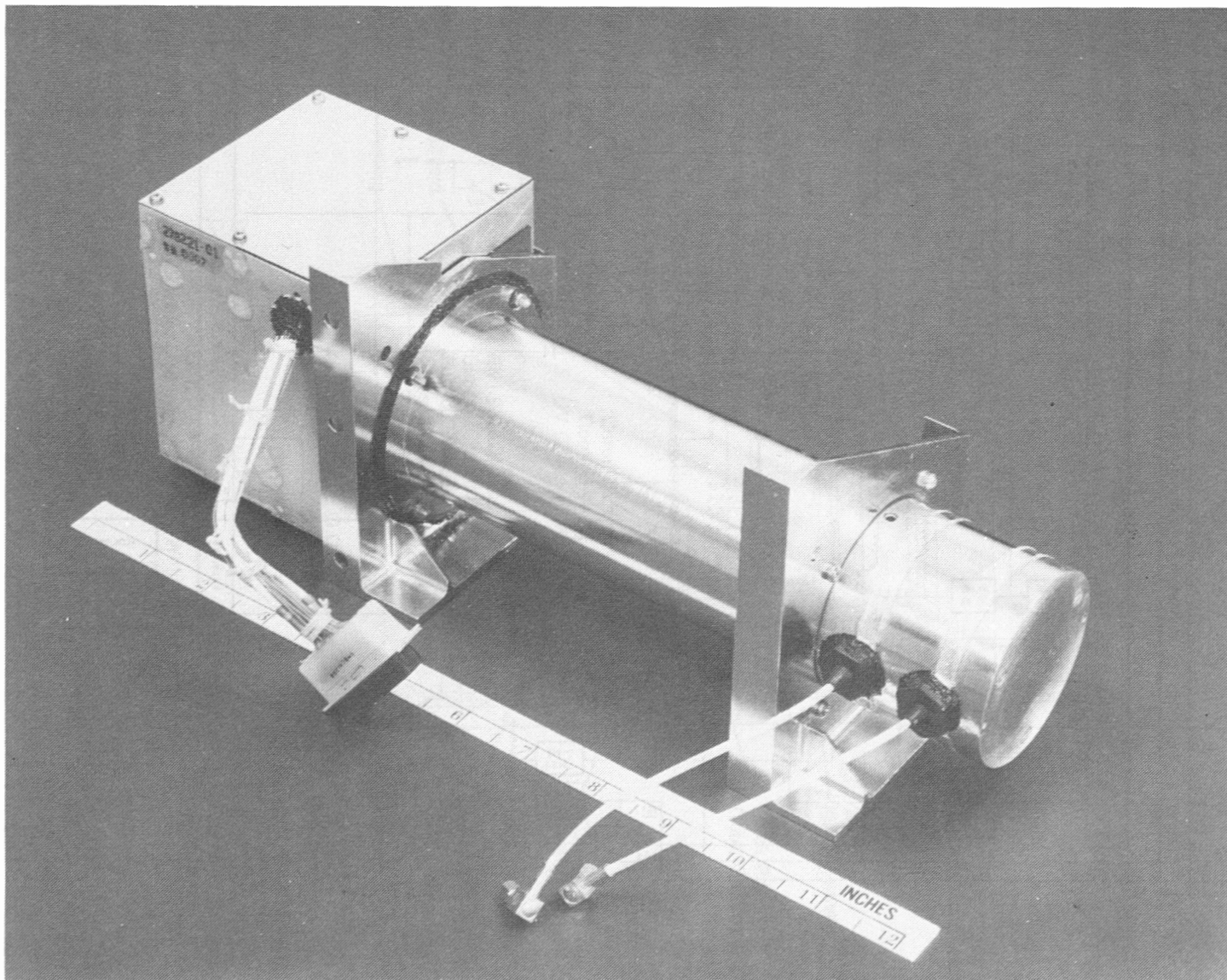


Figure 24.—High Energy Proton and Alpha Detector

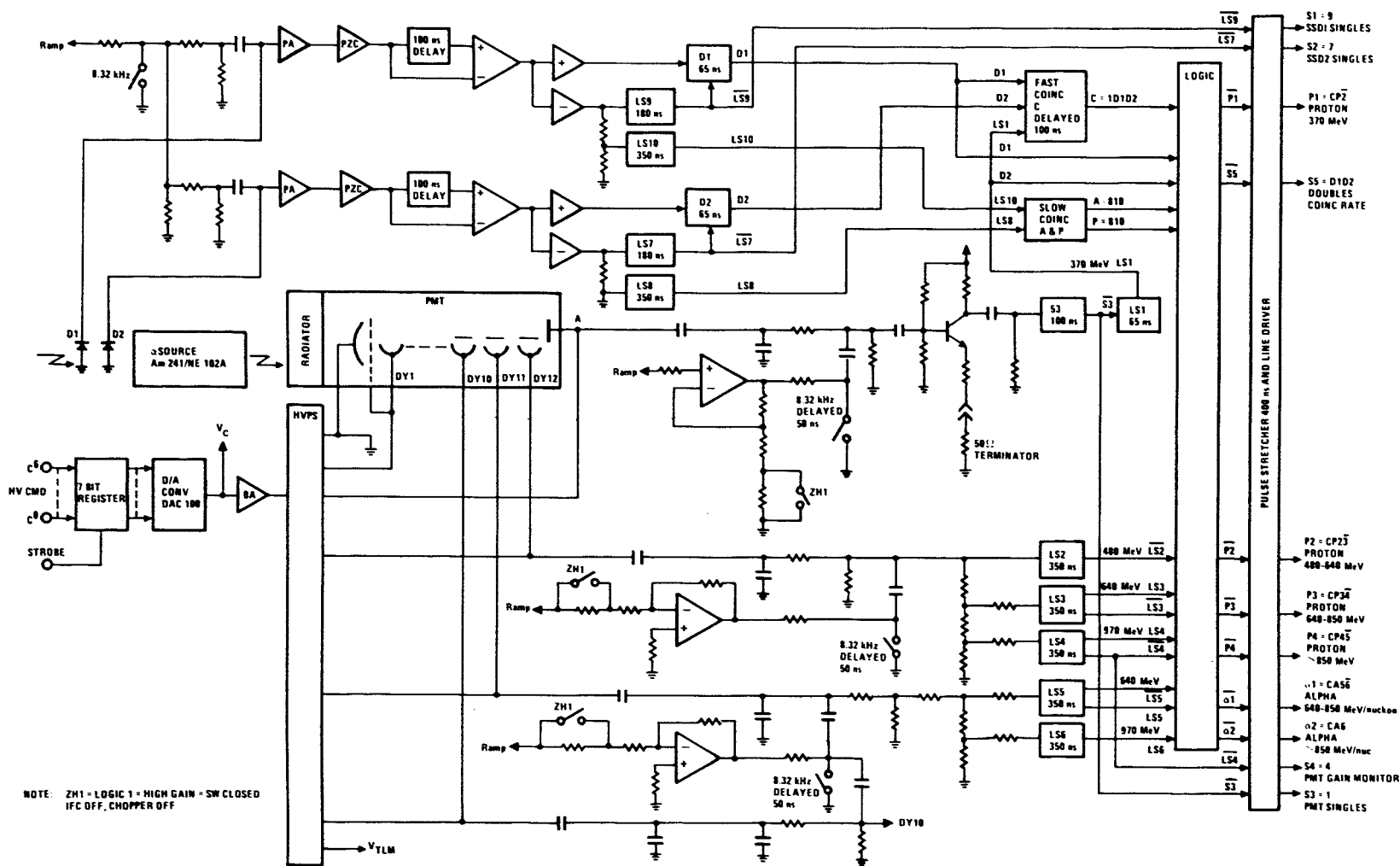
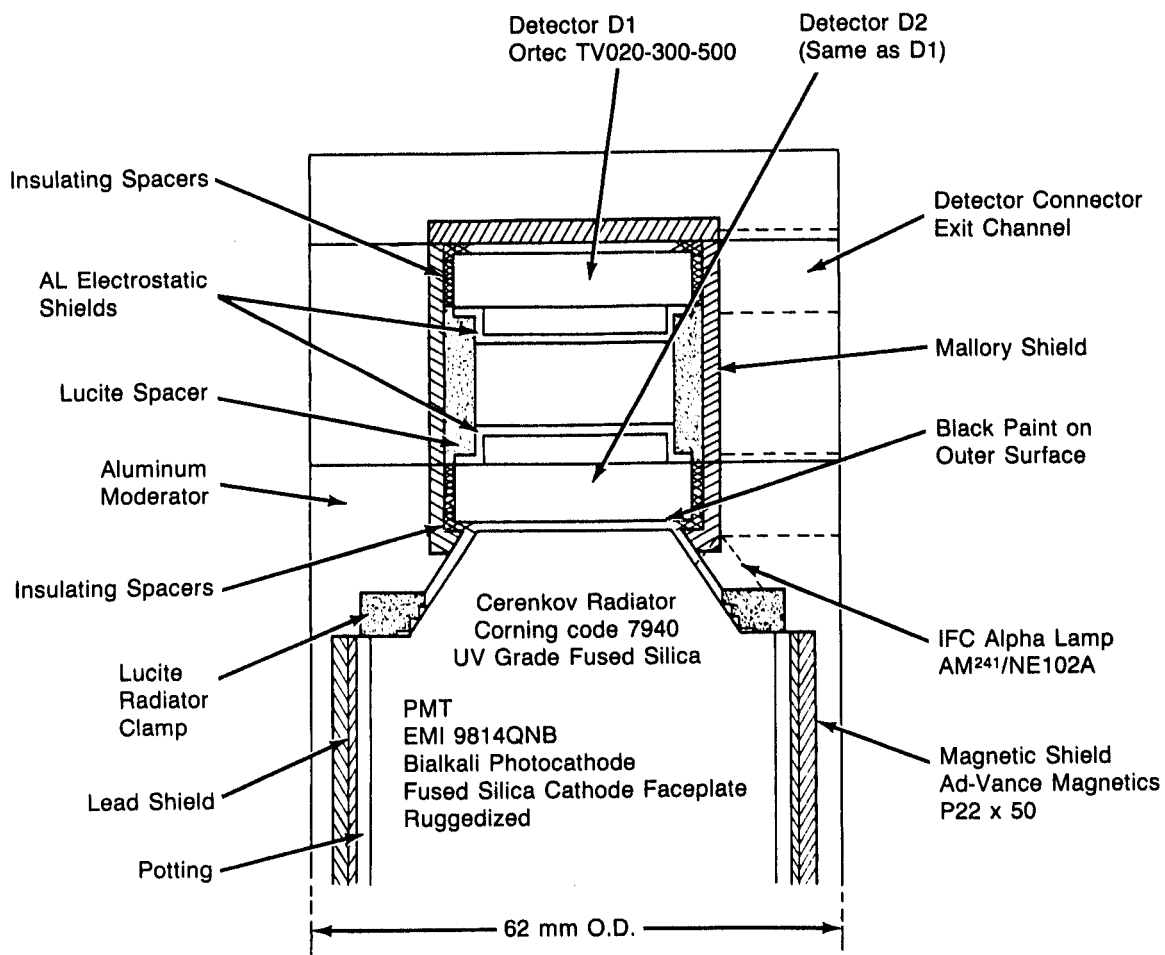


Figure 25.—HEPAD Block Diagram



Detector Area: 3 cm²
 Detector Separation: 2.9 cm
 Geometric Factor: $G \sim 0.9 \text{ cm}^2\text{-STER}$
 Acceptance Aperture: 68% of G Within $\leq 24^\circ$ Half-Angle
 100% of G Within $\leq 34^\circ$ Half-Angle

Figure 26.—HEPAD Telescope Assembly

TABLE 5. HEPAD OUTPUTS			
Data Channel	Observable	Count Interval (Nominal)	Nominal Max. Random Rate pps
P1	Protons 370-490 Mev	4 s	620
P2	" 490-620 "	"	420
P3	" 620-850 "	"	260
P4	" >850 "	"	260
A1	Alphas 640-875 Mev/nucleon	"	80
A2	" >875 MeV/nucleon	"	85
S1	SSD #1 Singles LS #9	94 ms	1.8×10^5
S2	SSD #2 Singles LS #7	"	1.6×10^5
S3	PMT Singles LS #1	"	5.6×10^4
S4	PMT Gain Monitor LS #4	2.5 s	2.0×10^3
S5	SSD #1, #2 Double Coincidences	1.2 s	2.0×10^4

S1-3 identify events exceeding the most sensitive pulse height (LS) thresholds associated with the two SSDs and the PMT, while S5 identifies time coincident events in the two SSDs which exceed these thresholds. S4 identifies the PMT events produced by the radioactive "pulser", all of which exceed the fourth PMT LS threshold.

The accuracies of the measurements and the boundaries of the corresponding energy bands are better than 20% in the following environments:

- a. Large hard solar proton event

$$J(>E) = 5.4 \times 10^5 e^{-E/5.8} \text{ protons}/(\text{cm}^2 \cdot \text{s}) \text{ isotropic}$$

- b. Large soft solar proton event

$$J(>E) = 1.6 \times 10^7 e^{-P/31} \text{ protons}/(\text{cm}^2 \cdot \text{s}) \text{ isotropic}$$

$$P = (E^2 + 1876E)^{1/2}$$

- c. Electron background

$$dJ/dE = 4 \times 10^3 E^{-3.3} \text{ electrons}/(\text{cm}^2 \cdot \text{s} \cdot \text{sr} \cdot \text{MeV})$$

where E represents particle energy in MeV.

Figure 26 shows the HEPAD telescope assembly. Two SSD surface barrier silicon detectors D1 and D2 (area 3 cm^2 , thickness $500 \mu\text{m}$, totally depleted) define an acceptance aperture of $\sim 24^\circ$ half-angle or geometric factor $\sim 0.9 \text{ cm}^2 \cdot \text{sr}$. All linear trajectories passing through these detectors also pass through the conical fused silica radiator (special PMT faceplate) which has an average thickness of $\sim 17 \text{ mm}$. For an isotropic environment, the probability distribution of path lengths in the conical radiator has a mean value of 1.05 times the average thickness so that the average Cerenkov radiation amplitude

should correspond to traversal of ~ 18 mm of silica. Silica is employed as the radiator to provide the desired proton energy threshold (~ 320 MeV) and to allow efficient transmission of the shorter wavelengths of the Cerenkov light (cutoff ~ 190 nm). Most of the area of the radiator's conical surface is bare to allow total internal reflection of incident Cerenkov light from all trajectories within the acceptance cone. Assuming an average quantum efficiency of 18% and full light collection efficiency within the 200–450 nm interval, 225 photoelectrons should be produced by axial protons of $\beta \approx 1$ where β is v/c .

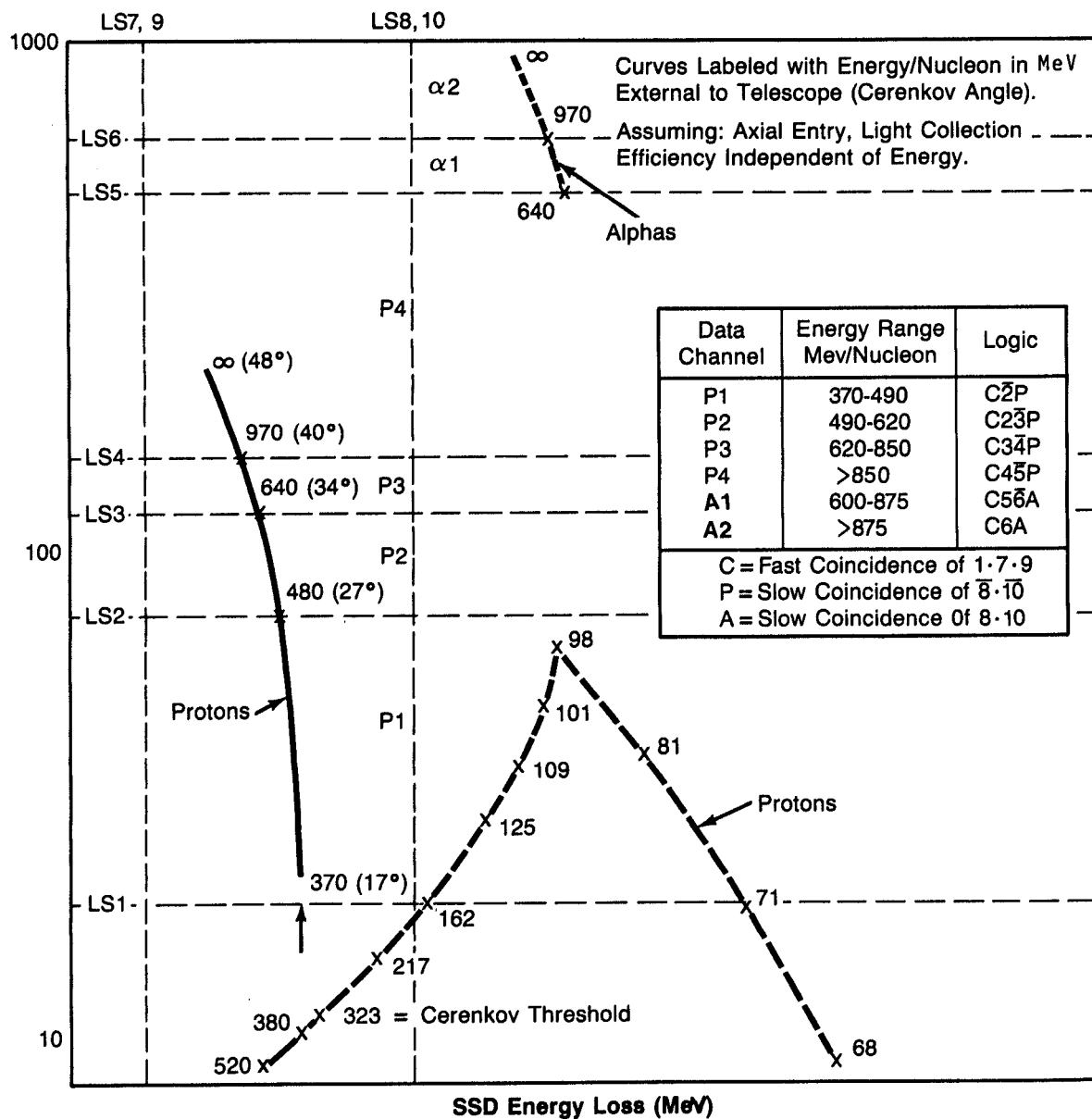
Mallory metal (high-Z) is employed to shield the detectors against bremsstrahlung generated by ambient electrons (thickness is one absorption length for $E < 350$ keV). Similarly, aluminum moderator (low-Z) is employed to shield these detectors against ambient electrons and protons and to suppress the bremsstrahlung radiated by the stopping electrons. Within the out-of-aperture solid angle, the moderator will stop protons of < 80 MeV and electrons of < 7 MeV. For in-aperture directions, the shielding is effective against protons of < 65 MeV and electrons of < 4 MeV and will absorb ~ 15 MeV from a 370 MeV proton. Shielding of the detectors from "upward"-entering protons of $E < 90$ MeV is supplied by the silica radiator and the magnetic shield, lead shield, and aluminum shell surrounding the PMT.

The Lucite spacer (see [Figure 26](#)) is used to position the detectors in the assembly, while insulating spacers prevent motion of the detector holders in a vibration environment and isolate signal ground (detector shell) from chassis ground. Similarly, the Lucite radiator positions the PMT with respect to the SSD, while contacting only a very small fraction of the radiator area. The aluminum electrostatic shields protect the inner, biased surfaces of the SSDs from EMI capacitively coupled from the structure. To allow monitoring of the PMT quantum efficiency and gain during operation, an Am^{241} radioactive source (5–10 nanocuries) coupled to an NE102A plastic scintillator (thickness $76 \mu\text{m}$ (0.003"), area 3×3 mm) is positioned near the conical wall of the silica radiator to illuminate the entire photocathode with fast light pulses of chosen amplitude ($\sim 30\%$ FWHM). The upbeam surface of the silica radiator is blackened to reduce the light collection efficiency for "upward-moving" particle trajectories which intersect D1 and D2.

5.3 Response to Radiation

[Figure 27](#) shows the nominal response of the silicon detectors and PMT to protons and alphas. The abscissa shows the energy lost in each silicon detector, while the ordinate shows either the number of photoelectrons produced in the PMT (solid curves) or the ionization energy loss in silica (dashed curve). The solid line trajectory for protons above 370 MeV is confined within the 125–500 keV abscissa range and the 21–500 photoelectron ordinate range, while the trajectory for alphas above 640 MeV lies above the 500 keV and 500 photoelectron levels. The data handling circuit associated with the telescope contains ten pulse height discriminators (level sensors = LS) at the abscissa and ordinate levels shown in [Figure 27](#), so that protons are distinguished from alphas on the basis of LS8 and 10 (silicon detectors) and LS5 (PMT). Energy analysis of each particle type is provided by the PMT LS1–6, while out-of-aperture events are suppressed by requiring a fast triple coincidence between LS1, 7, and 9 for any event to be counted.

The table on [Figure 27](#) shows the energy ranges of the data channels



— PMT response to Cerenkov Light Production in Silica (Photoelectrons)
 --- Ionization Energy Loss in Silica (MeV)

Figure 27.—HEPAD Telescope Response

provided by the HEPAD and the coincidence logic employed to obtain these signals. The dashed line indicates the energy dependence of scintillation produced in the radiator. This curve is not normalized with respect to the Cerenkov trajectories, since the normalization depends on the scintillation efficiency of the silica. This efficiency is sufficiently small that no distortion of the energy dependence of the Cerenkov light is produced by scintillation.

The detector thickness of 500 μm is a compromise between lower cost with lower bremsstrahlung sensitivity (smaller thickness) and greater S/N ratio (greater thickness). The radiator thickness is chosen sufficiently large so as to produce a PMT pulse of >100 photo-electrons for 850 MeV protons, restricting the statistical fluctuation in height of this pulse to about 10%, corresponding to a resolution of 170 MeV at 850 MeV. The center of the Am^{241} pulse height peak falls near LS4. The LS4 counting rate (~ 50 pps) is related to the overall PMT transfer function (silica transmission, PMT quantum efficiency, PMT gain) such that changes can be observed during quiescent periods.

5.4 HEPAD Application

The HEPAD senses the intensity in the local zenith direction of ambient solar and galactic protons above 370 MeV in four energy bands and of ambient solar and galactic alpha particles above 640 MeV in two energy bands.

The occurrence of large solar events with measurable proton flux in the energy range covered by the HEPAD is very infrequent. While infrequent, the occurrence of solar cosmic ray events with significant fluxes of particles above several hundred MeV is important for both scientific and operational reasons. Protons at the top of the atmosphere with energies greater than 60 MeV can penetrate to aircraft altitudes (24 km, 80,000 ft.) and with greater than about 650 MeV can penetrate the entire atmosphere and reach the earth's surface producing so-called ground level events. These very energetic events produce low altitude ionospheric effects, and may also constitute a radiation hazard at aircraft altitudes.

The last HEPAD on the NOAA Polar Orbiting satellites was flown on NOAA-7 launched on 6-23-81. The remaining four HEPADS were transferred to the GOES program for flight on GOES D, E, F and G.

5.5 Sample of HEPAD Data

Kolasinski has compared the inner zone spectrum measured by the HEPAD on TIROS with the AP-7 model published by Lavine and Vette. For $L = 1.20$, they give a characteristic flux J_0 of 644 protons/($\text{cm}^2 \cdot \text{s} \cdot \text{sr}$) for J perpendicular to the field at $B = 0.18$ gauss and an e-folding energy of $E_0 = 160$ MeV. (L is the maximum radius of a field line given in earth radii). Similarly at $B = 0.19$, they give $J_0 = 422$ and $E_0 = 140$ MeV. The HEPAD spectrum gives $E_0 = 145$ MeV and $J = 800$ protons/($\text{cm}^2 \cdot \text{s} \cdot \text{sr}$). For the very anisotropic pitch angle distribution of the trapped protons, this will be decreased to about 0.6 $\text{cm}^2 \cdot \text{sr}$ and the agreement will be poorer. However, the model would not be expected to agree with a single observation to better than a factor of two.

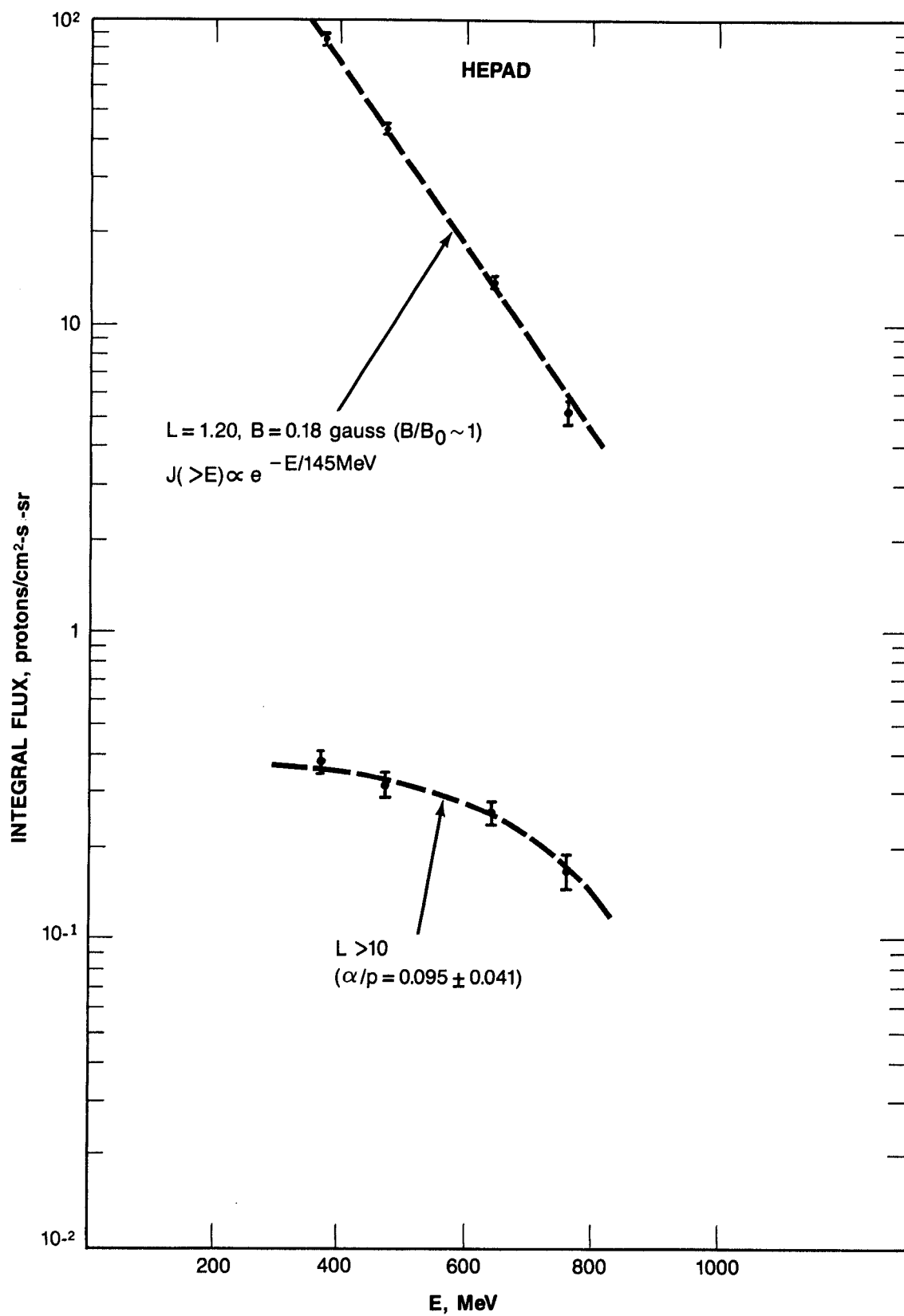


Figure 28.—Comparison of Flux Spectra by Kolasinski

Kolasinski made another check on the performance of the HEPAD using the natural background encountered in orbit. This is of two types: in the polar caps, the galactic cosmic ray background and at low latitudes, the intense inner zone trapped protons. For both types, it is possible to make comparisons with published data. Figure 28 shows Kolasinski's comparison of spectra obtained for these two cases.

To compare to the cosmic ray spectrum, it is necessary to convert to differential flux. For the interval 370-470 MeV, the HEPAD data give 0.061 protons/(cm²·s·sr) which is a differential flux of 6.1×10^{-4} protons/(cm²·s·sr·MeV). For an energy of 400 MeV published values range between 2×10^{-4} and 9×10^{-4} depending on the time in the solar cycle. Thus the agreement is as good as can be expected. Note also that the alpha-to-proton ratio, as shown by $(P3 + P4)/(A1 + A2)$ of 0.095, is reasonable.

6. DATA PROCESSING UNIT (DPU)

6.1 General Description

The Data Processing Unit takes the logic level pulses representing particle events in particular categories and processes them to provide data on the flux and spectrum for telemetering to the ground. In addition the DPU contains the power supplies (DC/DC converter) for the whole SEM and all interfaces with the spacecraft data, command, and power subsystems. The DPU has an analog multiplexer and A/D converter which provide SEM housekeeping data to the TIP data stream. A more limited number of voltages and temperatures are monitored by the Digital B and TIP Analog systems. A view of the unit is shown in Figure 29. A block diagram of the DPU is shown in Figure 30.

In the case of the MEPED and HEPAD data, the DPU operation is an accumulation of the number of events occurring in a fixed time interval. As the dynamic range of the observed flux is very large, the original, accumulated 19-bit number is converted to an 8-bit quasi-floating point representation (p. 61) to reduce the telemetry requirement. The various channels are multiplexed between accumulators and into the telemetry format to provide a sampling rate commensurate with the importance and rate of variation for the particular channel. For the TED data, the DPU carries out the summation over the energy sweep to obtain the total energy and detects the energy interval containing the maximum flux. Alternative telemeter formats (Appendix H) can be selected for the TED data to provide emphasis on different features of the TED submultiplexed data for different application.

6.2 DPU Functions

The DPU performs the following functions:

1. Accumulate pulse outputs from the TED, MEPED, and HEPAD particle detectors and provide count data.
2. Sample analog and digital housekeeping data from the particle

detectors and digitize the analog data to 8 bits.

3. Format the data above into a serial telemetry data stream to the TIROS Information Processor (TIP).

4. Provide analog and digital data from particle detectors and DPU directly to the TIP.

5. Receive, decode, and execute commands.

6. Provide a linear ramp and timing signals for the particle detector in-flight calibrators.

7. Provide power to the particle detectors from a DC/DC converter.

8. The DPU is the SEM interface to the spacecraft.

Appendices D, E and F contain information with cross references on the level sensors and detectors of which the various channels consist.

A block diagram of the DPU appears in Figure 30.

The DPU consists of the following circuits:

- a. Timing and Control
- b. Analog and Digital Multiplexer
- c. Particle Detector Data Processors
- d. A/D Converter
- e. Formatter
- f. Command Processor
- g. Ramp Generator and IFC Programmer
- h. Low Voltage (LV) Power Supply

a. The Timing and Control receives signals from the spacecraft and uses these signals to generate all the timing signals necessary within the DPU and the three particle detectors. The following timing signals are received by the DPU:

- a. 1/32 Hz sync (32 s is a major data frame period)
- b. 1 Hz sync
- c. 8.32 kHz
- d. A1 Select

Signals a and b are used to synchronize with the TIP major frame (32 s) and

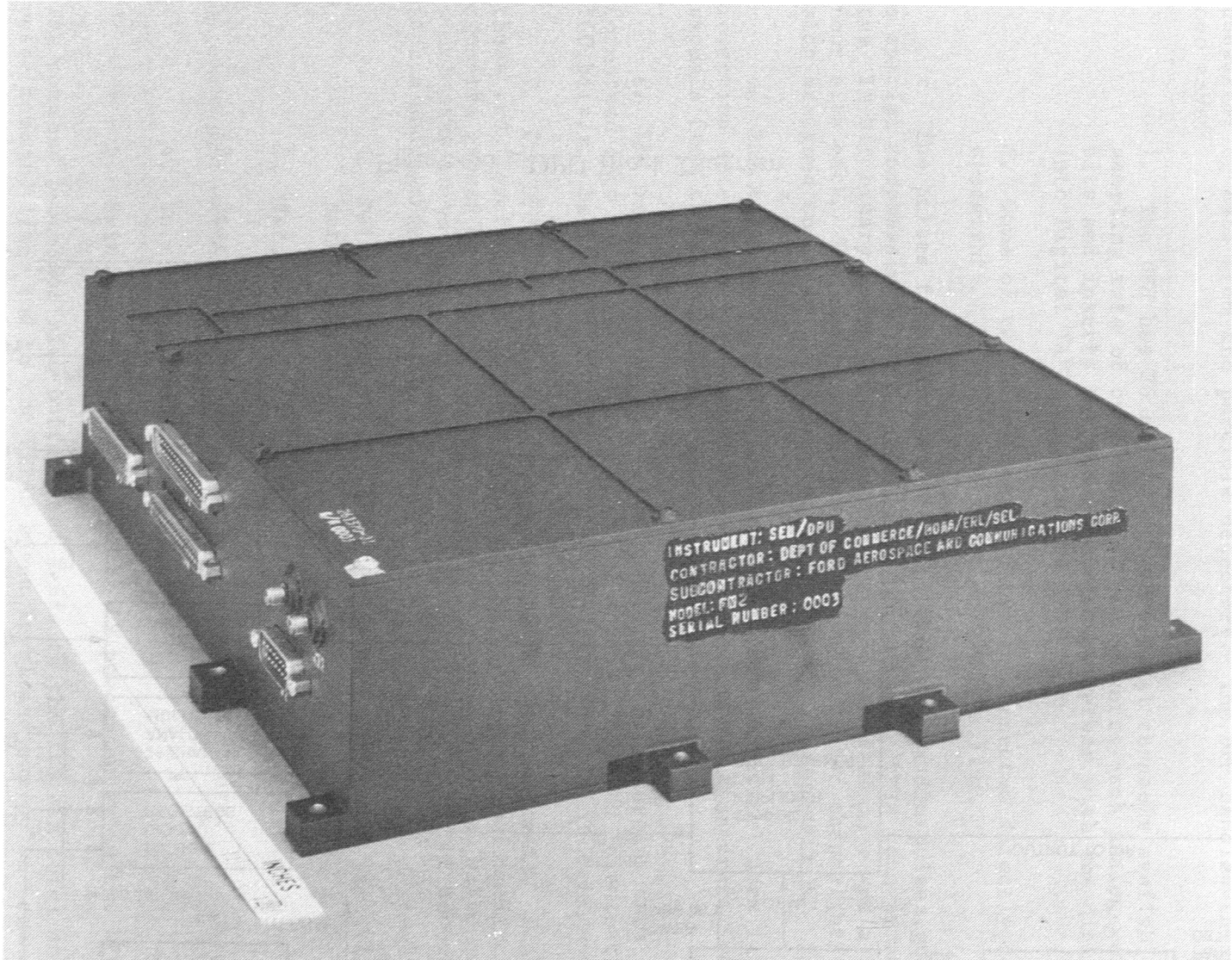


Figure 29.—Data Processing Unit

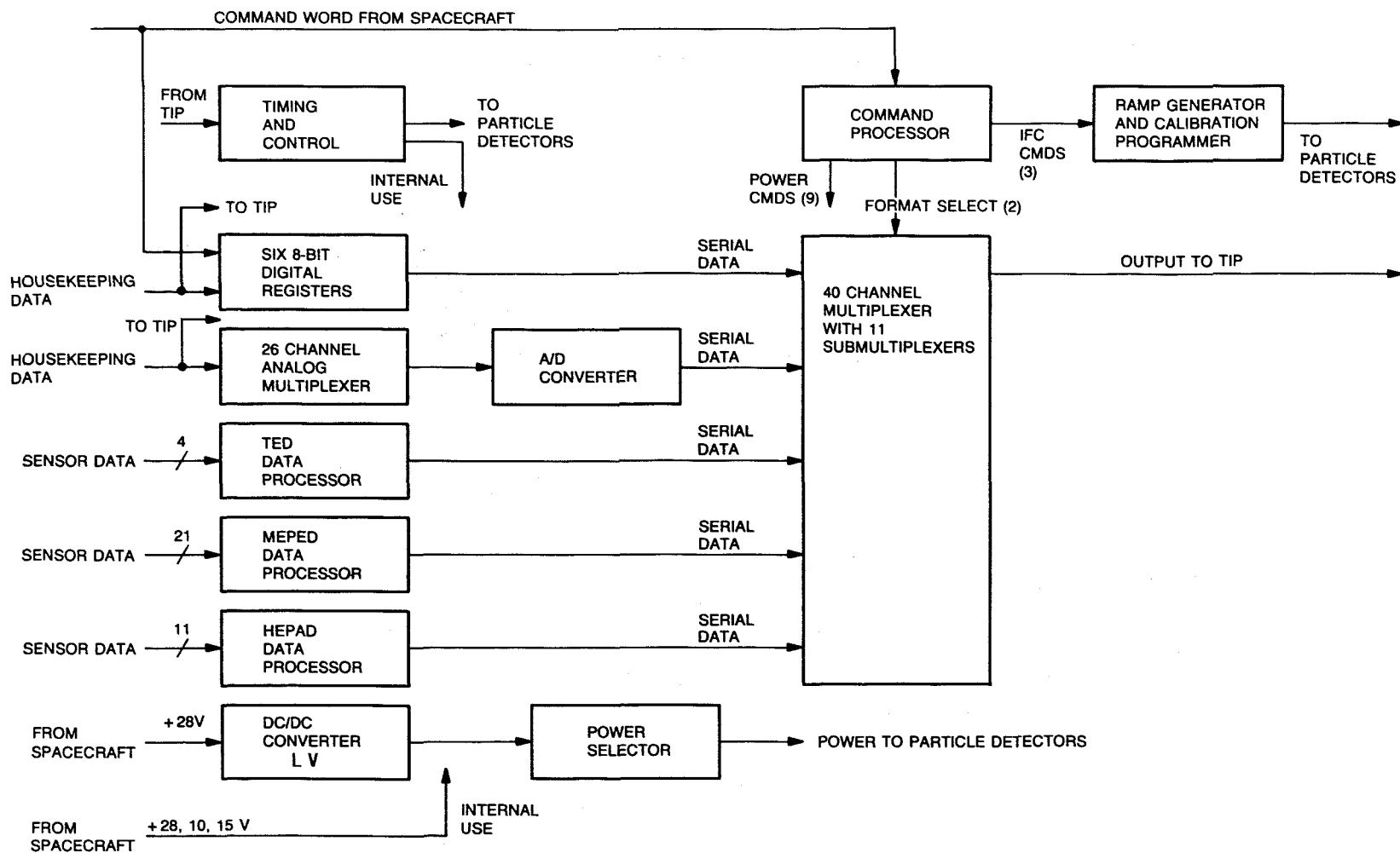


Figure 30.—DPU Block Diagram

minor frame (2 s). Signal c is used as the basic clock in all the circuits and is also the rate at which data are being transmitted to TIP. Signal d determines the time in a TIP frame of 100 ms when data from DPU are being transmitted. This signal is received only when TIP wants DPU data.

b. The Analog and Digital Multiplexer receives analog and digital housekeeping data from the particle detectors. The DPU handles this data in two ways:

1. The DPU has 26 analog and 48 digital channels available at a sampling rate of once in 32 s. It converts each analog word into 8 bits and inserts the converted data together with the digital data into Digital "A" Output to the TIP.

2. Some of the housekeeping data are connected directly to the spacecraft. Each source is on a separate line.

c. The pulses from the particle detectors are random pulses, counted in a special compression counter, the 623C. On command, this counter converts the 19-bit binary count into an exponent y and mantissa x; y and x having four bits each. The eight-bit number from each detector channel has a time slot assigned to it in the frame format as listed in Appendix H.

d. The A/D converter changes analog signals to digital form for insertion into Digital A. (Digital B is created in the spacecraft from analog signals from the SEM and other subsystems.)

e. The data from particle detectors and the housekeeping data are formatted into a major frame of 640 8-bit words. The data rate to the TIP is 160 bits/s. Data are sent only when an A1-select signal is received.

f. The DPU receives 12 command lines from the spacecraft. Eight of these are "level commands" which stay at the commanded level until changed from the ground by another command. The four remaining are "pulse commands" which stay on various short times (60 ms for NOAA-G). The DPU decodes these inputs and performs the following functions:

1. Switches the Power ON/OFF to each of the three particle detectors.

2. Establishes Mode 1 or Mode 2 of data transmission.

3. Starts calibration of the particle detectors.

4. Terminates the calibration.

5. Switches ON/OFF power to the LV power supply in the DPU.

The command processor also buffers and sends to the TED six level and one pulse command lines and to the HEPAD seven level and one pulse command lines.

g. The Ramp Generator and IFC Programmer, in response to a received command, generates a linear 0-8V ramp and corresponding timing signals necessary to perform the calibration of each particle detector.

The calibration sequence is self-terminating and may also be terminated on command before it runs its full course.

h. Low Voltage (LV) Power Supply

This module supplies power to the DPU and to each of the sensors. A DC/DC converter generates the following voltages from the spacecraft 28 volt main bus.

+6 volts	1610 mW
-6 volts	1150 mW
+12 volts	1430 mW
-12 volts	760 mW
+5 volts	3060 mW
+30 volts	880 mW
+350 volts	35 mW

	8925 mW

6.3 Symbols & Data Conversion

This section defines the data channel names and explains the data conversion from telemetered logarithmic compressed format to true count.

a. Data Coding. The following notation is used to refer to the various data channels:

channel names abc

where a = 0, 30, 90

 b = see table

 c = see table

For some channels a and c are not used.

Symbol a = view direction

0 = -X

30 = 30° from -X axis in -X, -Z plane

90 = 90° from -X axis along +Z *.

* In the case of the MEPED, this is only approximate to the angle from the -X axis.

Various alternate forms of these codes are used which include spaces, hyphens, and subscripts.

Symbol b

<u>Symbol</u>	<u>Type</u>	<u>Function/Source</u>
I	LOG	Ions/MEPED
P	LOG	Protons/MEPED, HEPAD
P	LOG**	Positive Ions/TED
E	LOG**	Electrons/MEPED, TED
S	LOG	Coincidence Counters/HEPAD
S	LOG	Singles Counters/HEPAD
A	LOG	Alpha Particles/HEPAD
DE	LOG	Diff. Energy, Electrons/TED
DP	LOG	Diff. Energy, Protons/TED
EF	LOG/Prescaled	Total Flux, Electrons/TED
PF	LOG/Prescaled	Total Flux, Protons/TED

** Except for EM, PM, see below.

Symbol c

1-8	Channel Number
m	With E or P, an integer identifying the channel in which max counts appeared.
M	With DE or DP, count in max channel
D	Directional
BK	Background
FD	Directional flux

b. Data Conversion

1. The particle counts are log compressed into a two part (y, x) floating point hexadecimal format by the several Type 623 Floating Point Processors in the SEM, all of which work in the 19-8 mode. Conversion from hexadecimal to actual count may be done using either Table 6 or 7 for all channels except EFD and PFD. (Note: the bit numbering is assigned in reverse order from that in Table 14.) The count listed is the lowest actual count fed into the 623 which results in the y,x listed.

TABLE 6. Algebraic Conversion of Log Function to Count

MSB								LSB
7	6	5	4	3	2	1	0	

where, for any log function,

y = Bits 7, 6, 5, and 4,

x = Bits 3, 2, 1, and 0.

Use the following equations with y and x decimal:

a) If y = 0 to 8:

$$\text{Count}^* = [(x + 16) 2^{(y + 6)}] + 1$$

Except: If y = 8 and x = 15, Count = 0.

* This conversion holds for all "log" functions except EFD and PFD
see 2. below

b) If y = 9: Count = x + 1.

c) If y = 10: Count = x + 17.

d) If y = 10 to 15: Count = [(x + 16) 2^(y - 10)] + 1.

The telemetered hexadecimal values can be converted into a monotonic format by adding binary seven to all y values, binary one to all x values, and adding any resulting carries to the y values.

TABLE 7. Look-up Conversion of Log Function to Count

x	0	1	2	3	4	5	6	7	
y									
0	1025	1089	1153	1217	1281	1345	1409	1473	0
1	2049	2177	2305	2433	2561	2689	2817	2945	1
2	4097	4353	4609	4865	5121	5377	5633	5889	2
3	8193	8705	9217	9729	10241	10753	11265	11777	3
4	16385	17409	18433	19457	20481	21505	22529	23553	4
5	32769	34817	36865	38913	40961	43009	45057	47105	5
6	65537	69633	73729	77825	81921	86017	90113	94209	6
7	131073	139265	147457	155649	163841	172033	180225	188417	7
8	262145	278529	294913	311297	327681	344065	360449	376833	8
9	1	2	3	4	5	6	7	8	9
10	17	18	19	20	21	22	23	24	10
11	33	35	37	39	41	43	45	47	11
12	65	69	73	77	81	85	89	93	12
13	129	137	145	153	161	169	177	185	13
14	257	273	289	305	321	337	353	369	14
15	513	545	577	609	641	673	705	737	15

x	8	9	10	11	12	13	14	15	
y									
0	1537	1601	1665	1729	1793	1857	1921	1985	0
1	3073	3201	3329	3457	3585	3713	3841	3969	1
2	6145	6401	6657	6913	7169	7425	7681	7937	2
3	12289	12801	13313	13825	14337	14849	15361	15873	3
4	24577	25601	26625	27649	28673	29697	30721	31745	4
5	49153	51201	53249	55297	57345	59393	61441	63489	5
6	98305	102401	106497	110593	114689	118785	122881	126977	6
7	196609	204801	212993	221185	229377	237569	245761	253953	7
8	393217	409601	425985	442369	458753	475137	491521	0	8
9	9	10	11	12	13	14	15	16	9
10	25	26	27	28	29	30	31	32	10
11	49	51	53	55	57	59	61	63	11
12	97	101	105	109	113	117	121	125	12
13	193	201	209	217	225	233	241	249	13
14	385	401	417	433	449	465	481	497	14
15	769	801	833	865	897	929	961	993	15

2. Conversion of Log Functions EFD and PFD To Count for the TED Flux Measurements

For the TED total flux measurements (only) a five-bit prescaler is used in the instrument to scale the count as the high voltage changes on the deflection plates, and the counting registers are preset to 1 (instead of 0 as for other channels). Correction for the additional count is not significant for counts above 33. The bits of the prescaler are not included in the readout except for cases where the true count is less than 8 (i.e., $y = 9$ and $x < 7$). In these cases the prescaler bits are included and the value of y is modified to overlay the normal (very high) range of $y = 6, 7, 8$, giving a "double valued" table. The correct value must be determined from EFM or PFM values.

a. If $y = 9$ and $x = 4, 5, 6$, or 7 , generate a new " x " by shifting the " x " bits left one position and entering the MSB of the prescale in the LSB position of x ; make the new value of $y = 6$, (e.g., If $x = 6$ (0990), shift the bits to make the new value of $x = 110$ P where P is the MSB of the prescale).

b. If $y = 9$ and $x = 2$ or 3 , generate a new " x " by shifting the " x " bits left two positions and entering the two MSB's of the prescale in the 2 LSB positions of x ; make the new value of $y = 7$.

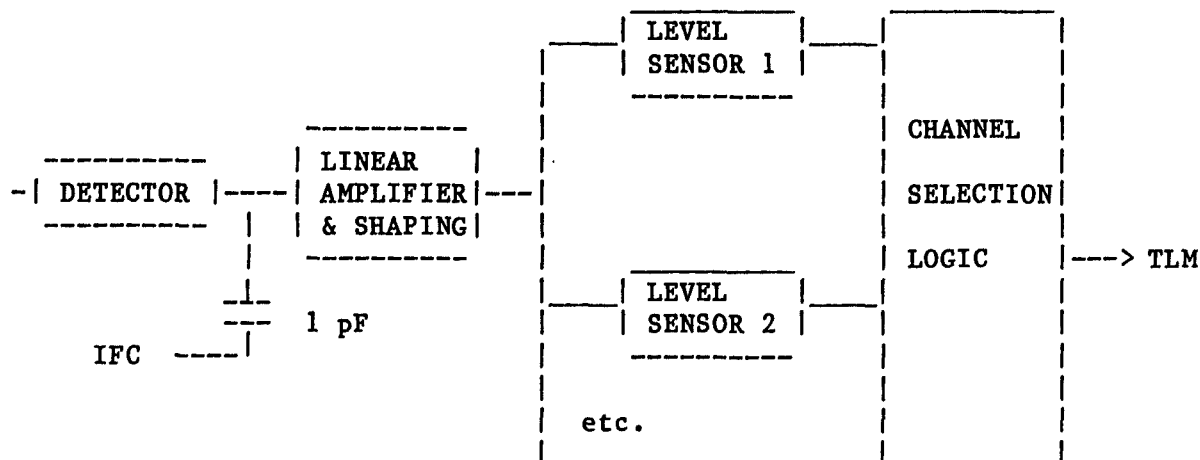
c. If $y = 9$ and $x = 1$ or 0 , generate a new " x " by putting this " x " bit in the MSB position of x and entering the 3 MSB's of the prescale in the 3 LSB of x ; make the new value of $y = 8$.

The alternate output in true count, where x and y are the newly generated values of x and y , then becomes:

TABLE 8. TED Prescaler True Count								
	$x = 0$	1	2	3	4	5	6	7
$y = 6$	THE HIGH VALUE							
$y = 7$	THE HIGH VALUE							
$y = 8$	0	1/8	1/4	3/8	1/2	5/8	3/4	7/8
$y = 9$	INVALID FOR THESE TED WORDS							
	$x = 8$	9	10	11	12	13	14	15
$y = 6$	4	4 1/2	5	5 1/2	6	6 1/2	7	7 1/2
$y = 7$	2	2 1/4	2 1/2	2 3/4	3	3 1/4	3 1/2	3 3/4
$y = 8$	1	1 1/8	1 1/4	1 3/8	1 1/2	1 5/8	1 3/4	1 7/8
$y = 9$	8	9	10	11	12	13	14	15

7. INFLIGHT CALIBRATION IFC

a. The HEPAD and MEPED are of the form



For each incident particle the detector produces a quantity of charge which is proportional to the energy deposited in the detector. This charge is converted to a voltage pulse and amplified until it is at a suitable level to apply to a Level Sensor each of which puts out a logic level pulse when the level is exceeded. It is usual to refer to the level in terms of the energy deposited in the detector. This is measured in electron volts (eV).

To calibrate, the electronic portion of the system is stimulated by injecting known quantities of charge at the input of each preamplifier in parallel with the detector using a small coupling capacitor driven from a low impedance source of "tail pulses". These are pulses with a fast rise and slow exponential decay. During the fast rise, a known charge ($Q = CV$) is injected and processed by the electronics exactly as if a particle had entered the detector.

The scale is established by the transfer scale of the detector w , the charge on one electron q and the capacitance of the IFC capacitor C .

$w = 3.62$ eV per charge pair released in the detector. (Ortec, 1985)

$q = 1.6021773 \text{ E-19}$ coulombs.

$C =$ approximately 1 pF.

$$\text{The scale is } \frac{q}{w C} = \frac{1.6021773 \text{ E-19}}{3.62 \times 1 \text{ E-12}} = 44.259 \text{ mV/MeV}$$

The scales in the appendices are based on 45 mV/MeV.

The pulses are amplitude modulated by a ramp (actually a stair-case of 1024 steps) which rises from zero to full scale in 192 seconds. The 192 s period is made by dividing the spacecraft 8320 Hz clock by $(13 \times 8 \times 15 \times 1024)$.

Levels for the level sensors are found by analysis of the output data on the ground. The analysis also checks system noise and long-term stability.

Upon receipt of the IFC ON command, the calibration generator in each of the instruments generates a sequence of calibration pulses, synchronized to the telemetry format. During the sequence, which is long compared to the read-out cycle of the instruments, the calibration pulse amplitude (and the equivalent energy) is linearly increased from zero to a peak value. By examining the sequence of readouts from an output channel during the calibration, it is possible to calculate the threshold energy level for that channel.

In the absence of noise in the channel, the simplest read-out sequence observed would be of the form

0 0 0 0 0 P C C C C C C C

where C is a constant called the "complete count" which depends on the tail pulse frequency (8.32 kHz) and the accumulation time. The energy level of the channel is calculated by linear interpolation between zero and the ramp peak energy. One intermediate value P, where $0 < P < C$, will occur if the level sensor turn-on occurs during an accumulation period. In most cases, because of sharing of accumulators, accumulation is not continuous so it is possible that P may not occur. If an intermediate value P is present, it is used to interpolate between telemetry word levels. If it is not present, then the accuracy of the interpolation is limited to word interval quantization.

In the MEPED, the calibration pulses are gated on and off on alternate readouts. So, out of 96 values telemetered in 192 s 48 contain IFC values. This is done to measure the ambient particle background, which is significant in orbit and must be subtracted from the calibration. On the ground, this background will normally be zero. Thus, on the ground the following sequence will appear

0 0 0 0 0 C 0 C 0 C 0 C 0, etc.

where again P may or may not appear.

In the lower energy channels of the MEPED and the singles channels of the HEPAD, the noise, which is due to the sum of noise from the detector and electronic noise from the preamplifier, is sufficiently large compared with the level sensor thresholds that it is necessary to keep track of the noise as a quantitative performance parameter. An increase of noise is of concern because in the extreme, it would cause one or more level sensors to trip continuously and render a channel or channels inoperative.

The noise performance of each detector-preamplifier chain can be measured by observing the calibration telemetry sequence from the lowest energy level sensor connected to that detector. The effect of the noise is to broaden the turn-on of the level sensor so that instead of one possible intermediate value we expect to see several, e.g.,

0 0 0 0 0 h i j k C C C C, etc.

where h, i, j, and k are partial values intermediate between 0 and C. Assuming gaussian noise statistics, the slope of the turn-on curve can be represented by a single parameter, the Full Width, Half Maximum (FWHM) value. This is the full width at half maximum amplitude of the resolution function

which is the differential of the turn-on curve we measure with the calibrator. Note that only one meaningful noise (FWHM) measurement is possible for each detector, using the lowest energy level. In some cases (the high energy omnidetectors in the MEPED, for instance), the the calibration data do not resolve the noise level. However, since the noise may be increased by a degraded detector or EMI, the value for FWHM should be monitored routinely.

b. The TED functions somewhat differently, although the interpretation of the calibration is similar.

Using the total count channels 0EFD, 0PFD, 30EFD, and 30PFD, the thresholds are determined in the same way as described for the other instruments. The thresholds have 4 different values which are selected on command, and cycled automatically during the calibration sequence. The variable threshold is used in orbit as a means of limit checking the channeltron performance, which is subject to degradation with time and radiation, to determine when operating voltage adjustments are required.

The IFC sequence also cycles the levels without applying artificial pulses so that the amplitude distribution of the detector outputs is obtained using natural events.

c. There are two major subdivisions of analysis, real time and non-real time. Because of time constraints, real time analysis of the raw data (conducted on all data at the telemeter rate) is limited to limit checks.

Non-real time analyses (conducted at a slower-than-telemeter rate) are done off-line for the following:

	<u>Thresholds</u>	<u>FWHM</u>	<u>Coincidence Efficiency</u>
TED	X		
MEPED	X	X	
HEPAD	X	X	X

d. Determination of Threshold

Table 9 lists the number of channels and number of data points per channel.

TABLE 9. IFC DATA								
Phase	1		2		3		4	
	NC	ND	NC	ND	NC	ND	NC	ND
TED	4	96	4	96	4	96	4	96
MEPED	7	48	15	48	11 2	48 12	NA	NA
HEPAD	7	48	7	48	7	48	7	48

NC = Number of channels. ND = Number of data points per channel.

These values are examined in non-real time to determine the number of minor frames from the start of the IFC phase with zero counts (O_1), the number of subsequent minor frames with partial counts (Y_1), and the number of subsequent minor frames with complete counts (X_1). If subsequent to a minor frame with a complete count, a minor frame appears with either a zero or partial count, an additional set of O, Y, X is generated. For example:

Minor frame #	1	2	3	4	5	6	7	8	9	10
Count	0	0	P	C	C	C	0	P	C	C

0 - Zero
P - Partial
C - Complete

O_1	Y_1	X_1	O_2	Y_2	X_2
2	1	3	1	1	2

The count required in a minor frame for a complete count, which depends on the particular channel being observed, is listed in Table 10. In addition to keeping the O, X, Y values, keep the data channel readout for all partial counts. The following is a format:

O_1, Y_1, X_1	O_2, Y_2, X_2 — — —
Data 1	Data 2

A checksum of O_1, Y_1, X_1 should equal the number of data points shown in Table 9. Note that in Phase 3, the MEPED has two channels $O1, 90I$ which have only 12 data points.

TABLE 10. Complete Counts	
Data Channel	Actual Count
<u>TED</u>	
abFD	8320
<u>MEPED</u>	
O1, 90I	33280
P6, P7, P8	16640
All Others	8320
<u>HEPAD</u>	
P1, P2, P3, P4, A1, A2	33280
S1, S2, S3	782
S4	20800
S5	9984

e. Determination of Full Width Half Maximum

Data for FWHM calculation varies in size per Table 11. Each has 48 data points per set.

TABLE 11. FWHM Data				
	Data Channels	Divide Data by	IFC Phase	Remarks
MEPED	0P1 0E1 90P1 90E1	8,320	1	<u>1/</u>
	P6 P7 P8	16,640	1	
HEPAD	S1 S2	782	1-4	<u>2/</u>
	S3	782	3,4	<u>3/</u>

1/ 0P1 and 90P1 channels have 2 FWHM Values--1 when the counts are increasing, the second when the counts are decreasing.

2/ There are 4 sets of 48 data points/channel (1 set/IFC phase). The average of the four values in each data time slot are used to calculate the FWHM.

3/ There are 2 sets of 48 data points for this channel (IFC Phase 3,4). The average of the 2 values in each data time slot are used to calculate the FWHM.

Let the data be identified by a step number I in the telemetered sequence. I varies from 1 to 48. For channels with more than one set, average the values which have the same I (see footnotes in Table 11). Divide all data by the numbers specified in Table 11 while maintaining the step number I for the resultants. Each new value is the fraction $F(Z,I)$, the area under the normal curve based on the assumption of a gaussian distribution of noise. Find values of Z from the table of F vs. Z, in Appendix A, page 93. Ignore values of F which exceed the range of the table.

Form a set of numbers Z,I. Because the counts include fluctuations, Z contains errors. Accordingly we make a least-square fit of the form $Z = a + b I$. However, the fit we need is $I = A + B Z$ where the intercept A is the threshold level and the slope B is the standard deviation, both in units of I. Solve for A and B using a and b. Convert from units of I to energy by multiplying by the end energy of the IFC ramp (given in Appendixes D and E) and dividing by the number of steps (typically 48) in the full sequence I to reach that end energy. All of the scales are based on 45 mV per MeV dissipated in the detector. The FWHM is analytically defined as 2 times the square root of $(2 \ln 2)$ times the standard deviation, so convert to FWHM by multiplying by 2.35482004.

Check this value of FWHM to see if it exceeds the limit (not listed here).

Example: MEPED Data Channel 0P1 IFC Phase 1

Data from NOAA6 in orbit, 1986 June 19 day 170 start IFC 12:02:57Z.

The count listed is the middle of the intervals listed in Table 7.
Divide Count by 8320.

Count	F	Z	I
1	.000120		7
4	.000481		8
18	.002163		9
75	.009014		10
265	.031851		11
785	.094351	-1.314483	12
1889	.227043	-.748657	13
3393	.407813	-.233185	14
5249	.630889	+.334222	15
6785	.815505	+.898380	16
7553	.907813	+1.327472	17
8065	.969351		18
7753	.931851		19

We make the least-square fit $Z = a + b I$ and solve for $I = A + B Z$.

$$A = -a/b \quad B = 1/b$$

We find that $A = 14.417917$, $B = 1.867308$ and $r^2 = 0.998652$

$$\begin{aligned} \text{Threshold} &= A \times 75 \text{ keV} / 48 \\ &= 14.417917 \times 75 / 48 = 22.53 \text{ keV cut-in} \end{aligned}$$

$$\begin{aligned} \text{FWHM} &= B \times (75 \text{ keV} / 48) \times 2.35482 \\ &= 1.867308 \times (75 / 48) \times 2.35482 = 6.871 \text{ keV} \end{aligned}$$

End of example.

f. Determination of Coincidence Efficiency.

For IFC phases 1 and 2, note the 48 values of A1, A2, P4 and S5. Convert all values to actual count.

For each of the following cases find I for the count nearest to the number listed here:

	increasing	decreasing
A1	8320	16640
A2	16640	--
P4	12979	16640

The A1 observation time is at a value halfway between the increasing and decreasing time determined above. For P4, as well as for A2, it is halfway between the I and 48.

Determine the efficiencies using Table 12.

TABLE 12. COINCIDENCE EFFICIENCY		
Data Channel	Double Coincidence Efficiency Observe S5 at I_0	Triple Coincidence Efficiency Observe Data Ch. at I_0
A1	$(S5 @ I_0)/9982$	$(A1 @ I_0)/33280$
A2	not used	$(A2 @ I_0)/33280$
P4	not used	$(P4 @ I_0)/33280$

Since Phase 2 is a repeat of Phase 1, there are two values determined for each of the efficiencies above. Average these values and report them as the double and triple coincidence efficiencies for those data channels.

For Phases 3 and 4, note the 48 values from each of the data channels P1, P2, P3, and S5.

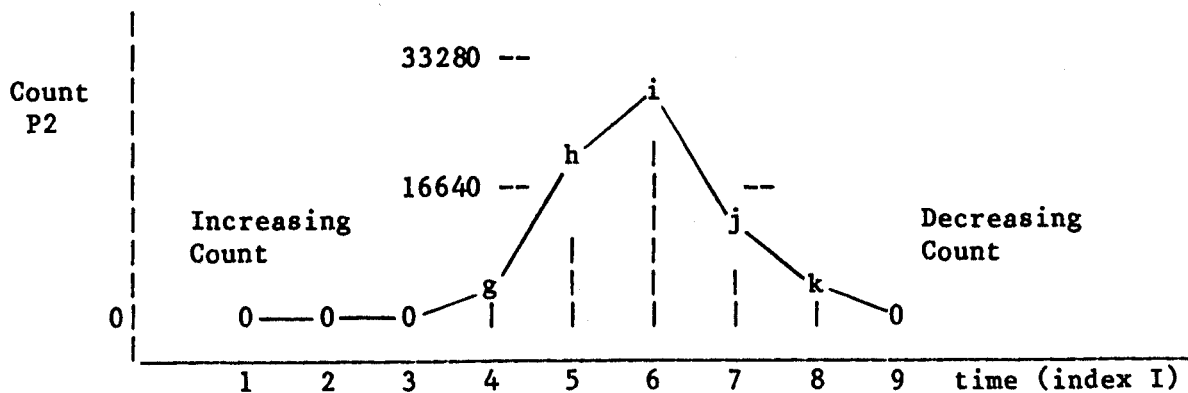
Use the same technique as in Phases 1 and 2 except pick I nearest these numbers (Table 13):

Table 13

	Count	Increasing	Decreasing	Efficiency
P1	8320	16640	(P1 @ I ₀)/33280	
P2	16640	16640	(P2 @ I ₀)/33280	
P3	16640	16640	(P3 @ I ₀)/33280	

Each data channel has two I values where the count is near the listed number because as the IFC ramp is increased, the cut-on threshold is passed and subsequently the cut-off threshold is passed. The values desired are at the points h and j shown on the following example:

Example



I for P2 near 16640 increasing is 5

I for P2 near 16640 decreasing is 7

The I halfway between these two is 6. Therefore the value of P2 for $I = 6$ is used in the equation to determine the triple coincidence efficiency.

End of example.

TED IFC

The TED IFC consists of 4 phases of 192 seconds each. See Appendix C. A 0-4 V ramp is put in. The threshold of the discriminator is determined for each of 4 channels at 4 attenuator settings; one for each phase. The TED stays in IFC Mode for 102.4 minutes after completion of the 4 phases (see note 2, p. 88).

Strobe #1 with SEM LINE 1 TRUE starts the TED/HEPAD IFC. The calibration starts anytime from 0-192 seconds after the command is given since the 192-second ramp must be at zero for the sequence to begin. This ramp is synchronized to the 32-second major frame. Therefore the IFC starts at the start of a major frame. In minor frame 285 word 20 bit 1, a "1" will appear indicating that the IFC began in that major frame, and will stay as long as TED/HEPAD IFC is on.

Each TED IFC phase calibrates a different gain/attenuator combination, that is, each calibrates one of the four TED levels. The 0° pulse height detector level is contained in word 20 minor frame 265 bits 1 and 2. The 30° pulse height detector level is contained in word 20 minor frame 265 bits 3 and 4. The levels from 1 to 4 are telemetered as binary names 00, 01, 10, 11. See p. 76, p. 89.

MEPED IFC

The MEPED IFC consists of three phases of 192 seconds each. The various ramp amplitudes are specified in Appendix D. IFC measures thresholds for 15 level sensors and FWHMs for 9 solid state detectors.

Strobe #1 with SEM LINE 2 True starts MEPED IFC. Bit 2 in minor frame 285 word 20 will go high in the major frame in which the IFC began.

Note: If the TED/HEPAD IFC is in progress do not send the "Start MEPED IFC" command. However, it is allowable to command both starts simultaneously.

HEPAD IFC

The HEPAD IFC consists of 4 phases of 192 seconds each. The ramp size in either energy or photoelectrons is specified in Appendix E. There are three values which must be calculated in non-real time for the HEPAD; thresholds for 10 level sensors, FWHM for 2 detectors and the photo multiplier tube (PMT) and double and triple coincidence counting efficiency for the electronic coincidence gates.

8. TELEMETRY

8.1 Data Transmission and Processing

The SEM data, which utilize two full words (8 bits each) in each 100 ms TIP minor frame, are dumped from tape in the spacecraft to the NOAA NESDIS CDA stations along with all other TIP data. It is then transmitted to Washington, D.C., by communication circuits. The SEM data stream is separated out along with relevant Digital B spacecraft analog data. Orbit information is added in the NESDIS computer system and the resultant data are transmitted to the SESC SELDADS II (Space Environment Laboratory Data Acquisition and Display System) computer in Boulder, Colorado where the data are stored for immediate operational use. Our present experience is that the most recent data we receive is about 100 minutes old.

SELDADS II archives on magnetic tape the raw data as received from NESDIS. These raw tapes are processed off line to produce the archive tapes as described in NOAA Technical Memorandum ERL SEL-71. SELDADS II presently (1986) keeps on line the most recent 8 days of raw data, as well as the most recent 32 days of certain processed data sets. Daily plots and status reports allow SEL staff to monitor the NOAA SEM.

8.2 Data Formats

Analog signals and digital data move from the SEM to the TIP in three different ways.

The Digital A data are sent as a serial data stream which contains all data and SEM housekeeping information. Digital B data are transmitted from the DPU to the spacecraft over parallel Digital B data lines where they are sub-multiplexed into the spacecraft Digital B data. The analog housekeeping is sent over parallel analog lines to the spacecraft where it is sub-multiplexed into the spacecraft analog words.

Appendix H gives the SEM Digital A output format. Also listed are the changes to this format for different modes.

The next several pages list the minor frame numbers where each datum appears in Digital A.

Table 14 shows the digital subcom words in digital A. Table 15 shows the analog words in digital A.

TED Data Location in Digital A

The TED data location within the TIP TLM format is shown in the following list:

<u>Data Channel</u>	<u>Minor Frame</u>	<u>Word</u>
ODE1	5, 85, 165	20
3ODE1	25, 105, 185	20
ODP1	45, 125, 205	20
3ODP1	65, 145, 225	20
ODE3	6, 86, 166	20
3ODE3	26, 106, 186	20
ODP3	46, 126, 206	20
3ODP3	66, 146, 226	20
ODE5	7, 87, 167	20
3ODE5	27, 107, 187	20
ODP5	47, 127, 207	20
3ODP5	67, 147, 227	20
ODE7	8, 88, 168	20
3ODE7	28, 108, 188	20
ODP7	48, 128, 208	20
3ODP7	68, 148, 228	20

<u>Data Channel</u>	<u>Minor Frame</u>	<u>Word</u>
0EBK	245	20
0PBK	246	20
0EM	9, 29, 49, 69, 89, 109, 129, 149, 169, 189, 209, 229, 249, 269, 289, 309	21 *
0PM	same as OEM	21 *
30EBK	247	20
30PBK	248	20
30EM	10, 30, 50, 70, 90, 110, 130, 150, 170, 190, 210, 230, 250, 270, 290, 310	20 *
30PM	same as 30EM	20 *
0EFD	16, 36, 56, 76, 96, 116, 136, 156, 176, 196, 216, 236, 256, 276, 296, 316	20
0PFD	same as 0EFD	21
30EFD	17, 37, 57, 77, 97, 117, 137, 157, 177, 197, 217, 237, 257, 277, 297, 317	20
30PFD	same as 30EFD	21
0DEM	18, 38, 58, 78, 98, 118, 138, 158, 178, 198, 218, 238, 258, 278, 298, 318	20
0DPM	same as 0DEM	21
30DEM	19, 39, 59, 79, 99, 119, 139, 159, 179, 199, 219, 239, 259, 279, 299, 319	20
30DPM	same as 30DE	21

* The "E" data are the first 4 bits of the word and the "P" data the second 4 bits.

MEPED Data Location in Digital A

<u>Data Channel</u>	<u>Minor Frame</u>	<u>Word</u>
OP1	0, 20, 40, 60, 80, 100, 120, 140, 160, 180, 200, 220, 240, 260, 280, 300	21
OP2	1, 21, 41, 61, 81, 101, 121, 141, 161, 181, 201, 221, 241, 261, 281, 301	20
OP3	same as OP2	21
OP4	2, 22, 42, 62, 82, 102, 122, 142, 162, 182, 202, 222, 242, 262, 282, 302	20
OP5	same as OP4	21
OE1	3, 23, 43, 63, 83, 103, 123, 143, 163, 183, 203, 223, 243, 263, 283, 303	20
OE2	same as OE1	21
OE3	4, 24, 44, 64, 84, 104, 124, 144, 164, 184, 204, 224, 244, 264, 284, 304	20
90P1	10, 30, 50, 70, 90, 110, 130, 150, 170, 190, 210, 230, 250, 270, 290, 310	21
90P2	11, 31, 51, 71, 91, 111, 131, 151, 171, 191, 211, 231, 251, 271, 291, 311	20
90P3	same as 90P2	21
90P4	12, 32, 52, 72, 92, 112, 132, 152, 172, 192, 212, 232, 252, 272, 292, 312	20
90P5	same as 90P4	21
90E1	13, 33, 53, 73, 93, 113, 133, 153, 173, 193, 213, 233, 253, 273, 293, 313	20
90E2	same as 90E1	21

<u>Data Channel</u>	<u>Minor Frame</u>	<u>Word</u>
90E3	14, 34, 54, 74, 94, 114, 134, 154, 174, 194, 214, 234, 254, 274, 294, 314	20
P6	same as 90E3	21
P7	15, 35, 55, 75, 95, 115, 135, 155, 175, 195, 215, 235, 255, 275, 295, 315	20
P8	same as P7	21
0I	0, 160	20
90I	20, 180	20

HEPAD Data Location in Digital A

<u>Data Channel</u>	<u>Minor Frame</u>	<u>Word</u>
P1	4, 44, 84, 124, 164, 204, 244, 284	21
P2	5, 45, 85, 125, 165, 205, 245, 285	21
P3	6, 46, 86, 126, 166, 206, 246, 286	21
P4	7, 47, 87, 127, 167, 207, 247, 287	21
A1	8, 48, 88, 128, 168, 208, 248, 288	21
A2	9, 49, 89, 129, 169, 209, 249, 289	20
S5	24, 64, 104, 144, 184, 224, 264, 304	21
S4	25, 65, 105, 145, 185, 225, 265, 305	21
S1	26, 66, 106, 146, 186, 226, 266, 306	21
S2	27, 67, 107, 147, 187, 227, 267, 307	21
S3	28, 68, 108, 148, 188, 228, 268, 308	21

TABLE 14. DIGITAL A SUBCOM WORDS					
Bit		Frame 265 Word 20	D1	Frame 266 Word 20	D2
(MSB)	1	TED (0E-0P)PHD bit 0		Level Command 0, (DCB 1)	
	2	TED (0E-0P)PHD bit 1		Level Command 1, (DCB 2)	
	3	TED (30E-30P)PHD bit 0		Level Command 2, (DCB 3)	
	4	TED (30E-30P)PHD bit 1		Level Command 3, (DCB 4)	
	5	TED Mode Status bit 0		Level Command 4, (DCB 5)	
	6	TED Mode Status bit 1		Level Command 5, (DCB 6)	
	7	TED On/Off		Level Command 6, (DCB 7)	
(LSB)	8	MEPED On/Off		Level Command 7, (DCB 8)	
Bit		Frame 285 Word 20	D3	Frame 286 Word 20	D4
	1	TED/HEPAD IFC On/Off		Pulse Command PC1	SEMDP
	2	MEPED IFC On/Off		Pulse Command PC2	SEMTD
	3	Low Voltage On/Off		Pulse Command PC3	SEMHD
	4	HEPAD Power On/Off		Pulse Command PC4	SEMPs
	5	Zero		Telemetry Mode 1 or 2	
	6	Zero		Zero	
	7	Zero		Zero	
	8	Zero		Zero	

Frame 305 Word 20 = Sync Pattern 1111 0011 = f3H D5

Frame 306 Word 20 = Sync Pattern 0101 0000 = 50H D6

Status of "bit 0" is determined by status of DCB 4, and status of "bit 1" is determined by status of DCB 5, when the affected variable was last addressed by a PC #2 strobe. (See "TED Commands", p. 88 and list p. 89.)

Pulse Command bits are "1" for one or two major frames after the corresponding pulse command is sent; otherwise they are "0".

In Table 14 PHD means pulse height detector referring to the setting of the TED level. D1 through D6 are names used in SEL printouts.

TABLE 15. HOUSEKEEPING SUBCOM in DIG A			
Minor Frame	Word	Cal Data Figure #	Signal Name
29	20	31-1	MEPED SSD Bias (Electron)
40	20	31-1	MEPED SSD Bias (Proton)
60	20	32	MEPED Omni Temperature
69	20	--	Spare
80	20	33	MEPED Electronics Temperature
100	20	32	MEPED Proton Telescope Temperature
109	20	--	Spare
120	20	32	MEPED Electron Telescope Temp.
140	20	32	DPU Temperature
149	20	--	Spare
189	20	--	Spare
200	20	--	Spare
220	20	31-1	TED Channeltron E HV
229	20	--	Spare
240	20	31-1	TED Channeltron P HV
260	20	32	TED Temperature
267	20	31-1	DPU +12V
268	20	31-1	TED Low Voltage Ramp
269	20	--	Spare
280	20	33	HEPAD HV PS
287	20	32	HEPAD Electronics Temperature
288	20	33	TED CEA
300	20	31-1	HEPAD SSD Bias
307	20	32	HEPAD PMT Temperature
308	20	31-1	DPU IFC Ramp
309	20	--	Spare

Typical telemetry values may vary from instrument to instrument. Test values for each instrument may be found in the End Item Data Package for that instrument.

The Digital B telemetry data provided by the SEM are shown in Table 16. All of the SEM Digital B data are also included in the SEM Digital A data.

TABLE 16. DIGITAL B TELEMETRY						
Signal Name	State*		Minor	Ch.	Word 8	Output
	Logic "1"	Logic "0"	Frame	No.	Bit no.	Circuit Figure 31
LV	Off	On	25	185	6	1
TED Power	Off	On	25	217	7	1
HEPAD Power	Off	On	25	249	8	1
MEPED Power	Off	On	26	26	MSB1	1
TED/HEPAD IFC On	Yes	No	26	58	2	2
MEPED IFC On	Yes	No	26	90	3	2
L D Cmd. LC0 (DCB-1)	1	0	26	122	4	2
L D Cmd. LC1 (DCB-2)	1	0	26	154	5	2
L D Cmd. LC2 (DCB-3)	1	0	26	186	6	2
L D Cmd. LC3 (DCB-4)	1	0	26	218	7	2
L D Cmd. LC4 (DCB-5)	1	0	26	250	LSB8	2
L D Cmd. LC5 (DCB-6)	1	0	27	27	1	2
L D Cmd. LC6 (DCB-7)	1	0	27	59	2	2
L D Cmd. LC7 (DCB-8)	1	0	27	91	3	2
Telemetry Format 1/2	1	2	27	123	4	3

* Logic "1" is a "True", "Low Voltage" state. All DIG B status bits are in Logic "1" state when the SEM is OFF.

Ch. No. refers to spacecraft telemetry channels, not to SEM DIG A channels.

The analog subcom telemetry data provided by the SEM are shown in Table 17. Equations relating values in engineering units to telemetered voltages are given in Table 18 (p. 80). Interface circuits for analog telemetry are shown in Figures 31 - 37. All of the SEM Analog Subcom Telemetry data are also included in the SEM Digital A data.

TABLE 17. ANALOG SUBCOM TELEMETRY					
This is not Digital A or B					
	Name	Output Fig.	Sub Com s	Minor Frame	Ch. No.
ATET	TED Temperature *	32	32	214	214
ACEA	TED CEA PS	34	32	222	222 **
AEPS	TED Channeltron E HV	34	32	119,279	119 **
APPS	TED Channeltron P HV	34	32	127,287	127
AMPT	MEPED Proton Telescope	32	32	135,295	135
	Temperature *				
AMET	MEPED Electron Telescope	32	32	230	230
	Temperature *				
AMSS	MEPED Proton Detector	35	32	143,303	143
	Bias Voltage				
AHPT	HEPAD PM Tube Temp. *	32	32	151,311	151
AHET	HEPAD Unit Temperature *	32	32	159,319	159
AMPV	HEPAD PM Supply Voltage	34	16	111,271	286
AHSS	HEPAD SS Detector Bias	35	16	4,164	294
	Voltage				
AIFC	DPU IFC Ramp	37	16	96,256	302
ADPU	DPU Temperature *	32	16	97,257	310
AMEL	MEPED Electronics Temp.	33	16	3,163	318
ALVR	TED LV Ramp	36	16	2,162	326

Notes:

* Indicates signals on the 28 V Analog Temperature Telemetry Bus. Temperature telemetry is available at all times when the +28V Analog Temperature Telemetry Bus is on, with one exception. MEPED electronics temperature, as well as all other non-temperature analog telemetry, is available only when the SEM is on.

** For NOAA-B through NOAA-G, these two telemetry signals are interchanged. (CEAPS MON is Channel 119, and CH E Bias Voltage is Channel 222).

1. The 32 and 16 second Analog Subcom data are read out in words 9, and 10 respectively, of each TIP Minor Frame.

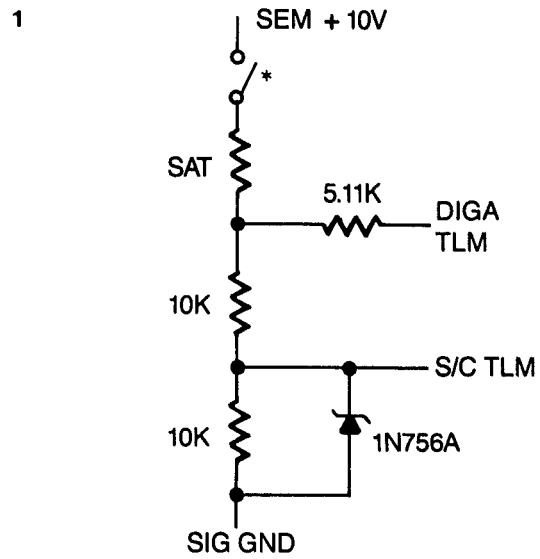
2. See Table 18 (p. 80) for equations.

TABLE 18. EQUATIONS FOR ANALOG TELEMETRY		
Channel Number	Name	Equation typical
214	TED Temperature	$0.463V^5 - 7.01V^4 + 42.33V^3 - 126.47V^2 + 199.58V - 169.19$
* 222	TED CEA PS	$313V + 178$
* 119	TED Ch. E HV level	$5.303V - 11.515$ round
127	TED CH. P HV level	$5.385V - 9.88$ round
135	MEPED P Tel. Temp.	$0.463V^5 - 7.01V^4 + 42.33V^3 - 126.47V^2 + 199.58V - 169.19$
230	MEPED E Tel. Temp.	$0.463V^5 - 7.01V^4 + 42.33V^3 - 126.47V^2 + 199.58V - 169.19$
143	MEPED P Det. Bias V.	$884.15V$
151	HEPAD PM Tube Temp.	$0.463V^5 - 7.01V^4 + 42.33V^3 - 126.47V^2 + 199.58V - 169.19$
159	HEPAD Unit Temp.	$0.463V^5 - 7.01V^4 + 42.33V^3 - 126.47V^2 + 199.58V - 169.19$
286	HEPAD PMT HV level	$88.29V - 110.07$ round
294	HEPAD SS Det. Bias V.	$889.16V$
302	DPU IFC Ramp	$1.6V$
310	DPU Temperature	$0.463V^5 - 7.01V^4 + 42.33V^3 - 126.47V^2 + 199.58V - 169.19$
318	MEPED Elect. Temp.	$0.235V^5 - 3.21V^4 + 18.09V^3 - 52.11V^2 + 89.98V - 103.97$
326	TED LV Ramp	V

V is the voltage passed from the SEM to the spacecraft which digitizes and telemeters the voltage to the ground. $V = 0.02n$ where n is the decimal value of the telemetered number. n ranges from 0 to 255 so V ranges from 0 to 5.10 volts.

See Table 17 (p. 79) for an output circuit list.

* For NOAA-B through NOAA-G, these two signals are interchanged.



* DigB 185 (LV conv) is connected directly to SEM + 10V (no switch)

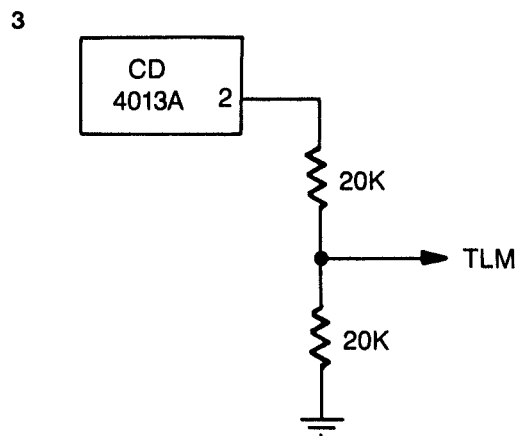
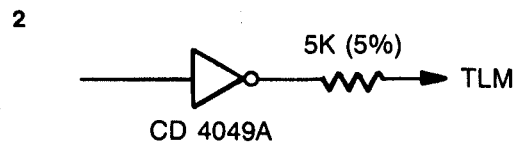
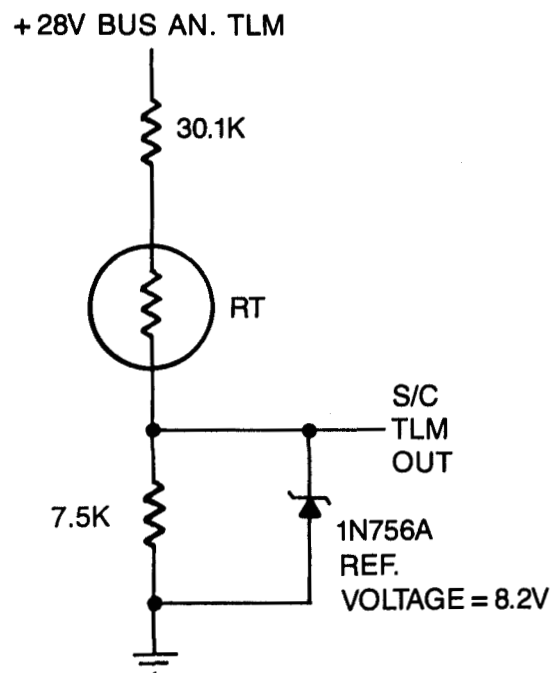


Figure 31.—Output Circuits



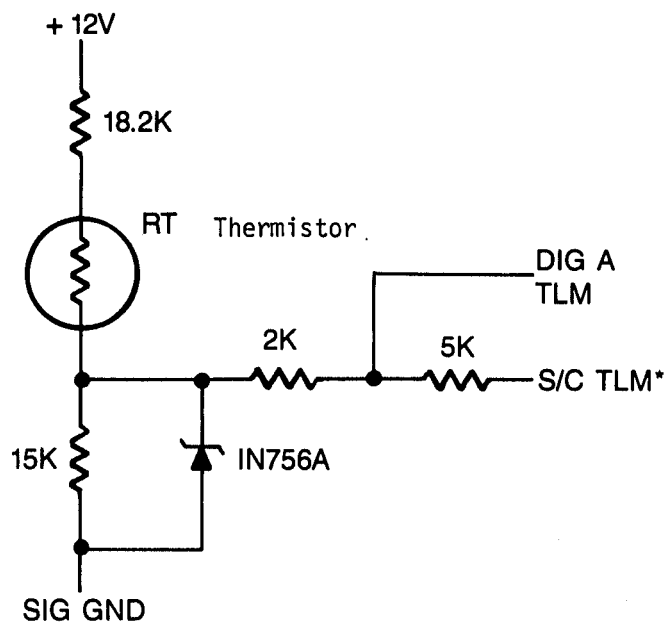
Typical six places for TIROS-N and NOAA-A to NOAA-D
 Typical four places for NOAA-E, F & G

Temp-°C	RT -KΩ	Vout - V
-40	88.27	1.67
-30	52.00	2.34
-20	30.50	3.08
-10	18.00	3.78
0	11.00	4.32
10	7.35	4.67
20	4.92	4.99
30	3.30	5.13
35	2.78	5.20

Best fit Polynomial:

$$\text{Temperature} = 0.463V^5 - 7.01V^4 + 42.33V^3 - 126.47V^2 + 199.58V - 169.19$$

Figure 32.—Spacecraft-Powered Temperature TLM Output Circuit



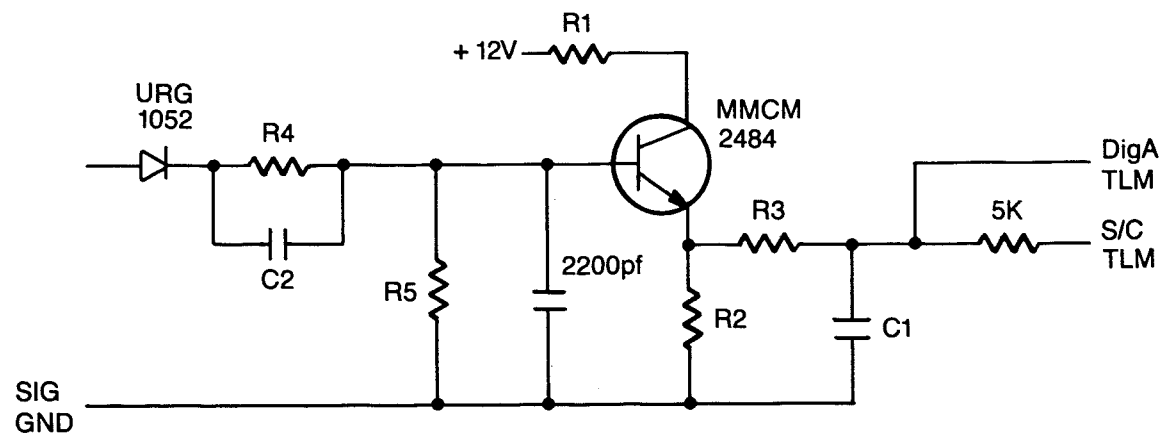
TEMP -°C	RT - KΩ	V Out -V
-40	88.27	1.482
-30	50.8	2.143
-20	30.0	2.848
-10	18.3	3.495
0	11.5	4.028
10	7.35	4.439
20	4.92	4.724
30	3.30	4.931
35	2.78	5.00

*The only SEM powered temperature telemetry contained in 16 second and 32 second subcoms of S/C telemetry is MEPED Electronics Temperature.

Best fit polynomial:

$$\text{Temperature} = 0.235V^5 - 3.21V^4 + 18.09V^3 - 52.11V^2 + 89.98V - 103.97$$

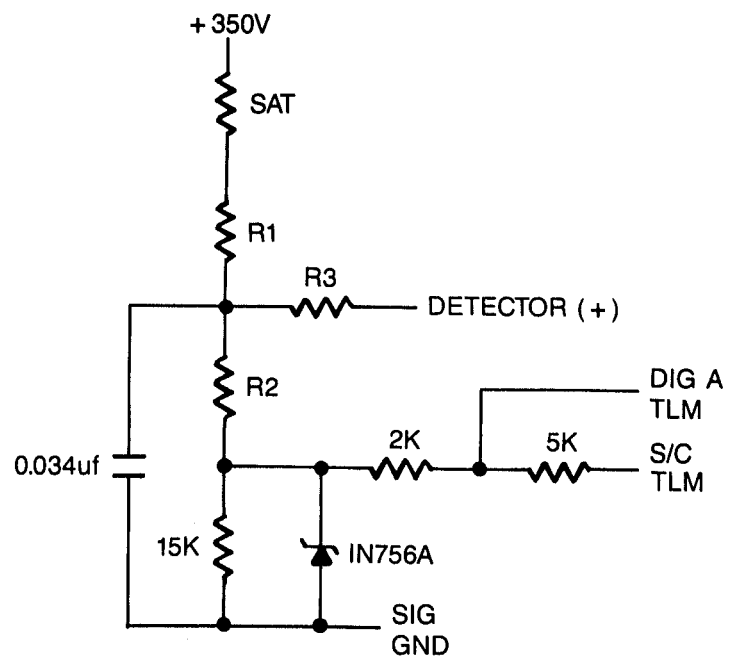
Figure 33.—SEM-Powered Temperature TLM Output Circuit



NAME	R1,R2	R3	R4	R5	C1	C2
E or P H V	100K	2.0K	1.17M	250K	0.01uf	470pf
CEA	51K	2.0K	590K	12.5K	0.47uf	470pf
HEPAD PMT	100K	9.1K	330K	250K	0.01uf	2200pf

Input is from a low-voltage point inside power supply before set-up transformer.

Figure 34.—HEPAD and TED HV Power Supply Monitor Analog TLM Output Circuit



	HEPAD	MEPAD
R1	Short	14.4M
R2	13M	2.94M
R3	4.32M	20M

Figure 35.—HEPAD/MEPAD Bias Voltage TLM Output Circuit

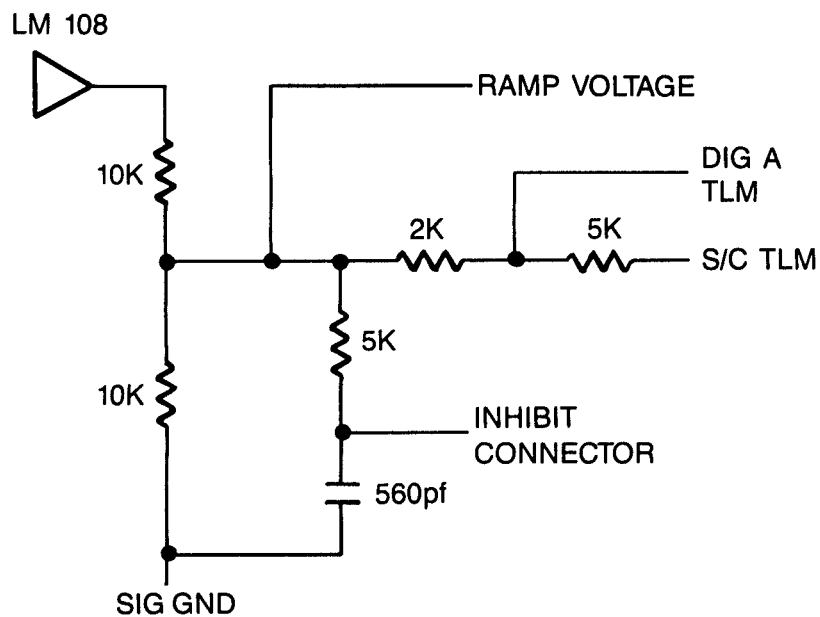


Figure 36.—TED LV Ramp TLM Output Circuit

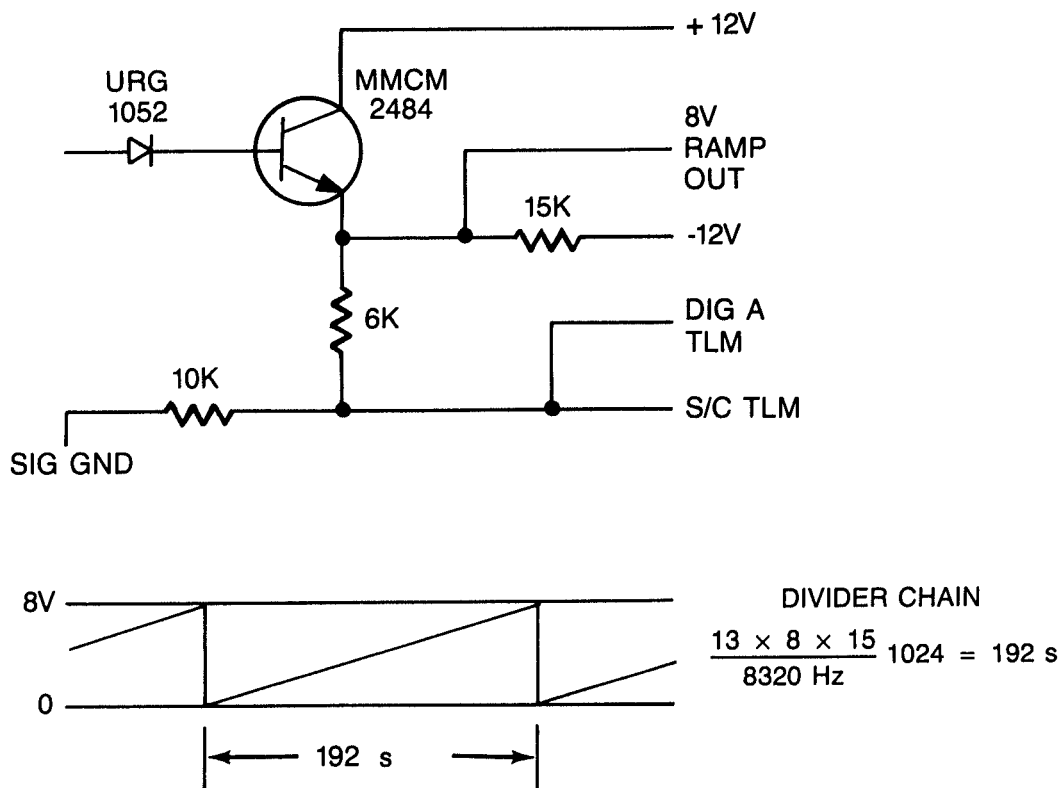


Figure 37.—DPU IFC Ramp TLM Output Circuit

9. COMMAND

9.1 General Information

The SEM command scheme consists of setting eight (8) two-state command lines from the spacecraft to the DPU to either "0" or "1". One of four two-state pulse command lines are then strobed which sets the command into the appropriate memory in the SEM.

All commands strobed with Pulse Command #4 (PC #4) operate latching relays. A "1" (0 volts) on the indicated Data Command Bit (DCB) line will set the state of the indicated relay. All other DCB lines should contain "0" unless the operator desires to change the state of more than one relay by means of a single PC #4 strobe. DCB lines have a second name "Level Command" (LC) as shown here with 0 to 7 numbers.

COMMANDS ACTIVATED BY A PC #4 STROBE				SOCC name SEMPLS	
SOCC name	Command Bit	Meaning of state "1"			
SML1	DCB 1 (LC#0)	MEPED	ON		
SML2	2 (LC#1)	MEPED	OFF		
SML3	3 (LC#2)	TED	ON		
SML4	4 (LC#3)	TED	OFF		
SML5	5 (LC#4)	HEPAD	ON		
SML6	6 (LC#5)	HEPAD	OFF		
SML7	7 (LC#6)	LV	ON		
SML8	8 (LC#7)	LV	OFF		

NOTES:

1. The LV power must be turned on first, by setting DCB 7 to "1" (True). It is wise to set DCB 8 to "0" (False) before sending PC #4 Strobe, since the status of DCB 8 cannot be determined when the instrument is OFF. Other bits may be set to "1", but it is not possible to turn on sensors with the same strobe which turns on the LV.
2. DCB 7 and DCB 8 must be set to "0" (False) before a strobe sent to turn on any of the sensors will be effective.
3. Turning LV off (DCB 8 = "1", followed by PC #4 strobe) also leaves all three sensor relays in the "OFF" position.

9.2 IFC and Format Commands

The Pulse Command 1 (PC #1) strobe with DCB 1 thru 6 sets logic states in the DPU. Any functionally correct combination on Data Command Bit (DCB) lines 1 thru 6 may be executed with a single PC #1 strobe.

COMMANDS ACTIVATED BY A PC #1 STROBE

SOCC name SEMDP

Command Bit	Meaning of state "1"
DCB 1 (LC#0)	Start TED/HEPAD IFC
2 (LC#1)	Start MEPED IFC Note 3
3 (LC#2)	don't care
4 (LC#3)	Terminate IFC
5 (LC#4)	Select TLM Format 1
6 (LC#5)	Select TLM Format 2
7 (LC#6)	don't care
8 (LC#7)	don't care

NOTES:

1. TED/HEPAD and MEPED may be calibrated separately by setting DCB 1 or DCB 2 to "1", or simultaneously by setting both DCB 1 and DCB 2 to "1". However, a second IFC command should not be sent during the following 16 minutes (except see Note 3), unless the "Terminate IFC" command is sent. Bad data may result.

2. When the TED/HEPAD IFC is commanded, the TED will continue in "IFC Mode" for 102.4 minutes after completion of the ramp calibration cycles. During this time, unless the "terminate IFC" command is sent, TED commands using PC #2 strobe (see page 89) will have no effect.

3. For correct results, MEPED IFC should not be commanded until the MEPED has been on for at least 20 minutes.

9.3 TED Commands

The Pulse Command #2 (PC #2) line is used to strobe six bits of the level commands (DCB lines 1 thru 6) into various holding registers in the TED. The three bits (DCB 3 thru 1) are used as a Register Address code and the remaining three (DCB 6 thru 4) as data bits. Two bits (DCB 8 and 7) are not used.

TED COMMANDS ACTIVATED BY A PC #2 STROBE * SOCC name SEMTD

Command Bit							Commanded TED State						
DCB	6	5	4	3	2	1							
1	M	N	0	0	0		Set 0° Level to Levels 1-4. (MN = 00 to 11) M is bit 1 N is bit 0						
1	M	N	0	0	1		Set 30° Level to Levels 1-4. (MN = 00 to 11)						
x	x	x	0	1	x		Not used						
L	M	N	1	0	0		Set Proton Channeltron HVPS -2635 V to -3850 V (Approx. -200 V steps). LMN = 000(min) to 111(max negative) binary.						
L	M	N	1	0	1		Set Electron Channeltron HVPS +2900 V to +4200 V (Approx. 200 V steps). LMN = 000(min) to 111(max) binary.						
E	P	C	1	1	0		E	Electron Channeltron HVPS ON/OFF 1 = ON Note 1					
							P	Proton Channeltron HVPS ON/OFF 1 = ON Note 1					
							C	CEA HVPS ON/OFF 1 = ON Note 1					
x	0	x	1	1	1		Normal TED MUX						
x	1	0	1	1	1		Electron Dwell						
x	1	1	1	1	1		Proton Dwell						

x = don't care

See note 2 p. 88

* - See Note 3 for PC #4 on p. 87

(1) The three high voltage power supplies cannot be commanded independently. When commanding any of the supplies, the appropriate bit for each supply must be set for the desired status of that supply following the strobe command.

9.4 HEPAD Commands

The Pulse Command #3 (PC #3) (SOCC name SEMHD) strobe line is used together with level commands DCB's 1 thru 7 to adjust the HEPAD PMT High voltage supply from 1500 volts to 2770 volts in 127 equal steps of 10 volts each.

The voltage is given by: $V = 1500 + 10A$

where A equals the decimal value of the bit setting of DCB's 1 thru 7 (DCB 1 - LSB; DCB 7 - MSB); DCB 8 = don't care.

10. ACKNOWLEDGMENTS

The total team with responsibility including the SEM encompasses the TIROSN/SEM project staffs at GSFC, NESS, SEL and FACC. Those primarily concerned with the detailed design of the SEM were:

Mr. Edward Petroka, FACC
Mr. Donald McMorrow, FACC
Dr. William Sandie, FACC
Dr. Stephen Lazarus, FACC
Dr. Marion C. Rinehart, FACC
Mr. Jacob Wezuiska

Those primarily concerned with reviewing the FACC design, monitoring the contract and assisting in instrument calibrations were:

Dr. W. Kolasinski, Aerospace Corp.
Dr. Bernard Blake, Aerospace Corp.
Mr. Norman Katz, Aerospace Corp.
Mr. Richard N. Grubb, SEL
Mr. Richard A. Seale, SEL
Mr. Robert O. Wales, GSFC
Mr. Martin Eiband, GSFC
Mr. Arthur Rubman, GSFC
Dr. Theodore Fritz, SEL
Dr. David Evans, SEL

Much of the information in this document was supplied by the following individuals:

TED - Dr. David Evans, SEL
MEPED - Dr. Theodore Fritz, SEL
HEPAD - Dr. Herbert Sauer, SEL
Archive Data Format - Ms. V. J. Hill, SEL
HEPAD Calibration - Dr. Frederick Hanser, Panametrics Corp.
Dr. Bach Sellers, Panametrics Corp.

Currently the scientific responsibility within SEL for the operation of the SEM is:

Dr. David Evans - TED
Dr. Herbert Sauer - MEPED and HEPAD

11. REFERENCES

- Crutzen, P. J., I. S. A. Isaaksen, G. C. Reid, "Solar Proton Events: Stratospheric Sources of Nitric Oxide", Science 189, 457, 1975.
- Husky, John W., "The TIROS-N/NOAA Operational Satellite System", paper presented at the NOAA Scientific Colloquium on May 3, 1979, in Washington D.C. and on May 5, 1979, in Geneva, Switzerland.
- Kolasinski, W. A., private communication
- Lavine, James P., James I. Vette, "Models of the Trapped Radiation Environment, Volume VI: High Energy Protons" Goddard Space Flight Center NASA SP-3024 Washington 1970.
- IGRF several papers
- Peddie, N. W., "International geomagnetic reference field - its evolution and difference in total field intensity between new and old models for 1965 - 1980", Geophysics 48 1691, 1893.
- - "International Geomagnetic Reference Field 1975", JGR 81 5163-5164 Oct 1975.
- J. of Geomagnetism and Geoelectricity 34 '#6 307-422 1982.
- Ortec, The Whys and Wherefores of Charged Particle Detector Spectrometry, EG&G Ortec, Oak Ridge, May 1985, page 6.
- Rinehart, Marion C., "Cerenkov Counter for Spacecraft Application", Nuclear Instruments and Methods 154, 303-316, 1978.
- Schwalb, Arthur, "The TIROS-N/NOAA A-G Satellite Series", NOAA Technical Memorandum NESS 95, Washington, March 1978, Reprinted 1982.

12. REFERENCE DOCUMENTS

END Item Data Package: Proto Flight Model WDL-TR7773, 30 Jan 1978

END Item Data Package: Flight Unit WDL-TR7773-1, 1 Apr 1978

END Item Data Package: Flight Unit WDL-TR7773-2, 21 Jul 1978

END Item Data Package: Flight Unit WDL-TR7773-3, 23 Sep 1978

END Item Data Package: Flight Unit WDL-TR7773-4, 26 Oct 1978

END Item Data Package: Flight Unit WDL-TR7773-5, Feb 1979

END Item Data Package: Flight Unit WDL-TR7773-6, Mar 1979

END Item Data Package: Flight Unit WDL-TR7773-7, 6 Jun 1979

TIROS-N Unique Interface Specification for the Space Environment Monitor
IS-2280264, RCA Corp, Princeton, First issued December 6, 1976

V.J. Hill, D.S. Evans, H.H. Sauer, TIROS/NOAA Satellite Space Environment
Monitor, Archive Tape Documentation, NOAA Technical Memorandum,
ERL SEL-71, Boulder, January 1985

H. H. Sauer, An Atlas of Polar Cap Energetic Particle Observations
Volume I. TIROS-N: 1 January 1979 to 28 February 1981,
NOAA Data Report ERL SEL-3, Boulder, August 1984

TIROS-N SEM Data Reduction and Calibrations Cycle Analysis Manual, Rev. C, R.
Seale, NOAA SEL, Boulder, March 1, 1977

Space Environment Monitor for the TIROS-N Satellite Technical Performance
Specification and Statement of Work, NOAA SEL, Boulder, June 12, 1975

Space Environment Monitor for TIROS-N Satellite, Subsystem Instruction Manual
WDL-TR7683, Ford Aerospace Communications Corp., Palo Alto, Jan. 1978
Volume I: Data and Procedures
Volume II: Drawings and Parts List

APPENDIX A

Table of the area F under the normal curve.

Used for Determination of Z in FWHM Calculation.

F(Z)	1-F(Z)	Z	F(Z)	1-F(Z)	Z
.500000	.500000	.00	.805105	.194895	.86
.507978	.492022	.02	.810570	.189430	.88
.515953	.484047	.04	.815940	.184060	.90
.523922	.476078	.06	.821214	.178786	.92
.531881	.468119	.08	.826391	.173609	.94
.539828	.460172	.10	.831472	.168528	.96
.547758	.452242	.12	.836457	.163543	.98
.555670	.444330	.14	.841345	.158655	1.00
.563559	.436441	.16	.846136	.153864	1.02
.571424	.428576	.18	.850830	.149170	1.04
.579260	.420740	.20	.855428	.144572	1.06
.587064	.412936	.22	.859929	.140071	1.08
.594835	.405165	.24	.864334	.135666	1.10
.602568	.397432	.26	.868643	.131357	1.12
.610261	.389739	.28	.872857	.127143	1.14
.617911	.382089	.30	.876976	.123024	1.16
.625516	.374484	.32	.881000	.119000	1.18
.633072	.366928	.34	.884930	.115070	1.20
.640576	.359424	.36	.888768	.111232	1.22
.648027	.351973	.38	.892512	.107488	1.24
.655422	.344578	.40	.896165	.103835	1.26
.662757	.337243	.42	.899727	.100273	1.28
.670031	.329969	.44	.903200	.096800	1.30
.677242	.322758	.46	.906582	.093418	1.32
.684386	.315614	.48	.909877	.090123	1.34
.691462	.308538	.50	.913085	.086915	1.36
.698468	.301532	.52	.919243	.080757	1.4
.705401	.294599	.54	.933193	.066807	1.5
.712260	.287740	.56	.945201	.054799	1.6
.719043	.280957	.58	.955435	.044565	1.7
.725747	.274253	.60	.964070	.035930	1.8
.732371	.267629	.62	.971283	.028717	1.9
.738914	.261086	.64	.977250	.022750	2.0
.745373	.254627	.66	.986097	.013903	2.2
.751748	.248252	.68	.991802	.008198	2.4
.758036	.241964	.70	.995339	.004661	2.6
.764238	.235762	.72	.997445	.002555	2.8
.770350	.229650	.74	.9986501	.0013499	3.0
.776373	.223627	.76	.9997674	.0002326	3.5
.782305	.217695	.78	.9999683	.0000317	4.0
.788145	.211855	.80	.9999966	.0000034	4.5
.793892	.206108	.82	.9999997	.0000003	5.0
.799546	.200454	.84			

For 1 - F(Z), Z is negative.

From NBS 55 1964 p. 966

APPENDIX B

SEM IFC

Length: 4 phases.
Each phase consists of 6 major frames, 192 seconds.

IFC Ramp: 192 Seconds, 0 to 8 volts.

During spacecraft testing, it is assumed that both IFC commands are given simultaneously.

APPENDIX C

TED IFC Details

4 Phases--192 Seconds Each

1 Ramp 0 to 8.0 V divided down to 1 volt.

Each phase is run with a different attenuator setting.

1. Discriminator Thresholds--Determine the threshold on each of 4 channels during each IFC phase and limit check.

Channels with thresholds: OEFD, OPFD, 30EFD, 30PFD.

Channels with no threshold check but which probably have a complete count:

ODE1, ODE3, ODE5, ODE7

30DE1, 30DE3, 30DE5, 30DE7

ODP1, ODP3, ODP5, ODP7

30DP1, 30DP3, 30DP5, 30DP7

OEM, 30EM, OPM, 30PM

ODEM, ODPM, 30DEM, 30DPM

2. Background Check--Limit check the OEFD, OPFD, 30EFD, 30PFD channels for appropriate levels.

3. With ASE, check the DE, Em, and DEM channels.

Note: Use of ASE requires the TED to be in a vacuum.

APPENDIX D

MEPED IFC Details

3 Phases--192 seconds each. The 4th phase is not used.

Ramps: 0 to 8 V divided down to the amplitudes listed below.

<u>Detector</u>	<u>Amplitude</u>	<u>Phase</u>	<u>Peak Energy</u>
D1 D2 D3	0-3.375 mV	1	75 keV
D1 D3	0-144 mV	2	3.2 MeV
D1	0-450 mV		10 MeV
D2	0-1.35 V	3	30 MeV
D3	0-144 mV		3.2 MeV
D4, D5, D6	0-54 mV	1-3	1.2 MeV

1. Determine FWHM for 9 detectors during Phase 1 using data channels 0P1, 90P1, 0E1, 90E1, P6, P7, P8 limit check.
2. Limit check other channels for spurious counts.
3. Determine thresholds of 15 level sensors during three phases as follows and check limit. (Note: All channels except P6, P7, P8 are both 90° and 0°.)

Phase I

	<u>Level Sensors</u>	<u>Data Channel</u>
Proton	1, 7	P1
Electron	1	E1
OMNI	1-3	P6, P7, P8

Phase II

Proton	2-5	P2, P3, P4
Electron	1-4	E1, E2, E3
OMNI	1-3	P6, P7, P8

MEPED IFC (cont.)

Phase III

Proton	1, 8	P5
Ion	6	I
Electron	1-4	E1, E2, E3
OMNI	1-3	P6, P7, P8

4. Background limit check--During the IFC sequence, the DPU automatically gates the IFC pulses on/off at a 1/2 Hz rate so that the preamp alternately sees background and background plus calibration.

5. During periods with no IFC, check all channels for backgrounds which exceed limits.

APPENDIX E

HEPAD IFC Details

4 Phases---192 seconds each

3 Ramps

<u>Detector</u>	<u>Amplitude</u>	<u>Phase</u>	<u>Energy</u>
D1, D2	0 to 16, 0 to 9 mV	1-4	0-0.76 MeV
PMT		1, 2	0-800 photoelectrons
PMT		3, 4	0-320 "

1. Determine FWHM for 2 detectors and PMT and check limits.

<u>Detector</u>	<u>Data Channel</u>	<u>IFC Phase</u>	<u>Remarks</u>
D1	S1	1-4	Avg. of 4
D2	S2	1-4	Avg. of 4
PMT	S3	3, 4	Avg. of 2

2. Determine thresholds of 10 level sensors during 4 phases as follows and check limits.

Phase 1, 2 (High Gain)

<u>Level Sensor</u>	<u>Data Channel</u>	<u>Remarks</u>
1	S3	Avg. of 2 readings
7	S2	
9	S1	
4, 5	P4	*
5	S4	
10, 6	A1	*
6	A2	

* The first LS determines the cut on threshold; the second the cutoff.

APPENDIX E (cont.)

HEPAD PARAMETERS (CONT.)

Phase 3, 4 (Low Gain)

<u>Level Sensor</u>	<u>Data Channel</u>	<u>Remarks</u>
1	S3	Avg. of 2 readings
7	S2	
9	S1	
9, 2	P1	*
2, 3	P2	*
3, 4	P3	*
4, 8	P4	*

*The first LS determines the cut on threshold; the second the cutoff.

3. Determine the double and triple coincidence efficiency for six pairs of level sensors as follows and check limits.

<u>Level Sensor</u>	<u>Data Channel</u>
9, 2	P1
2, 3	P2
3, 4	P3
4, 5	P4
10, 6	A1
6	A2

4. During periods with no IFC, check all channels for backgrounds which exceed limits.

APPENDIX F

Detector and Level Sensor Cross Reference

Data Channel	Levels Used	Thresholds Determined			FWHM			Remarks
		Level Sensor		IFC Phase	Detector		IFC Phase	
		Rising Slope	Falling Slope		Rising Slope	Falling Slope		
MEPED								
OP1	1, 2, 7	1	7	1	OD1	OD2	1	1/
90P1	1, 2, 7	1	7	1	90D1	90D2	1	
OP2	2, 3, 7	2	3	2				
90P2	2, 3, 7	2	3	2				
OP3	3, 4, 7	3	4	2				
90P3	3, 4, 7	3	4	2				
OP4	4, 5, 7	4	5	2				
90P4	4, 5, 7	4	5	2				
OP5	5, 6, 8	5	8	2, 3				2/
90P5	5, 6, 8	5	8	2, 3				2/
OI	6	6		3				
90I	6	6		3				
P6	1	1		1, 2, 3	D4		1, 2, 3	
P7	2	2		1, 2, 3	D5		1, 2, 3	
P8	3	3		1, 2, 3	D6		1, 2, 3	
OE1	1, 4	1	4	1	OD3		1	
90E1	1, 4	1	4	1	90D3		1	
OE2	2, 4	2	4	2, 3				
90E2	2, 4	2	4	2, 3				
OE3	3, 4	3	4	2, 3				
90E3	3, 4	3	4	2, 3				

APPENDIX F (Cont'd)

Data Channel	Levels Used	Thresholds Determined			FWHM			Remarks
		Level Sensor		IFC	Detector		IFC	
		Rising Slope	Falling Slope		Rising Slope	Falling Slope		
HEPAD								3/
S1	9	9		1-4	D1		1-4	
S2	7	7		1-4	D2		1-4	
S3	1	5		1,2				
S4	5	5		1,2				
P1	1,7,9,2,8,10	9	2	3,4				
P2	1,7,9,2,3,8,10	2	3	3,4				
P3	1,7,9,3,4,8,10	3	4	3,4				
P4	1,7,9,4,5,8,10	4	8	3,4				4/
A1	1,7,9,5,6,8,10	10	6	1,2				
A2	1,7,9,6,8,10	6		1,2				
TED								
OEFD								5/
OPFD								
3OEFD								
3OPFD								

1/ Level sensors 3, 4, and 5 can be determined from the cut on (rising slope) or cutoff (falling slope) in two adjacent data channels. It is only necessary that one or the other method be used.

2/ Channel P5 has an "or" logic condition of 1, 5, 7, 8. LS 5 is measured in IFC phase 2 with the 5, 6, 8 logic. LS 8 is measured in IFC phase 3 with the 1, 5, 7, 8 logic.

3/ Same note as 1/ except level sensors 2, 3, 4, 5, and 6 are involved.

4/ LS 5 is determined during phases 1 and 2. LS 8 is measured during phases 3 and 4.

5/ The TED has only one level sensor per channel; the level however can be set to 4 discrete values by gain and attenuator settings. Each IFC phase measures one gain/attenuator condition.

APPENDIX G

Integration Time

Channel		
<u>TED</u>	All Channels	1 s
<u>MEPED</u>	0I 90I	8 s
	All Other Data Channels	1 s
	see notes below	
<u>HEPAD</u>	All Primary Data Channels	4 s
	S1, S2, S3	94 ms
	S4	2.5 s
	S5	1.2 s

During MEPED IFC, the DPU alternately looks at MEPED background for 1 second and the IFC signal for 1 second while at the same time multiplexing between telescopes.

During MEPED IFC the integration time for 0I and 90I is 4 seconds.

APPENDIX H

Digital A Telemeter Assignments Telemeter Data by Minor Frame Number

TED Mode 1 = normal

DPU Mode 1 = TLM format 1

0	20	40	60	80	100	120	140
0I	90I	MEP P	MEP	MEP	MEP P	MEP E	DPU
	Bias	Bias	Omni T	E1 T	Tel T	Tel T	T
0P1	-	-	-	-	-	-	-
1	21	41	61	81	101	121	141
0P2	-	-	-	-	-	-	-
0P3	-	-	-	-	-	-	-
2	22	42	62	82	102	122	142
0P4	-	-	-	-	-	-	-
0P5	-	-	-	-	-	-	-
3	23	43	63	83	103	123	143
0E1	-	-	-	-	-	-	-
0E2	-	-	-	-	-	-	-
4	24	44	64	84	104	124	144
0E3	-	-	-	-	-	-	-
P1	S5	P1	S5	P1	S5	P1	S5
5	25	45	65	85	105	125	145
0DE1	30DE1	ODP1	30DP1	0DE1	30DE1	ODP1	30DP1
P2	S4	P2	S4	P2	S4	P2	S4
6	26	46	66	86	106	126	146
0DE3	30DE3	ODP3	30DP3	0DE3	30DE3	ODP3	30DP3
P3	S1	P3	S1	P3	S1	P3	S1
7	27	47	67	87	107	127	147
0DE5	30DE5	ODP5	30DP5	0DE5	30DE5	ODP5	30DP5
P4	S2	P4	S2	P4	S2	P4	S2
8	28	48	68	88	108	128	148
0DE7	30DE7	ODP7	30DP7	0DE7	30DE7	ODP7	30DP7
A1	S3	A1	S3	A1	S3	A1	S3
9	29	49	69	89	109	129	149
A2	MEP E B	A2	spare	A2	spare	A2	spare
OEM OPM	- -	- -	- -	- -	- -	- -	- -
10	30	50	70	90	110	130	150
30EM 30PM	- -	- -	- -	- -	- -	- -	- -
90P1	-	-	-	-	-	-	-
11	31	51	71	91	111	131	151
90P2	-	-	-	-	-	-	-
90P3	-	-	-	-	-	-	-

12	32	51	72	92	112	132	152
90P4	-	-	-	-	-	-	-
90P5	-	-	-	-	-	-	-
13	33	53	73	93	113	133	153
90E1	-	-	-	-	-	-	-
90E2	-	-	-	-	-	-	-
14	34	54	74	94	114	134	154
90E3	-	-	-	-	-	-	-
P6	-	-	-	-	-	-	-
15	35	55	75	95	115	135	155
P7	-	-	-	-	-	-	-
P8	P8	P8	P8	P8	P8	P8	P8
16	36	56	76	96	116	136	156
OEFD	-	-	-	-	-	-	-
OPFD	-	-	-	-	-	-	-
17	37	57	77	97	117	137	157
30EFD	-	-	-	-	-	-	-
30PFD	-	-	-	-	-	-	-
18	38	58	78	98	118	138	158
ODEM	-	-	-	-	-	-	-
OPDM	-	-	-	-	-	-	-
19	39	59	79	99	119	139	159
30DEM	-	-	-	-	-	-	-
30DPM	-	-	-	-	-	-	-
<div> <div>2 s</div> <div>4 s</div> <div>8 s</div> <div>16 s</div> </div>							

MEPED Code abc a = 0, 90 for 0 and 90 degrees
 b = E, P for electrons and protons
 c = 1 to 3 for electron energy
 1 to 6 for proton energy
 BK for background

aE1 aE2 aE3 aP1 aP2 aP3 aP4 aP5
 30 100 300 keV 30 80 250 800 2500 keV

if a is missing: b = P
 P6 P7 P8
 16 35 70 MeV

Energy numbers are the low ends of the ranges.
 The list here does not indicate which signals are for a finite range
 and which are integral.

TED 1 DPU 1

This page fits at the right of page 102.

160	180	200	220	240	260	280	300
01	901	spare	TED E ch PS	TED P ch PS	TED T	HEP PMT PS	HEP Bias
OP1	-	-	-	-	-	-	-
161	181	201	221	241	261	281	301
OP2	-	-	-	-	-	-	-
OP3	-	-	-	-	-	-	-
162	182	202	222	242	262	282	302
OP4	-	-	-	-	-	-	-
OP5	-	-	-	-	-	-	-
163	183	203	223	243	263	283	303
OE1	-	-	-	-	-	-	-
OE2	-	-	-	-	-	-	-
164	184	204	224	244	264	284	304
OE3	-	-	-	-	-	-	-
P1	S5	P1	S5	P1	S5	P1	S5
165	185	205	225	245	265	285	305
ODE1	30DE1	ODP1	30DP1	0EBK	TED bits	bits	sync f3
P2	S4	P2	S4	P2	S4	P2	S4
166	186	206	226	246	266	286	306
ODE3	30DE3	ODP3	30DP3	0PBK	DCB 1-8	PC1-4	sync 50
P3	S1	P3	S1	P3	S1	P3	S1
167	187	207	227	247	267	287	307
ODE5	30DE5	ODP5	30DP5	30EBK	DPU12V	HEP ELT	HEP PMTT
P4	S2	P4	S2	P4	S2	P4	S2
168	188	208	228	248	268	288	308
ODE7	30DE7	ODP7	30DP7	30PBK	TED ramp	TED CEAPS	DPU ramp
A1	S3	A1	S3	A1	S3	A1	S3
169	189	209	229	249	269	289	309
A2	spare	A2	spare	A2	spare	A2	spare
OEM OPM	- -	- -	- -	- -	- -	- -	- -
170	190	210	230	250	270	290	310
30EM 30PM	- -	- -	- -	- -	- -	- -	- -
90P1	-	-	-	-	-	-	-
171	191	211	231	251	271	291	311
90P2	-	-	-	-	-	-	-
90P3	-	-	-	-	-	-	-

172	192	212	232	252	272	292	312
90P4	-	-	-	-	-	-	-
90P5	-	-	-	-	-	-	-
173	193	213	233	253	273	293	313
90E1	-	-	-	-	-	-	-
90E2	-	-	-	-	-	-	-
174	194	214	234	254	274	294	314
90E3	-	-	-	-	-	-	-
P6	-	-	-	-	-	-	-
175	195	215	235	255	275	295	315
P7	-	-	-	-	-	-	-
P8	-	-	-	-	-	-	-
176	196	216	236	256	276	296	316
0EFD	-	-	-	-	-	-	-
0PFD	-	-	-	-	-	-	-
177	197	217	237	257	277	297	317
30EFD	-	-	-	-	-	-	-
30PFD	-	-	-	-	-	-	-
178	198	218	238	258	278	289	318
ODEM	-	-	-	-	-	-	-
OPDM	-	-	-	-	-	-	-
179	199	219	239	259	279	299	319
30DEM	-	-	-	-	-	-	-
30DPM	-	-	-	-	-	-	-
				24 s			
							32 s

xxx minor frame number

yyyy data in word 20

zzzz data in word 21

- means same as at left.

Where data have two codes:

4 bits are used by each (frame 9, 10).

TED code abc

a = 0, 30 for 0 and 30 degrees

in b E = electrons

P = protons

In TED codes E and P do not appear alone.

TED Mode	Proton Dwell			DPU Mode 1 = TLM format 1			
5	25	45	65	85	105	125	145
ODP1	3ODP1	ODP1	3ODP1	ODP1	3ODP1	ODP1	3ODP1
6	26	46	66	86	106	126	146
ODP3	3ODP3	ODP3	3ODP3	ODP3	3ODP3	ODP3	3ODP3
7	27	47	67	87	107	127	147
ODP5	3ODP5	ODP5	3ODP5	ODP5	3ODP5	ODP5	3ODP5
8	28	48	68	88	108	128	148
ODP7	3ODP7	ODP7	3ODP7	ODP7	3ODP7	ODP7	3ODP7
9	29	49	69	89	109	129	149
OPM OPM	--	--	--	--	--	--	--
10	30	50	70	90	110	130	150
3OPM 3OPM	--	--	--	--	--	--	--

16	31	51	71	91	111	131	151
OPFD	-	-	-	-	-	-	-
OPFD	-	-	-	-	-	-	-
17	37	57	77	97	117	137	157
3OPFD	-	-	-	-	-	-	-
3OPFD	-	-	-	-	-	-	-
18	38	58	78	98	118	138	158
ODPM	-	-	-	-	-	-	-
ODPM	-	-	-	-	-	-	-
19	39	59	79	99	119	139	159
3ODPM	-	-	-	-	-	-	-
3ODPM	-	-	-	-	-	-	-

continued on next page

TED Mode Electron Dwell is same as Proton Dwell except all P symbols listed here in rows beginning with 5 - 10, 16 - 19 are E.

This page fits at the right of page 106.

165	185	205	225	245	265	285	305
ODP1	30DP1	ODP1	30DP1	OPBK			
166	186	206	226	246	266	286	306
ODP3	30DP3	ODP3	30DP3	OPBK			
167	187	207	227	247	267	287	307
ODP5	30DP5	ODP5	30DP5	30PBK			
168	188	208	228	248	268	288	308
ODP7	30DP7	ODP7	30DP7	30PBK			
169	189	209	229	249	269	289	309
OPM OPM	--	--	--	--	--	--	--
170	190	210	230	250	270	290	310
30PM 30PM	--	--	--	--	--	--	--

176	196	216	236	256	276	296	316
OPFD	-	-	-	-	-	-	-
OPFD	-	-	-	-	-	-	-
177	197	217	237	257	277	297	317
30PFD	-	-	-	-	-	-	-
30PFD	-	-	-	-	-	-	-
178	198	218	238	258	278	298	318
ODPM	-	-	-	-	-	-	-
ODPM	-	-	-	-	-	-	-
179	199	219	239	259	279	299	319
30DPM	-	-	-	-	-	-	-
30DPM	-	-	-	-	-	-	-

TED normal

DPU mode 2 = TLM format 2

45	65	125	145	205	225
ODE1	30DE1	ODE1	30DE1	ODE1	30DE1
46	66	126	146	206	226
ODE3	30DE3	ODE3	30DE3	ODE3	30DE3
47	67	127	147	207	227
ODE5	30DE5	ODE5	30DE5	ODE5	30DE5
48	68	128	148	208	228
ODE7	30DE7	ODE7	30DE7	ODE7	30DE7

APPENDIX I

Acronyms and Letter Groups

CDA	Command and Data Acquisition
CEAPS	Cylindrical Electrostatic Analyzer Power Supply
DCB	Data Command Bit also Digital Command Bit
DPU	Data Processing Unit
FACC	Ford Aerospace and Communications Corporation
GSFC	Goddard Space Flight Center of NASA
IFC	In-Flight Calibration
LC	Level Command
LD	Level Detector
HEPAD	High Energy Proton and Alpha Detector
HVPS	high voltage power supply
MEPED	Medium Energy Proton and Electron Detector
NESDIS	National Environmental Satellite Data and Information Service, NOAA
PC	Pulse Command
SAT	Select at Test (means choose value during manufacture)
S/C	Spacecraft
SEL	Space Environment Laboratory, NOAA, Boulder
SELDADS	SEL Data And Display System
SEM	Space Environment Monitor
SESC	Space Environment Service Center, SEL, NOAA, Boulder
SOCC	Satellite Operations Control Center of NESDIS, Suitland, Maryland
SSD	Solid State Detector
TED	Total Energy Detector
TIP	TIROS Information Processor
TLM	Telemeter

- - - - -